

Introduction to “Mach Effect Propulsion, an Exact Electroelasticity Solution”

José J. A. Rodal¹

Rodal Consulting

Research Triangle Park, North Carolina

[Editors' comment: Rodal's research article was considered too lengthy to fit well into the chapter, being the length of a small monograph, so here is just Rodal's introduction to his article which is located in Appendix D, at the end of the proceedings.]

This is a general introduction to my article in Appendix D, which presents a comprehensive analysis of a mathematical modeling of the experiments performed by Woodward and Fearn using piezoelectric stacks (known for over 100 years as Langevin stacks, since P. Langevin first invented and developed them). Up to now, Woodward and Fearn have analyzed these experiments without taking into account the effect of damping or stiffness (neither the quality factor of resonance nor any other form of damping measure, nor the modulus of elasticity nor any other form of stiffness measure appears in their equations) in the modeling of the response in their experiments. The Woodward and Fearn experiments are experiments conducted as closely as possible to the natural frequency. It is known that for zero damping, the response at the natural frequency would have infinite amplitude, which is physically impossible, which is why it is imperative to take damping into account. Similarly the vibration response is dependent on the stiffness of the system, and not just the masses involved, hence it is imperative to take into account the modulus of elasticity of the system components in the analysis of the response.

The Woodward and Fearn experiments are not quantum mechanics or particle physics experiments nor cosmological measurements dealing with verification of gravitational theories. Instead, they are dynamic measurements performed in a macroscopic man-made dynamic system, a Langevin stack of piezoelectric plates. Also, the Woodward and Fearn experiments have not been conducted for a Mach Effect Gravitational Assist (MEGA) drive floating freely in space, but instead for one attached at the back end to a bracket at the end of a torsional pendulum whose center of rotation is fixed to terra firma. Hence a mathematical analysis of these experiments has to concentrate on macroscopic aspects like materials science (phase transitions, crystallography), mechanics of materials (piezoelectricity, electrostriction, fracture mechanics, etc.), dynamic analysis, unsteady heat transfer and other aspects of continuum mechanics rather than aspects common to general relativity like cosmological measurements or aspects more familiar to fundamental physics experiments like quantum mechanics or particle physics. The mathematical analysis of the Woodward and Fearn experiments involves interdisciplinary aspects like mechanics of materials and structural dynamics that aerospace engineers are familiar with, but with (brittle anisotropic piezoelectric and electrostrictive) materials that may be familiar only to a segment of people interested in space propulsion.

Due to the fact that the disciplines involved in these experiments may not be familiar to people specializing in specific areas like general relativity or space propulsion, many things discussed in my article (in Appendix D) may at first glance perhaps appear insignificant or unimportant, for example, the reason why materials science (phase transitions, crystallography), and mechanics of materials (piezoelectricity, electrostriction, fracture mechanics, etc.) are discussed in some detail. A specific example is the discussion of the bolts that hold the stack. This is important because the materials involved in the experiment are very brittle materials that need to be pre-compressed (using bolts) to stop cracks from propagating and to therefore behave as structural materials able to take tension. The stiffness of the bolts used to pre-compress the sandwich stack of piezoelectric plates plays an important role in the stiffness of the stack of piezoelectric plates, and hence is necessary to take into account when modeling these experiments. The length of the paper is due to these numerous interdisciplinary aspects which are discussed.

Following is a short description of the sections covered in my article, which gives an overview of what is being discussed, and where, and allows the reader to jump to certain sections and skip other sections if she prefers. The figures, tables, references and pertinent details are in Appendix D.

¹ jrodal@alum.mit.edu

SECTION 1, PIEZOELECTRICITY, THE LANGEVIN TRANSDUCER AND PZT

In the first section, after a brief overview of the history of piezoelectricity, the role of the tail and front masses in achieving a desired natural frequency is discussed. Next is discussed the piezoelectric materials involved in the experiments of Woodward and Fearn, brittle materials that cannot function for transducer purposes without application of an initial compressive stress. The various physical behaviors of the materials used in these experiments are discussed: elastic, ferroelectric, piezoelectric, electrostrictive and pyroelectric. Most of the section is dedicated to a discussion of the material science issues associated with these experiments, including the phase diagram and associated crystallography in different phases, the transition temperature associated with a change from tetragonal or rhombohedral ferroelectric to a centrosymmetric cubic dielectric, the importance of proximity to the morphotropic phase boundary to favor enhancement of the piezoelectric coefficient, the poling process, the fact that the materials involved are doped, and that hard doping (involving acceptors) or soft doping (involving donors) can substantially impact the material properties exhibited by these materials.

SECTION 2, THE MEGA LANGEVIN STACK

Next, the second section deals with the specific construction of the Langevin stack used in the experiments of Woodward and Fearn. The MEGA Langevin stack has a tail mass made of brass and a front mass made of aluminum, with a stack of piezoelectric plates between the end masses, which is compressed by stainless steel bolts in tension. My analysis concludes that it would be better to use a copper tail mass, or optimally, a silver tail mass, because of thermal diffusivity considerations, due to the unsteady heat transfer that occurs as a result of internal heat generated inside the piezoelectric plates from the vibratory motion of the stack. The analysis and experimental results show that the passive piezoelectric plates used in the MEGA stack act as strain gauges, and not as accelerometers, due to the fact that the MEGA stack is purposely driven near the natural frequency resonance. The piezoelectric plates and brass electrodes in the stack are adhered with an epoxy adhesive in a sandwich sequence where the piezoelectric plates are connected mechanically (as springs) in series and electrically (as capacitors) in parallel. My analysis shows that it would be better to use a filled polymer adhesive to decrease the thermal expansion of the adhesive (in relation to the thermal expansion of the electrodes and the piezoelectric plates), increase the thermal diffusivity of the adhesive, and increase the strength of the adhesive. It also would be better to use an adhesive with a higher glass transition temperature than the one presently used, because the glass transition temperature of the present adhesive is much lower than the Curie temperature of the piezoelectric plates presently used in the MEGA stack and therefore acts as the weak link in the system. The piezoelectric plates presently used have a negative coefficient of thermal expansion, and therefore it would be better to replace the stainless steel bolts presently used to compress the stack with bolts having a much smaller coefficient of thermal expansion, like invar bolts, as the bolts result in compression being lost during heating of the stack which leads to damage and loss of functionality of the piezoelectric plates.

SECTION 3, VARIATION OF INERTIAL MASS FROM HOYLE-NARLIKAR COSMOLOGY

The third section takes off from the re-derivation by Fearn (using Hoyle-Narlikar's theory without the creation field) of the inertial mass fluctuation equation originally derived by Woodward. I derive the force differently from previous derivations by Woodward and Fearn, using the relativistic kinetic energy and purposely avoiding any use of the energy mass equivalence relation. I clearly identify the terms that are neglected. Only three assumptions are involved: 1. Hoyle-Narlikar's theory (dropping the creation field), 2. that the speed of material points is negligibly small compared to the speed of light and 3. that the second derivative with respect to time of the natural logarithm of the rest mass is negligibly small compared to the second derivative with respect to time of the kinetic energy per unit mass.

SECTION 4, THE MEGA DRIVE MODEL: 2 UNEQUAL MASSES CONNECTED BY A VISCOELASTIC PIEZOELECTRIC/ELECTROSTRICTIVE STACK

The fourth section discusses the MEGA drive mathematical model: 2 unequal masses connected by a stack of compressed viscoelastic piezoelectric/electrostrictive plates. The calculated natural frequency of the MEGA Langevin stack using book values for the material properties compares very well with the previously reported MEGA experiments.

SECTION 5, THE MACH EFFECT FORCE: ANALYSIS OF INPUT VARIABLES

Section five starts by discussing the exact analytical calculation of the Mach effect force on the center of mass as the product of the total mass times the acceleration of the center of mass. Most of this section is dedicated to a detailed discussion of the proper values of the input variables for the model. Although some of the input parameters have unquestionable values (like the gravitational constant or the speed of light) and other parameters are straightforward to measure (like the geometrical dimensions and the masses), other parameters are not, and therefore they deserve a thorough discussion. Prominent among these are the constitutive properties, since the materials involved in the MEGA drive experiments are anisotropic (different material properties in different directions), and their properties are a complex function of frequency, temperature, electric field, initial stress, fatigue life and electromechanical history, including polarization history. Material properties for which the material supplier gives book values still need to be carefully assessed. For example, in the rare case where the supplier gives the test conditions under which the material properties were measured, those test conditions may be unrepresentative of the MEGA stack testing conditions, and hence the input properties have to be carefully converted. Most importantly, previous derivations of the Mach effect force have not used the proper constitutive equations: they have used the voltage as the field variable. The proper field variable to use in electroelastic constitutive equations is the electric field (see Maxwell's equations) instead of the voltage. Previous Mach effect force derivations have used this improper constitutive equation and inconsistently used as an input the piezoelectric values based on the electric field (hence using different physical units, which has led to inconsistencies). Particular attention is dedicated to an examination of the value of the electrostrictive tensor physical component value, since this material property has such small value for the piezoelectric material used in MEGA experiments, palling in comparison to the piezoelectric effect, that it is not provided by the material supplier. The (fourth order) electrostriction tensor components can be properly defined in terms of the electric field or in terms of the polarization field. These constitutive properties are properly analyzed mathematically and the correct transformation is derived, which leads to a consistent value for the electrostrictive property to use in the analysis. Hysteresis in the strain vs. electric field or in the polarization vs. electric field domain are shown to be negligible for the MEGA experiments conducted up to now because of the low level of electric field applied in the experiments. For the MEGA drive experiments, much more important than nonlinearities like hysteresis, are the issues associated with the brittle nature of the piezoelectric materials employed. The electric field used for the MEGA experiments is ten times larger than the industry standard reliability limit for the electric field in piezoelectric ceramics. Furthermore, as previously discussed, due to thermal expansion mismatch between the piezoelectric stack and the stainless steel bolts, necessary pre-compression is progressively lost as the stack heats up due to internal heat generation, and therefore the piezoelectric stack becomes more prone to damage due to micro-crack propagation. I show that MEGA experiments should be conducted taking impedance vs. frequency spectra measurements of the MEGA drive stack immediately before and immediately after conducting the MEGA experiment, so that one knows the electromechanical fatigue state of the piezoelectric ceramic being tested ahead of the test, and can assess the level of damage suffered by the piezoelectric as a result of the test.

SECTION 6, THE MACH EFFECT FORCE: OUTPUT ANALYSIS

Section six analyzes the numerical results of different Mach effect force experiments. In addition to calculating the MEGA experiments conducted by Woodward and Fearn, the behavior of a MEGA drive floating freely in space is analyzed. A very small amplitude (a few nanoNewtons) subharmonic Mach effect force response due to the electrostrictive effect is calculated to take place at one half the first piezoelectric natural frequency. The magnitude of the Mach effect force at the first piezoelectric natural frequency is

several thousands of times larger than the subharmonic electrostrictive resonance (as expected, since the value of the piezoelectric tensor component is 24 million times greater than the value of the electrostrictive tensor component and the applied electric field is not high enough to compensate for this difference). As the first fundamental frequency due to piezoelectricity is approached from lower or higher frequencies that are more than the (dimensionless) damping ratio (the ratio of the actual damping to the critical value of damping) away from the resonant frequency peak, the Mach effect force response is directed towards the tail (brass) big mass, in agreement with the experiments of Woodward and Fearn. Inside a bandwidth enveloped by the damping ratio, the Mach effect force response changes direction and is instead directed in the opposite direction, towards the front (aluminum) small mass, reaching a peak value at the piezoelectric natural frequency that is seven times greater than the peak value reached in the direction towards the tail mass. It is necessary to have equipment that can lock on this frequency with a bandwidth much smaller than the damping ratio to lock onto this peak Mach effect force. This is very difficult to do because as the MEGA Langevin stack vibrates, heat gets internally dissipated inside the piezoelectric plates, which raises the temperature, which changes the dimensions of the stack, as well as the piezoelectric and electrostrictive properties, hence the natural frequency changes during operation, and it needs to be chased within this small bandwidth. To achieve the highest Mach effect forces, it is better to have a material with a higher quality factor of resonance, but the higher the quality factor of resonance, the smaller this bandwidth around the natural frequency, hence the higher the quality factor of resonance, the more difficult it is to find and stay at the value of frequency at which Mach effect forces have larger values.

Fearn and Woodward tested the MEGA drive with several different tail (brass) masses while keeping everything else constant. They found that there was an optimal tail (brass) mass that maximized their measured Mach effect force. I show that this “optimal tail mass” is not a fixed characteristic of a piezoelectric Langevin stack, but it is an experimental artifact due to the restrained-end condition in the experiments run by Fearn and Woodward. A MEGA drive floating free in space will not exhibit an optimal tail mass, but the greater the tail mass the better, with diminishing returns as the tail mass gets larger, approaching an asymptotic value at infinite tail mass. For the experiments run by Fearn and Woodward, with a restrained-end, there is a different optimal tail mass that depends on how far the excitation frequency is from the natural frequency, and it depends on the stress and electrical history of the piezoelectric material.

SECTION 7, CONCLUSIONS

The final section states the conclusions of this study. I have selectively pointed out several of these conclusions in the previous synopsis of each section. The calculated direction of the Mach effect force and the optimal tail (brass) mass are shown to compare excellently with Woodward and Fearn’s experimental data.

Section seven also discusses that in order for theoretical calculations to match experimental results (based on book values of material properties) it is necessary to introduce an ad-hoc factor. I show that Woodward and Fearn effectively used an ad-hoc factor of 0.2% multiplying the book value of the piezoelectric constant in their Mach effect force calculations of their MEGA drive experiments. In order to match the magnitude of the experimentally measured Mach effect force in Woodward and Fearn’s MEGA experiments, it is also necessary in my analysis to introduce an ad-hoc factor of 0.4% multiplying the piezoelectric constant and the electrostrictive coefficient. This factor is about 100 times smaller than the coupling coefficient one would expect based on electromechanical coupling. Since the total Mach effect force is comprised of the multiplication of three excitation factors (two factors due to piezoelectricity and one factor due to electrostriction), the total ad-hoc coupling factor for the Mach effect force is quite small: of the order of one millionth ($10^{-2} \times 10^{-2} \times 10^{-2} = 10^{-6}$). The following explanations are considered to explain this ad-hoc coupling factor:

- Arguable reality (and magnitude) of the Mach effect propulsion hypothesis
- Neglected gradients of mass terms
- Neglected counterbalancing inertial mass fluctuations due to effects other than kinetic energy
- Material properties: modulus of elasticity and masses
- Material properties: piezoelectric and electrostrictive properties
- Material nonlinearity: strain vs. electric field hysteresis

- Material nonlinearity: polarization vs. electric field hysteresis
- Thermal effects
- Fracture mechanics and fatigue, including electromechanical history
- Mach effect inertial mass fluctuations may affect only a portion of the total mass

Upon examination of these possible explanations it is clear that several of the above explanations cannot be responsible for the coupling factor of 10^{-2} needed to match Woodward and Fearn's experimental results. Woodward stated in his book that it was not clear to him where exactly (within the affected masses) the mass fluctuations took place. I conclude that indeed, if the Woodward mass fluctuation propulsion hypothesis is real, the most plausible explanation for the small value of the coupling factor seems to be that the mass fluctuations most significantly take place over a small proportion of the total inertial mass. However, why the coupling factor on the piezoelectric and electrostrictive forces should be 10^{-2} or the coupling factor on the total Mach effect force should be 10^{-6} is unclear, as for example the electron-proton mass ratio is 5.446×10^{-4} .

DISCUSSION

During Rodal's talk, he gives a formula for a static solution to the displacement of the two masses in Jim's Mach Effect device, it has in it the electrostrictive parameter of the lead zirconate titanate, PZT (Steiner & Martins, Inc.'s SM-111, a modified form of PZT-4 or Navy Type I) material in it.

Fearn There are very few references that have the value of the electrostrictive parameter of PZT-4 in them, this equation shows how you can experimentally determine the value for electrostriction for a given stack at a certain temperature and frequency.

Rodal Yes, I only found 3 references that had enough data on experimentally measured values of electrostriction for PZT formulations to ascertain an estimate of the electrostrictive parameter of hard-doped PZT.

Meholic Does the natural frequency change with temperature, so as you run the device would it change natural frequency as it heats up?

Rodal Yes— the natural frequency will decrease with higher temperature (since the stiffness decreases with temperature) and will change with thermal, electrical, and stress-strain history. The PZT material is also very brittle, with very low value of fracture toughness. The scanning electron microscope image I showed reveals the presence of large voids between the grains. Those voids can coalesce and form cracks than can propagate and result first in softening (lower natural frequency), damage and eventual failure of the stack. Pre-compression has to be applied to the stack with bolts in tension, so that the PZT is not exposed to tension, to avoid the crack opening mode.

Hathaway Can you determine theoretically how much torque you need to put on the bolts for optimum thrust ?

Rodal We should not talk about the torque on the bolt but rather the bolt should be tightened based on the stress on the stack. The compression should be performed based on the magnitude of the compressive stress and not on torque level. You need to keep the stress constant, therefore you need to change the force (therefore change the torque) when you change the cross-sectional diameter of the stack. A smaller diameter stack made with the same material and having the same void volume, should use less force (and hence less torque) than a larger diameter stack. Once the optimal pre-compression stress is determined for a given piezoelectric material, all stacks made with the same material and having the same void volume content should be compressed to the same level of stress, which will often mean different levels of torque (depending on dimensions and depending on the void volume content). This is very important to maximize fatigue life. Insisting on blindly applying the same torque to all stacks without measuring the resulting compressive stress and ensuring the same stress is the wrong thing to do: it results in stacks having different stiffness,

hence different natural frequencies, and also in shorter lifetimes of the stacks.

Buldrini *Nembo was not seated near a microphone and the question is hard to hear but the gist of it is the following...* Does the aluminum bracket have any effect on the natural frequency of the stack?

Rodal I took a good look at that. Either by luck or as a result of trial and error, the brackets in use are thin enough so that the stack behaves as a free-free resonant spring with lumped masses attached at its ends, at the resonant frequency, for stiffness purposes, disregarding damping. (However, the rubber pad at the end acts like a damper fixed at one end, and hence it impacts the force measurement). The support is not stiff enough (compared with the stiffness of the stack) to act as a stiff mechanical clamp. The bracket is able to flex and accommodate the natural frequencies of a free-free stack. We actually tested this, we used a piece of very thin aluminum as a bracket so thin it was easy to bend by hand and Heidi was worried it would not support the weight of the stack. Heidi ran one PZT stack with brass tail mass and aluminum head mass on Keith Wanser's SR-780 impedance analyzer with the $\sim 0.72\text{mm}$ thick (2.7 g) aluminum bracket and ten separate runs of the regular $\sim 3.21\text{mm}$ thick (6.8 g) aluminum bracket and all tests gave the same impedance spectrum (José shows a slide of the impedance spectrum with the different brackets showing the same results with both brackets). So we are quite sure that the bracket is effectively decoupling the device from the balance beam, for stiffness purposes, and is not significantly influencing the natural frequency of a free-free stack.

Broyles What were the bolts made of that hold the stack together?

Fearn There are 12 stainless steel bolts. Six 4:40 cap screws attach the brass to the mount bracket and six 2:56 cap screws run through the aluminum end cap on the outside of the PZT stack and enter the threaded brass mass. These hold the stack in place and have heat shrink around them for electrical insulation.

Broyles Stainless steel may not be the best material for the bolts. The heating effect comes from the stack I assume, and that is causing the shift in natural frequency?

Rodal The function of the bolts is to apply an initial compressive stress on the stack, its purpose being to avoid any tension during vibration, because the piezoelectric PZT material is very brittle and it will fail if tension is applied to it or if cracks can grow in crack opening mode. The coefficient of thermal expansion in the thickness direction of the plates of the piezoelectric material used in the MEGA stack PZT-4 (Navy Type I) is negative (the plate shrinks in the thickness direction due to an increase in temperature) during its first heating, particularly as the temperature gets near $100\text{ }^\circ\text{C}$ ($\alpha = -6 \times 10^{-6}$ per $^\circ\text{C}$ at $100\text{ }^\circ\text{C}$). By comparison the coefficient of thermal expansion of metals like stainless steel is positive (it expands with temperature). The coefficient of thermal expansion of stainless steel has a magnitude about 3 times greater ($\alpha = +17 \times 10^{-6}$ per $^\circ\text{C}$). During subsequent heating cycles, the magnitude of the coefficient of thermal expansion of PZT-4 substantially decreases ($\alpha = -1 \times 10^{-6}$ per $^\circ\text{C}$ at $100\text{ }^\circ\text{C}$). This behavior (the fact that the PZT shrinks in the thickness direction, mainly during its first heating) is due to stress relaxation and softening of the PZT-4 material. So you are right, this entails a loss of compressive stress as the PZT-4 is heated. The problem is the thermal history dependence of the properties of PZT-4, particularly its stress relaxation behavior. To substantially ameliorate this behavior, all PZT stacks should be run through a first vibration run, and the compressive stress should be checked once again, and the torque should be re-applied if necessary, after that initial run to accommodate the stress relaxation of PZT-4. This will take care of the stress relaxation as well permanent shakedown (due to vibration) that takes place during initial heating, which is substantial. To accommodate further stress-relaxation, one can use, for example spring fasteners. Heidi has used Belleville springs to accommodate stress-relaxation of the stack. However, in practice, the use of Belleville springs did not result in any significant difference in the natural frequency or the forces measured with the MEGA stack.

Meholic It appears the only cooling, at the moment, is at the ends of the stack, by the brass mass and the aluminum end cap.

Rodal The heating is internally generated inside the volume. Cooling can only be provided through surfaces, hence a priority should be to maximize the amount of surface through which cooling is provided and to minimize the amount of internal volume generating the heat. The surface to volume ratio should be maximized, subject to other constraints (generating maximizing force). Passive cooling, using metal conductors as a heat sink is much more efficient than active cooling. Aside from changing the geometry (for example, instead of just providing heat sinks at the ends, to also provide metal heat sinks inside the stack

and on its exterior cylindrical surface), the materials used need to be re-examined. The present choice of brass for the tail mass is a non-optimal choice. Copper would be a much better choice because copper has 3.5 times higher thermal conductivity and 3.4 times higher thermal diffusivity than brass, at practically the same density. The spot price for copper is about 50 cents per 100 grams (the typical mass of the tail mass in the MEGA drive) while brass sells for about 30 cents for 100 grams, so that the cost of copper (instead of brass) should not be an issue. Silver is even better: it has 3.7 times higher thermal conductivity than brass and 5 times higher thermal diffusivity than brass. What matters is thermal diffusivity because it is the material property governing transient heat transport: it measures the time rate of heat transfer from the hot side to the cold side. Silver sells for about \$60 per 100 grams. Is that unaffordable for the MEGA drive?

More questions were about to be asked ... coffee was being brought in...

Fearn Perhaps we should have a little break (we've just had two back-to-back theory talks) have some coffee and continue the discussion after we all calm down and relax a little ...

Audience laughter – coffee is up next –

APPENDIX D

Mach Effect Propulsion, an Exact Electroelasticity Solution

José J. A. Rodal¹

Rodal Consulting

Research Triangle Park, North Carolina

Mathematical models and numerical results for the Mach Effect Gravitational Assist (MEGA) drive are presented. The MEGA drive is shown to be a Langevin stack where the piezoelectric and electrostrictive effects resulting from an oscillating electric field excitation are used to produce a Mach effect force. An exact electroelasticity solution is obtained for a Langevin (MEGA) piezoelectric/electrostrictive stack. The calculated natural frequency of the Langevin stack compares very well with previously reported MEGA experiments. The calculated direction of the Mach effect force and the optimal tail brass mass are also shown to compare excellently with MEGA experimental data. The reported optimal tail (brass) mass of the MEGA experiments is shown to be an experimental artifact associated with dissipative end fixity. For a MEGA drive free in space there is no optimal mass tail mass, but rather, the Mach effect force increases as a decaying exponential rapidly approaching an asymptotic value for increasing tail mass of the Langevin (MEGA) stack.

CONTENTS

1. Piezoelectricity, the Langevin transducer and PZT
2. The MEGA Langevin stack
3. Variation of inertial mass from Hoyle-Narlikar cosmology
4. The MEGA drive model: 2 unequal masses connected by a viscoelastic piezoelectric/electrostrictive stack
5. The Mach effect force: analysis of input variables
6. The Mach effect force: output analysis
7. Conclusions

1. PIEZOELECTRICITY, THE LANGEVIN TRANSDUCER AND PZT

First, a short history of piezoelectricity, the invention of the Langevin transducer, and lead (Pb) zirconate titanate (PZT):

- 1880: Pierre and Jacques Curie started research at the *École de Physique et Chimie* (nowadays *École supérieure de physique et de chimie industrielles de la ville de Paris*, ESPCI), on crystal electro-elastic properties that led to the discovery of piezoelectricity.
- 1888: Paul Langevin entered ESPCI and helped Pierre Curie with further piezoelectric experiments. Later, he attended Cambridge University and studied in the Cavendish Laboratory under Sir J. J. Thomson. Langevin returned to the Sorbonne and obtained his Ph.D. from Pierre Curie in 1902.

¹ jrodal@alum.mit.edu

- 1905: Langevin, aged 34, became Professor and in 1906 succeeded P. Curie (who died instantly in 1906, aged 46, as a consequence of a road accident) as head of the piezoelectric laboratory at ESPCI.
- 1916, 100 years ago (World War I): invention of piezoelectric stack sonar, P. Langevin and C. Chilowsky awarded 1916 French patent 502,913 and 1917 US Patent 1,471,547 for first ultrasonic submarine detector. It described a sandwich stack of thin quartz crystals, 15 mm long, bonded to steel masses. Resonant frequency: 50 kHz. Time taken by the signal to travel to the enemy submarine and echo back to the ship was used to calculate the distance.
- 1940's: (World War II): discovery of ferroelectricity (demonstrating that it could exist in simple oxide materials, and it was not always associated with hydrogen bonding): barium titanate BaTiO_3 . In 1941, H. Thurnauer and J. Deaderick filed US Patent 2,429,588 for doping studies of BaO and TiO_2 which produced ceramics with enhanced dielectric permittivity. Later, more precise studies by Wainer and Solomon in the USA (1942), Ogawa and Waku (1944) in Japan and Wul and Goldman (1945) in Russia. von Hippel at MIT (USA) published his WWII work demonstrating ferroelectric switching in BaTiO_3 in 1946. US firm Sonotone in 1947 marketed BaTiO_3 phonograph pickups.
- 1950's: 1952: invention of lead zirconate titanate (PZT) $\text{Pb}[\text{Zr}_x\text{Ti}_{1-x}]\text{O}_3$ ($0 \leq x \leq 1$) at Tokyo Institute of Technology by Y. Takagi, G. Shirane and E. Sawaguchi. 1953: E. Sawaguchi published the phase diagram for PZT. 1957: US firm Clevite trademarked the name PZT and developed the formulations for PZT-4, PZT-5, PZT-6, PZT-8, etc. and secured their patents.

Langevin (see Fig. 1 for a photo of Langevin at the 5th Solvay conference) realized that there was a limit as to how thick piezoelectric plates could be made to make effective piezoelectric transducers for underwater acoustic applications (sonar). For this reason, to this date, sonar and ultrasonic-application transducers are often composed of a sandwich stack of piezoelectric plates. The sandwich stack of piezoelectric plates is attached to a tail (or back) mass at the rear, and a head (or front) mass at the front, facing the acoustic medium (for example, water, for a sonar transducer).

The attached masses allow the transducer to match the frequency required for particular applications. (The mechanical natural frequencies of the Langevin stack are dictated by the masses and by the longitudinal stiffness of the stack). This way, the stack is resonant at the desired operating frequency with the mass of the piezoelectric element being a small component of the overall mass. In the original patents by Langevin, the piezoelectric stack is compressed between the two masses by a central bolt, Fig. 3. Other transducers use instead a number of bolts around the outside perimeter of the stack to apply compression. This compressive stress is necessary because the piezoelectric materials often used for these transducers are brittle ceramics formed by a sintering process (the process of compacting ceramic particles and forming a solid mass, by applying pressure and heat, at a temperature below the melting temperature). The resulting ceramic plate is a brittle polycrystalline material, with low fracture toughness, due to the voids created during the forming process and which are present between the sintered ceramic grain boundaries (grains with typical dimensions of 2 micrometers, Fig. 2), that can coalesce into cracks. Therefore these discs easily fracture under low magnitude tensile stress. The purpose of the initial compressive stress on the stack is to ensure that the ceramic discs never experience tension but instead oscillate between greater and lesser levels of compression during ultrasonic vibration. During assembly of the stack under controlled conditions, the bolt(s) is(are) tightened to provide a precise amount of compressive stress (typically 15 to 30 MPa=2,200 to 4,400 psi for hard stacks).

Lead Zirconate Titanate (PZT) is a ceramic that is:

- Ferroelectric: it has spontaneous electric polarization which can be reversed with a large enough electric field.



FIG. 1: Attendees of the 5th Solvay International Conference, *On electron and photons*, Brussels, October 1927, 17 of these 29 participants were or became Nobel Prize winners. (Photo credit: B. Couprie, Institut International de Physique de Solvay)

- Piezoelectric: it displays extremely large (relative to other materials) dielectric and piezoelectric constants when the solution has near equal parts of lead titanate and lead zirconate solution. The piezoelectric PZT plate develops a voltage difference across its two faces when compressed or stretched (with the polarity of the electric field depending on the sign of the strain). This is called the direct piezoelectric effect and it is used for stress or strain sensing applications. This effect is used to measure the dynamic strain, using passive PZT plates, in the Mach effect Langevin stack that has been used in the experiments of Woodward and Fearn at California State University, Fullerton. These passive PZT plates measure the strain through the thickness of the PZT, resulting from the stress transmitted from the other plates in the stack, and hence act essentially as strain gauges. One should be cautious not to interpret the reading from these passive plates as measuring anything but strain, for example as measuring acceleration, because the relationship between the measured strain and the acceleration is very dependent on the equations of motion, specifically the amount of damping and the difference between the excitation frequency and the natural frequency. Scientific piezoelectric accelerometers are restricted to operating at excitation frequencies lower than 3 dB below the first natural frequency (in other words, approximately below $\frac{1}{2}$ of the first natural frequency). This $\frac{1}{2}$ of the first natural frequency limit marks the frequency where the measuring error becomes 30%. If the exciting frequency becomes closer to the natural frequency, the error becomes much larger. The PZT also deforms when an external electric field is applied across its faces in direct linear proportion to the applied electric field. This is called the inverse piezoelectric effect and it is used for actuator applications as in ultrasonic transducers, or as in the active PZT plates in the Mach effect Langevin stack that have been used in the experiments of Woodward and Fearn, to produce the force.
- Electrostrictive: this is a much smaller effect in PZT than the inverse piezoelectric effect. It deforms when an external electric field is applied across its faces, in proportion to the square of the applied electric field. This electrostrictive feature is usually ignored in most PZT applications, but it is essential to produce the Mach effect force in the Langevin stack that has been used in the experiments of Woodward and Fearn.
- Pyroelectric: a PZT plate develops a voltage difference across its two faces when it experiences a temperature change. Therefore, it can be used as a sensor to measure temperature differences.

The above properties have made PZT piezoelectric ceramics the most prominent and useful electroceramics since they were first marketed in 1957 by US firm Clevite, who trademarked the name PZT and developed the formulations for PZT-4, PZT-5, PZT-6, PZT-8, etc., under the scientific leadership of Hans Jaffe (Ph.D. Goettingen, 1934) and Bernard Jaffe [1], and was awarded their patents. The US Navy standardized several of these types of PZT (Navy Types I, II, III, etc., where Navy Type IV is barium titanate instead of lead zirconate titanate) originally developed by Clevite, in a military standard [2]. PZT, besides being brittle, cannot readily withstand contact stresses, wear, high humidity, or aggressive media, therefore a housing is used in many applications. In some Langevin stack designs the metal housing itself (which serves the purpose of protecting the brittle piezoelectric material from fluid attack, etc.) has been used as the pre-stressing spring, instead of using bolts.

For most underwater acoustic applications the front mass usually is made lighter than the back mass, in order to increase the displacement amplitude at the front end, facing the acoustic medium, Fig. 4. For sonar applications the front end is also widened to a larger flat radiation surface at the acoustic end to provide good acoustic matching with the water. The ratio of the back mass to the front mass has a significant effect on the acoustic radiation. The lighter the head mass, compared to the back mass, the greater the velocity of the head mass, and the greater the sonic pressure level generated. In order to decrease the mass of the front mass, the material selected for the head mass should have a low density, while preserving a high ratio of stiffness to mass density, so that the speed of sound in the head mass is relatively high. Aluminum satisfies these conditions and therefore aluminum is commonly used for the head mass.

For applications different than sonar, such as sonochemistry (the application of ultrasound to chemical reactions, using acoustic cavitation) and ultrasonic surgery, ultrasonic cleaning, ultrasonic welding, ultrasonic machining, etc., that require amplification of the displacement amplitude and focusing the oscillatory energy into a spot, the front mass is connected to a long horn (also known as sonotrode, acoustic wave guide, booster, plunger, or ultrasonic probe). Another purpose of the long horn is to prevent tensile stresses on the brittle piezoelectric actuator, resulting for example from dynamic bending moments or dynamic torques at the tip of the horn. These horns can have different cross-sectional profiles in the longitudinal direction: stepped, exponential, conical, catenoidal, or a composite of different profiles. The horn is usually bolted to the front mass. The whole assembly (back mass, stack, front mass and horn) is impedance matched to maximize

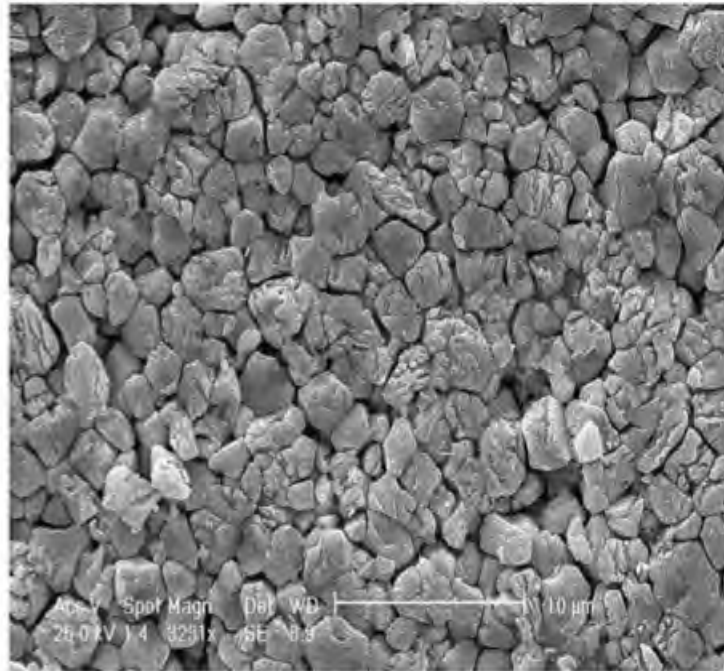


Fig. 2. A typical image of the PZT sample observed by using a scanning electron microscope (Philips XL30), showing that the averaged grain size is about 2 μm and there are many pores in the sintered ceramics. The sample was mechanically polished with 3 μm alumina suspension and then chemically etched with the solution, 50 ml 36.6% HCl acid plus 10 drops of HNO₃ acid, for five minutes at room temperature.

FIG. 2: Scanning electron microscope (SEM) image of lead zirconate titanate (PZT-4, Navy Type I, supplied by Morgan Matroc) grain structure, showing an average grain size of 2 μm and several inter-granular voids. (Image from Fig. 2 of [5])

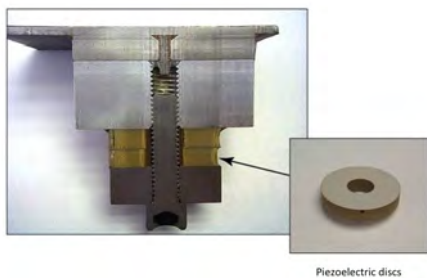


FIG. 3: Langevin Ultrasonic transducer. Piezo disc shown enlarged on the right. (Image from John Fuchs at John's Corner Technical Blog)

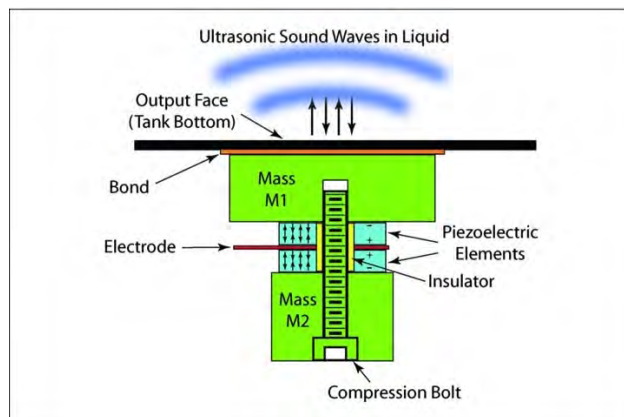


FIG. 4: Langevin Ultrasonic transducer, for underwater acoustic applications. (Image from John Fuchs at John's Corner Technical Blog)

energy transfer to the tip of the horn. The total length of the whole transducer assembly is designed to be

an integer multiple of the half wavelength of vibration.

The tail mass is usually considered the least important part when compared with the head mass and the stack. Its main function is to be a counter mass to the head mass to produce a two-mass (the head and the tail masses), 1-spring (the stack) resonant system. To increase the radiated power and bandwidth of the transducer, the mass of the tail mass should be as large as possible. The back mass, due to being the largest mass, has a major influence on the resonant frequency of the transducer. Hence, the material selected for the tail mass must have a high density to satisfy this need with a reasonable volume, and it must have a high stiffness to have a high speed of sound. Therefore, steel is commonly used as the material for the tail mass. For high frequency designs where the volume needs to be small, tungsten is also used. In most ultrasonic applications, the transducer is driven by a continuous sinusoidal wave source tuned to the first natural frequency of the Langevin transducer. Langevin transducers usually work at a frequency range from 20 kHz to 200 kHz.

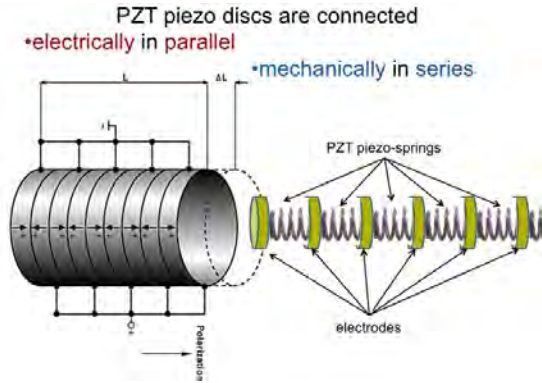


FIG. 5: Langevin piezoelectric stack. Lead zirconate titanate (PZT) discs are connected electrically in parallel and mechanically in series.

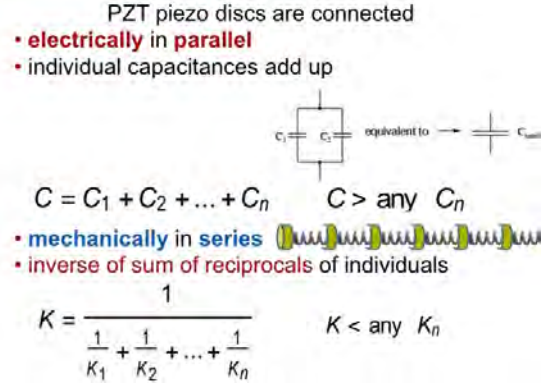


FIG. 6: Capacitors are connected electrically in parallel and springs are connected mechanically in series.

To this date, sonar transducers are often composed of a sandwich stack of piezoelectric discs or plates connected mechanically in series, and electrically in parallel so as to result in the largest displacement for a given level of voltage excitation, Figs. 5 and 6. The piezoelectric plates are placed so that their positively poled faces contact a positive electrode. The negatively poled faces of the plates, including the front and the back masses, are at negative or ground potential and complete the circuit of the piezoelectric stack. The faces of the piezoelectric ceramic elements are sometimes coated with a conductive material (like silver) to enhance this electrical connection to the electrodes. Each piezoelectric plate in the Langevin stack can be idealized as behaving like a spring in the thickness direction of the piezoelectric plate. The stress in the longitudinal direction at the interface of each piezoelectric plate with the electrode and the next piezoelectric plate in the sandwich construction of the stack has to satisfy stress continuity. This means that if the cross-sectional areas of the piezoelectric plates are identical, the transmitted force must be continuous. It is simple to show that if the force is continuous, this implies that the springs representing each piezoelectric plate are connected in series. The effective stiffness of the stack is the inverse of the sum of the reciprocals of the individual stiffness of each piezoelectric plate in the stack. This means that the larger the number of piezoelectric plates, the longer the stack, the lower the effective stiffness of the stack. The simplest equivalent circuit representation of each piezoelectric plate is a capacitor in parallel with a resonant circuit composed of another capacitor, an inductor and a resistance in series. As Monkman et.al. state in page 92 of [6], piezoelectric actuators are basically capacitive elements; this means that current only flows during the charging process (while the actuator is providing motion) and so long as leakage currents and losses can be kept small, force is maintained at the end of the stroke without the need of supplying additional energy. Since the piezoelectric plates are connected electrically in parallel, this means that each of these equivalent circuits is connected in the stack in parallel. Capacitances in parallel add up, therefore the Langevin stack results in an actuator which provides a motion that is a multiple of the number of piezoelectric plate capacitances in the Langevin stack, but whose stiffness decreases as the inverse of the sum of the reciprocals of the individual stiffness of each piezoelectric plate in the stack. Hence if the design goal is to amplify the displacement, the number of plates in the Langevin stack should be maximized while, if the goal is to have the highest stiffness and highest natural frequency, then the lower the number of piezoelectric plates the better, Fig. 6.

Comparing a Langevin piezoelectric stack made with hard PZT piezoelectric plates with an electromagnetic

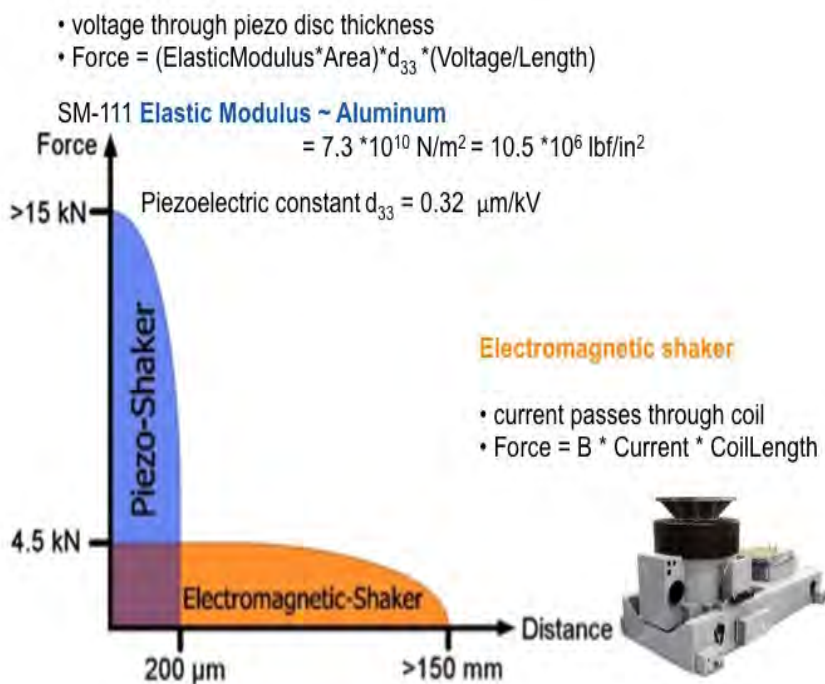


FIG. 7: Piezoelectric Shaker compared with Electromagnetic Shaker. (Images from Piezosystem Jena and from Thermotron Electromagnetic Shakers)

shaker, one notices a significant difference between them. An electromagnetic shaker, Fig. 7, provides a much larger displacement than a hard PZT Langevin stack, but a significantly smaller force. This is because the force provided by the electromagnetic shaker is effectively given by the magnetic field times the current times the coil length. On the other hand the hard PZT Langevin stack provides a much greater force with a much smaller displacement. This is because the hard PZT Langevin stack's force is proportional to the modulus of elasticity of the hard PZT (which is close to the modulus of elasticity of aluminum) times the cross-sectional area of the PZT plates, times the piezoelectric coefficient in the longitudinal direction of the stack, times the electric field (applied voltage to each piezoelectric plate in the stack divided by the thickness of the piezoelectric plate). The force provided by the PZT Langevin stack can be much greater than that of an electromagnetic shaker because it relies on the high modulus of elasticity of the PZT. This is the reason why electromagnetic shakers have to be made very large, much larger than the cross-sectional area of Langevin stacks, to provide similar forces. On the other hand, the piezoelectric stack provides a much smaller displacement because the piezoelectric strain effect in a piezoelectric material like hard PZT is very small (less than 200 micrometer displacement for a typical stack), particularly when compared to an electromagnetic shaker (typically over 100 mm). As Monkman et.al. state in page 92 of [6], piezoelectric actuators are basically capacitive elements whose force is maintained at the end of the stroke without the need of supplying additional energy (ignoring losses), and this is in complete contrast with electromagnetically driven actuators like electromagnetic shakers, where energy must continue to be supplied if the full actuator force is to be maintained.

Lead zirconate titanate (PZT) is the ferroelectric material used in the Langevin ultrasonic transducers tested for the Mach effect in the MEGA (Mach effect Gravity Assist) drive, Figs. 8 and 9. The chemical formula of PZT is $\text{Pb}[\text{Zr}_x\text{Ti}_{1-x}]\text{O}_3$ (where x is the mole fraction, with possible range $0 \leq x \leq 1$; and best properties typically $0.47 \leq x \leq 0.52$). The piezoelectric properties of PZT ceramics are a result of their molecular structure. The largest piezoelectric effects are observed when the mole fraction of titanium (Ti) and zirconium (Zr) are close to 0.5, in the transitional region between the tetragonal and rhombohedral perovskite crystal phases (perovskite: a type of crystal structure like the one in calcium titanium oxide (CaTiO_3), ${}^X\text{II}A^{2+} {}^V\text{IB}^{4+} X_3^{2-}$ where A and B are two cations (a positively charged ion), with A atoms larger than B atoms, and where X is an anion (a negatively charged ion) that bonds them, with the oxygen anion in the face centers). In the transitional area between the tetragonal and rhombohedral phases there

is a significant polarization variation. (A crystalline structure is polarized if the average position of all of its positive ions is not the same as the average position of all of its negative ions.) This transitional area is called the morphotropic phase boundary (MPB). Examining the phase diagram, Figs. 8 and 9, it is apparent that multiple crystalline structures can exist near this boundary.

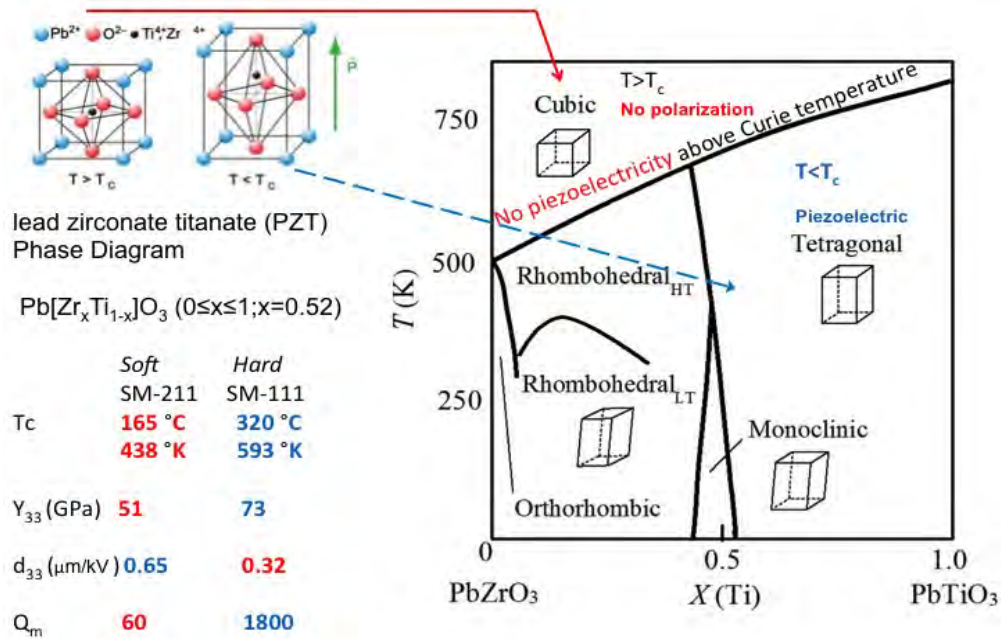


FIG. 8: Phase diagram and properties of lead zirconate titanate (PZT). (Background phase diagram from Fig. 1 of Shindo et.al. [3])

The Curie temperature (T_c) for a ferroelectric material is defined as the transition temperature such that the material is ferroelectric below T_c and dielectric above T_c . Materials in their ferroelectric state (below T_c) are piezoelectric: they have a spontaneous electric polarization as their structures are unsymmetrical. In the ferroelectric state the spontaneous polarization can be reversed by a suitably strong applied electric field in the opposite direction; the polarization is therefore dependent not only on the current electric field but also on its history, yielding a hysteresis loop (when plotting polarization versus electric field). Above T_c , the material's spontaneous electric polarization changes to induced electric polarization. Above T_c the material is in a dielectric state and therefore it has no electric polarization in the absence of an applied electric field. The electric dipoles are unaligned and have no net polarization. Electric susceptibility only occurs above T_c . Above T_c the structure has cubic symmetry: the crystal structure is centrosymmetric and hence there is no dipole moment. In perovskite structures the dipole is created by movement of the central ion in the crystal structure. Below T_c the central ion moves out of the centrosymmetric location and so the charges no longer balance and this results in a net dipole. Once the temperature drops below T_c , the crystal structure becomes tetragonal or rhombohedral resulting in an electric dipole moment. These non-cubic structures have over 14 stable domain configurations at the MPB giving them great flexibility during polarization. The region of the MPB near the T_c favors enhancement of the longitudinal piezoelectric coefficient and longitudinal susceptibility.

Materials in their ferroelectric state (below T_c) can be forced to have their dipoles aligned in a particular direction by a process called poling. The poling process involves aligning the individual dipole moments, so that they point in the same general direction. This is accomplished by exposing the crystal to a constant electric field in the desired direction. Under the electric field, dipoles that are not parallel to the electric field lines experience a torque, and so they are turned to the same direction as the electric field. When the electric field is removed from the material in the ferroelectric state (below T_c), the dipoles remain fairly aligned, and the material is said to be "poled" in that direction. Poling usually is done by heating the material above the T_c , applying the electric field, cooling below the T_c , and finally halting the electric field. The result is

a “remanent” polarization as well as a permanent deformation. The piezoelectricity is maintained as long as the material is not de-poled, which can happen for example if the material is exposed to a temperature above T_c , or to an extreme electric field or to high stress conditions. For example, later exposure to a high magnitude electric field causes polarization reversal, leading to the hysteresis loop shown by ferroelectrics.

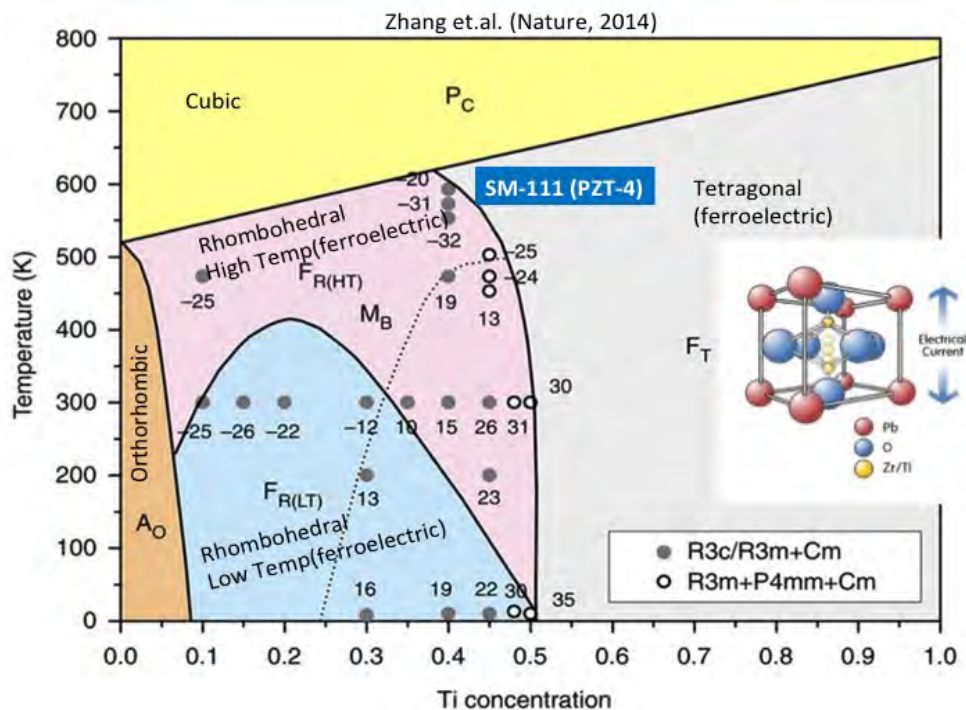


FIG. 9: Phase diagram of lead zirconate titanate (PZT) (Background image from Fig. 7 of Zhang et.al. [4]).

The perovskite structure is very tolerant to element substitution (doping) – therefore the terms “hard doped” and “soft doped” are frequently used. Even small amounts of a dopant ($\sim 1\%$) may cause large changes in the material properties. Most types of piezoelectric ceramic materials, including PZT, are supplied as doped materials, and can be differentiated based on whether they are “hard doped” or “soft doped,” or simply “hard” and “soft” for short. Ferroelectric ceramics like PZT are usually “hard” doped with acceptors, which create oxygen (anion) vacancies, or “soft” doped with donors, which create metal (cation) vacancies and facilitate domain wall motion in the material. Acceptor “hard” doping results in hard PZT while donor “soft” doping results in soft PZT. In general, soft PZT has a higher piezoelectric constant, but larger internal losses, and greater material damping (low quality of resonance Q_m) due to internal friction. Donor dopants are usually lanthanum (La), niobium (Nb), antimony (Sb) or tungsten (W), and are incorporated at a lattice site of lower valency. They increase the dielectric constant (relative electric permittivity up to 3,000), and increase the coupling constant (up to 0.7), but also increase electrical and mechanical losses (decrease the mechanical quality factor of resonance Q_m).

In hard PZT, domain wall motion is pinned by the impurities thereby lowering the losses in the material (increasing quality of resonance Q_m), but this is usually at the expense of a reduced piezoelectric constant. Hard doping ions are usually from the group of transition metals like iron (Fe), manganese (Mn), nickel (Ni) and cobalt (Co), and are incorporated at a lattice site of higher valency. They reduce the dielectric constant, the coupling factor, and reduce the damping (they raise the quality factor of resonance Q_m), while improving aging properties. They also increase the stability of the ceramic with respect to electrical or mechanical (stress) de-polarization. The best performing piezoelectric material used up to now in Mach effect experiments has been a hard doped proprietary modified form of PZT-4 (Navy Type I) ceramic, having the supplier’s (Steiner & Martins) trade name “SM-111.” Another material from the supplier Steiner & Martins with trade name “SM-211” was tried, with awful results. From the properties given by the supplier one can ascertain that SM-211 is a soft ferroelectric ceramic. Comparing these:

TABLE I: Table of Hard/Soft PZT material properties.

Material PZT type	Steiner & Martins designation	T_c		Y_{33} (GPa)	d_{33} ($\mu\text{m}/\text{kV}$)	Q_m
		$^{\circ}\text{C}$	K			
Hard	SM-111	320	593	73	0.32	1800
Soft	SM-211	165	438	51	0.65	60

It is clear that the hard PZT has much higher mechanical quality factor of resonance (Q_m), higher Curie temperature (T_c), and higher stiffness (Y_{33}), while the soft material's only redeeming value is a higher value of the piezoelectric coefficient (d_{33}). It is not surprising that the hard PZT gave much higher Mach effect force, due to its much higher quality factor of resonance (Q_m) and higher stiffness (Y_{33}), that more than compensate for the lower value of the piezoelectric coefficient (d_{33}). Also the lower value of T_c for soft PZT is an issue for the application because the PZT gets hotter as it vibrates, and the quality factor of resonance (Q_m) degrades as the temperature gets closer to T_c .

2. THE MEGA LANGEVIN STACK

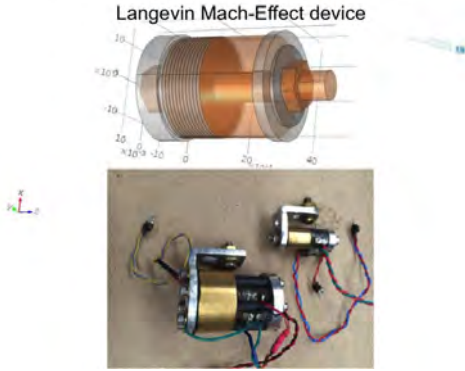


FIG. 10: Top: Drawing of Mach effect device with central bolt as per original Langevin transducer design, Bottom: two different sizes of Mach effect (MEGA) drives shown using a Langevin transducer design. The smaller one has a central bolt, the larger uses 6 concentric bolts equally spaced around the periphery.

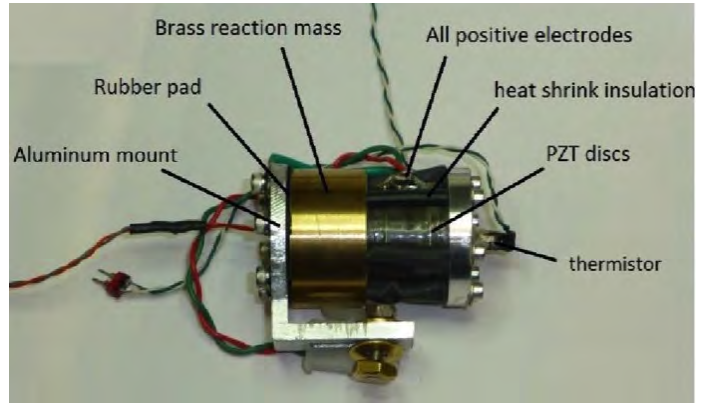


FIG. 11: Parts of the MEGA (Mach effect Gravitational Assist) drive stack: a Langevin transducer, namely, from right to left: aluminum head mass, PZT stack, brass tail mass, and supported by an aluminum bracket at its tail end.

Looking at the images, Figs. 10 and 11, for the MEGA (Mach effect Gravitational Assist) drive stack, one can see that it is a typical Langevin stack, very similar to the typical Langevin transducers that have been used for decades in many applications: with a small aluminum head mass, a stack of PZT-4 (US Navy Type I) plates, and a tail mass made of brass (instead of more common choices like steel or tungsten) reportedly because it was desired to provide a heat sink for thermal diffusion of heat generated by dissipation in the PZT stack during vibration. It would be better to use a copper tail mass instead of brass for this purpose since copper has 3.5 times thermal conductivity of brass, with practically the same density, as shown in Table 2.

Also of great importance, for the MEGA stack vibrating during tests at the resonant frequency of the stack (typically between 20 to 100 kHz, depending on the length of the stack), what matters for the duration of typical experimental MEGA tests are the material properties governing transient heat conduction: the unsteady state of heat transfer. The material properties involved are: thermal conductivity divided by the heat capacity per unit volume (the product of the heat capacity per unit mass times the mass density), this property is called thermal diffusivity. The thermal diffusivity measures the time rate of heat transfer from

the hotter side to the colder side. The higher thermal diffusivity, the faster that heat moves through the material, essentially because the material conducts heat quickly relative to its heat capacity per unit volume. If two materials have the same thermal conductivity, the material with lowest value of heat capacity per unit volume will have the highest thermal diffusivity, because it will transport heat faster in the unsteady state of heat transfer. It is obvious from Table 2, that the present choice of brass for the tail mass is not optimal. All the other materials in Table 2 (including tungsten, which has 2.2 times the mass density) have higher thermal diffusivity. Among this group of metals, silver has the highest thermal conductivity and thermal diffusivity. Copper has 3.4 times greater thermal diffusivity than brass. Hence copper has 3.5 times thermal conductivity and 3.4 times thermal diffusivity of brass and it would make a better choice for tail mass of the MEGA drive to conduct and thermally diffuse the heat generated in the PZT stack, at practically the same mass density. Concerning cost, as of this writing (November 2016) the spot price for silver is 59 US dollars per 100 grams, while copper sells for approximately fifty cents: 0.49 US dollars per 100 grams, and brass sells for 0.29 US dollars per 100 grams.

TABLE II: Table of thermal properties of a few possible metals to use for end mass for the MEGA drive compared with piezoelectric PZT, Butyl rubber pad and epoxy adhesive, properties at room temperature

Material	Density kg/m ³	Heat Cap. J/(kg K)	Therm. Cond. W/(m K)	Therm. Diff. m ² /s
PZT-5	7650	350	1.3	0.049×10^{-5}
Unfilled epoxy Bisphenol A	1150	1100	0.17	0.013×10^{-5}
Unfilled Butyl rubber (IIR) pad	920	1950	0.13	0.0072×10^{-5}
Aluminum	2700	900	205	8.44×10^{-5}
Brass	8730	380	109	3.29×10^{-5}
Copper	8960	386	385	11.13×10^{-5}
Gold	19320	126	314	12.90×10^{-5}
Silver	10490	233	406	16.61×10^{-5}
Tungsten	19250	134	173	6.71×10^{-5}

Since the tail mass used for the MEGA drives is only about 100 grams, the cost of copper should not be an issue. Also, there are no experimental concerns with copper’s magnetic properties as compared to brass, since the relative magnetic permeability of copper is closer to 1, the value for free space. Copper is slightly diamagnetic, with relative magnetic permeability of 0.999994, compared to high tensile brass CZ114 or HT1 with a relative magnetic permeability of 1.05 (a value higher than several types of stainless steels). From the values shown in Table 2 it is evident that the present choice of aluminum for the head mass is an ideal choice to fulfill the requirement of low mass density, high thermal conductivity, high thermal diffusivity, and speed of sound typical of metals. Fearn et.al. on page 1512 of [9] write “The temperature of the aluminum cap is seen to rise much faster than the brass mass which is also slower to cool,” and on page 1513, they write “the temperature rise in the aluminum is on the order of 18 degrees Celsius and that of the brass mass is about 8 degrees,” Figs. 12 and 13. This information is consistent with thermal diffusivity of aluminum being 2.56 times higher than thermal diffusivity of brass, and therefore shows that it would be better to use copper or (preferably silver) for the back mass, to rapidly diffuse the temperature internally generated in the piezoelectric stack, instead of the present choice of brass, which has lower thermal diffusivity.

On page 111 of his book [57], Woodward states: “In this case, since vibration getting to the suspension was a background concern, thin rubber pads were added to the system between the brass reaction masses and aluminum mounting brackets.” In a private communication, James Woodward stated that the rubber pad thickness is $\frac{1}{16}$ of an inch (1.59 mm) and that the rubber came from a tire’s inner tube. The standard type of rubber used for inner tubes is butyl rubber, a synthetic rubber, copolymer of isobutylene with isoprene, with a common technical abbreviation: IIR, which stands for isobutylene isoprene rubber. As shown on Table 2, the thermal conductivity and thermal diffusivity of butyl rubber is very low, so this rubber pad acts as a thermal insulator between the tail (brass) mass and the aluminum mounting bracket.

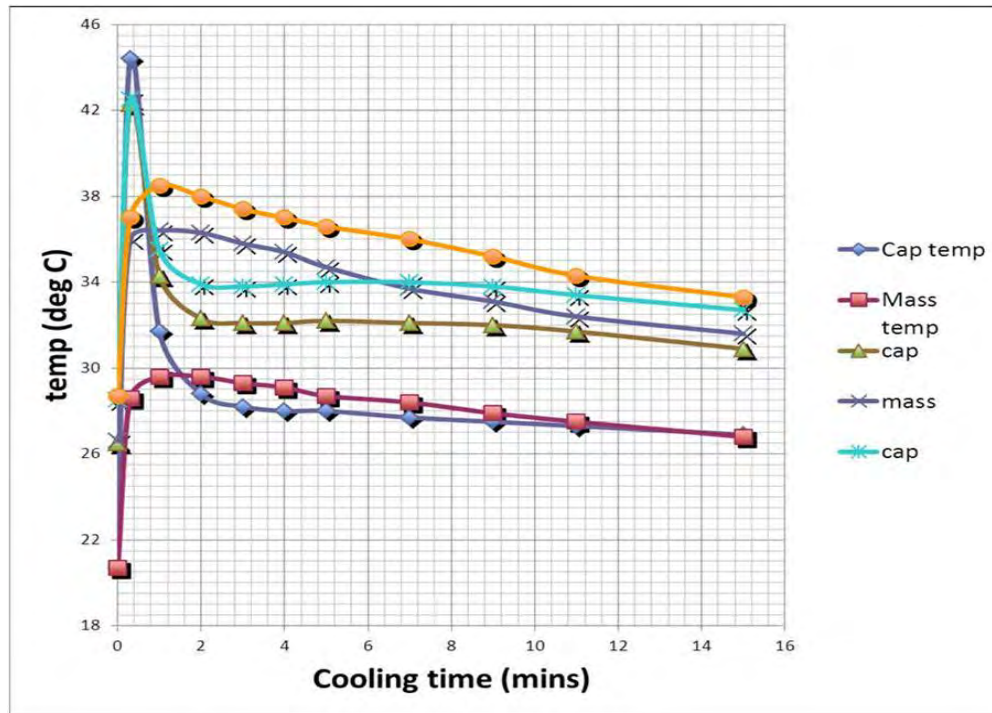


FIG. 12: Temperature ($^{\circ}\text{C}$) vs. time (min) for a MEGA stack experiment by Fearn and Woodward, during a typical 14 second run, at different locations in the front aluminum mass (star-turquoise, diamond-dark-blue and triangle-green-brown) and tail brass mass (square-red, x-gray and circle-orange), from Fig. 4 of [9].

In the MEGA drive, the Langevin PZT stack is excited by the converse piezoelectric effect where an electric field (an applied voltage difference across the thickness of each PZT plate) induces mechanical strains (under free-ends boundary conditions) or an applied stress (under mechanical constraints, or under dynamic conditions). The direct piezoelectric effect, where the piezoelectric material (PZT) responds to strain by generating an electric voltage, is used in one or more pairs of passive 0.3 mm thick piezoelectric plates in the MEGA drive Langevin stack, for the purpose of dynamic strain measurements.

These passive PZT plates measure the strain, through the thickness of the PZT, resulting from the stress transmitted from the other plates in the stack. They act essentially as strain gauges. One should not interpret the reading from these passive plates as measuring anything but strain, for example as measuring acceleration, particularly for the case of this MEGA Langevin stack operating at an excitation frequency very close to the first natural frequency of the Langevin stack. An accelerometer should be operated, as a measuring instrument, in the so-called flat response region of vibration response (p.58 of Den Hartog [10], p.80 of Scanlan and Rosenbaum [11], and p.62 of Clough and Penzien [12]). Scientific piezoelectric accelerometers are restricted to operating at excitation frequencies lower than 3 dB below the first natural frequency of the vibrating system defining the accelerometer (in other words, approximately below $\frac{1}{2}$ of the first natural frequency).

The first natural frequency of the vibrating system is dictated, of course, by the stiffness and masses composing the accelerometer vibrating system. In the case of the MEGA Langevin stack under free-free conditions, this natural frequency is dictated by both end masses (in Fearn and Woodward's experiments: the front aluminum mass and the back brass mass), the mass of the PZT stack and the stiffness of the PZT stack between the end masses. This limit, restricting the excitation frequency to be below $0.5f_o$, $\frac{1}{2}$ of the first natural frequency, marks the frequency where the measuring error becomes 30%. (At approximately $0.3f_o$, $\frac{1}{3}$ of the first natural frequency, the error is 10%, while at approximately $0.2f_o$, $\frac{1}{5}$ of the first natural frequency, the error is 5%). If the exciting frequency becomes closer to the natural frequency, the error becomes much larger (the measured strain becomes unrepresentative of the acceleration, due to the fact that close to the natural frequency the damping term in the equations of motion starts to dominate the amplitude of the response). For the MEGA drive experiments, Fearn and Woodward purposefully operate the stack at an

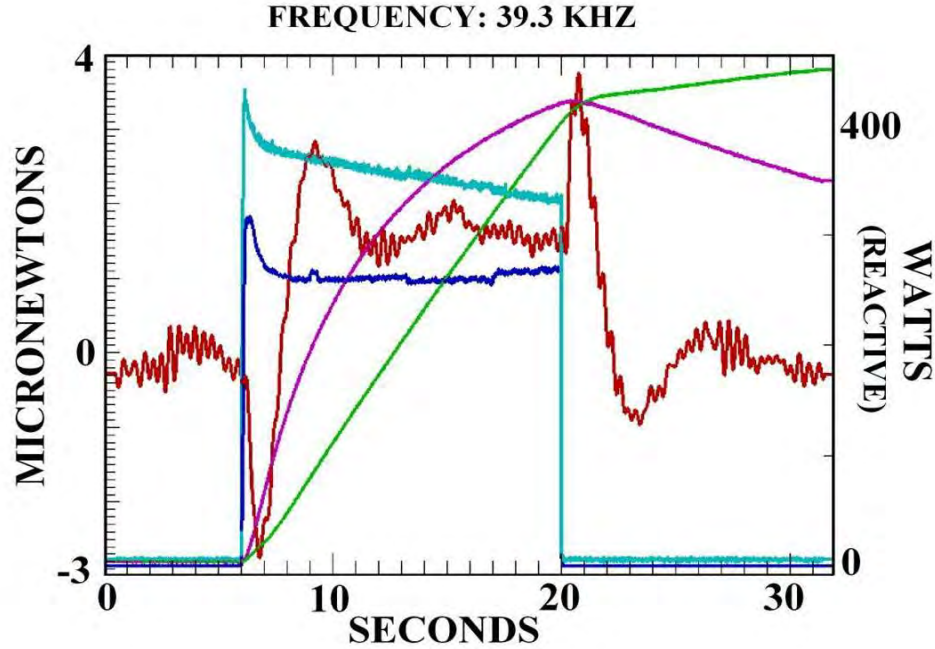


FIG. 13: Force (μN , left vertical) vs. time (sec, bottom horizontal), power (W, right vertical) vs. time (sec) and temperature (not scaled) vs. time (sec) for a MEGA experiment. Power duration: 14 sec. Excitation frequency: 39.3 kHz (labeled at the top, the upper horizontal axis is not a frequency scale). Force is indicated with a red trace and power with a dark blue trace. Positive force is directed from the aluminum mass towards the brass mass.

Negative force is directed from the brass mass towards the aluminum mass. After the transient (with initial negative peak towards aluminum mass, followed by positive peak towards brass mass) there is a fairly steady force with a magnitude of $2 \mu\text{N}$ towards the brass mass. This is followed by another transient (first peaking positively towards the brass mass and then negatively towards the aluminum mass). The turquoise trace (labeled in [9] as accelerometer) is from the passive PZT plates that measure strain through their thickness (not acceleration, since the excitation frequency is very close to the natural frequency) and it is not scaled. The green trace is the temperature from thermistor embedded in the back brass mass, while the magenta trace is from thermistor in the front aluminum mass. Temperatures are not to scale, but Fearn et.al. write that “the temperature rise in the aluminum is in the order of 18 deg C, and that of the brass mass is 8 deg C.” Image from Fig. 3 of [9].

excitation frequency closer than $\frac{0.75}{Q_m}$ to the natural frequency of the Langevin stack (which has a mechanical-quality-factor-of-resonance (Q_m) equal to 190). Therefore, for the MEGA drive experiments conducted by Fearn and Woodward, the output of the passive PZT plates is unrepresentative of the acceleration, and instead should be interpreted strictly as representing solely the strain through the thickness of the PZT plate.

The PZT presently used for the MEGA drive is supplied by Steiner & Martins Inc. with trade name SM-111, which is a modified PZT-4 (US Navy Type I). It is shaped like a thin circular plate (disc), of 19 mm diameter. The piezoelectric PZT-4 disc is electrically poled through the thickness and it has a silver coating on the surfaces. Stacks have been constructed with 8 discs 2 mm thick and other stacks with 16 discs 1 mm thick. The electrodes are made of brass of the same diameter, 0.05 mm thick, and with holes in them, for the adhesive to penetrate through. The adhesive is a low viscosity liquid bisphenol A based epoxy containing n-butyl glycidil ether. It is supplied by E. V. Roberts with trade name Hexion Epon resin 815C and it is cured with E. V. Roberts Versamid 140 (presently named RF61 Epoxy curing agent), which is a polyamide resin based on dimerized fatty acid and polyamines. The brass electrodes are sanded before applying the adhesive. The stack is compressed under bolt tension and then cured in an oven for 1 hour at 120°C . Therefore the glass transition temperature (T_g) of the epoxy adhesive used to adhere the electrodes to the piezoelectric material is significantly lower than the Curie temperature (T_c) of the piezoelectric material (320°C for SM-111 PZT-4). Therefore the glass transition temperature of the adhesive used for present MEGA drive experiments constitutes a lower threshold for the piezoelectric integrity of the MEGA drive.

Instead of using an unfilled epoxy as in the present MEGA stack, it would be better to use a filled adhesive, for several reasons, including increasing thermal conductivity (Table 3) and possibly increasing the electrical conductivity. Also a filled epoxy will have a reduced coefficient of thermal expansion, more compatible with the coefficients of thermal expansion of the electrodes and the piezoelectric plates. Also a polymer adhesive filled with inorganic fillers will have a higher modulus of elasticity closer in stiffness to the stiffness of the electrodes and the piezoelectric plates. Also filled adhesives are stronger, particularly regarding important properties like shear strength, and their properties with respect to temperature drop less precipitously than unfilled adhesives. The thermal conductivity of the unfilled Epon epoxy used for the MEGA stack is only 0.17 W/(mK), which is only 0.04% of thermal conductivity of copper and only 0.08% of thermal conductivity of aluminum, and 11% to 16% of thermal conductivity of PZT, hence the unfilled epoxy adhesive acts as a thermal insulator between the PZT and the copper (or brass). To improve thermal conductivity of the adhesive, fillers like Aluminum Nitride and Boron Nitride are known to raise thermal conductivity to 1.4 to 1.7 W/(mK), depending on the size of the filler and filler content. Therefore, an epoxy filled with Aluminum Nitride or Boron Nitride would match thermal conductivity of PZT, instead of acting as a thermal insulator. Other possible choices are to use an adhesive with higher glass transition temperature. For example Creative Materials 124-41 is a polyimide adhesive with a glass transition temperature exceeding 250 °C. Such an adhesive would provide an upper temperature limit more commensurate with the Curie temperature of SM-111. Also this adhesive is claimed to have a thermal conductivity of 11 W/(mK), which is 69 times more conductive than the presently used unfilled epoxy. Adhesives using micronized silver are claimed to have a thermal conductivity exceeding 7.5 W/(mK), almost 50 times thermal conductivity of the unfilled epoxy presently used for the MEGA drive, such silver-filled adhesives would also have significantly greater electrical conductivity.

TABLE III: Table of thermal conductivity of unfilled and filled adhesives at room temperature, compared with piezoelectric PZT and different metal electrode materials (present MEGA drive experiments use brass electrodes)

Material	Thermal Conductivity (W/(m K))
Brass	109
Copper	385
Silver	406
PZT-5	1.3
Unfilled epoxy Bisphenol A	0.17
Aluminum Nitride filled epoxy	1.4 to 1.7
Boron Nitride filled epoxy	1.4 to 1.7
Silver filled epoxy	7.5
Creative Materials 124-41 polyimide	11

The adhesive method of making a piezoelectric stack has a number of disadvantages due to the properties of the adhesive. For example, the adhesive used for the MEGA stack is more than an order of magnitude more compliant than the piezoelectric material, so it lowers the stiffness of the stack. The adhesive used for the MEGA drive is also not electrically or thermally conductive, therefore it acts as a thermal and as an electrical insulator, which is detrimental to the functioning of the stack. Also the adhesive used for the MEGA drive has low fracture toughness, and due to the abrupt change in stiffness between the adhesive and the electrode and the piezoelectric materials being adhered to, it is a source of delamination for fracture mechanics and fatigue. Furthermore, the coefficient of thermal expansion for the adhesive is considerably larger than the coefficient of thermal expansion of the electrodes and of the piezoelectric material, which introduces thermal stresses upon changes in temperature. Finally, the glass transition temperature (T_g) of the adhesive is considerably lower than the Curie temperature (T_c) of the piezoelectric material. This results in a lower upper temperature that the piezoelectric stack can be operated at without losing its integrity. Besides the old fabrication method used for the MEGA drive of stacking (laminating) a plurality of piezoelectric plates by adhering them to the sandwiched electrodes, there is a newer fabrication method called co-sintering. In co-sintering, layers of molded sheets (green sheets) containing an organic binder of piezoelectric ceramic are stacked before sintering and layers of electrodes are sandwiched in between them before sintering, thermally pressing them into an incorporated form, and sintering the whole stack together.

This newer fabrication method can fabricate a compact and higher-performance stack (laminate) element, because the piezoelectric ceramic layers can be formed thinner and because thermal press can obviate a need for use of the adhesive. However, the co-sintering fabrication process becomes technically more complex, since residual stresses between the ceramic and the electrodes have to be considered, and hence the thickness of the electrode is a major consideration in this process. The thickness of the electrode needs to be considered, as well as the thickness and stiffness of the piezoelectric ceramic layers, and the sintering temperature. In US Patent 6114798 by Maruyama et.al [13] the authors discuss such a con-sintering process and state that electrodes thicker than 5 micrometers (0.003 to 0.005 mm), or 10% of the thickness of the electrodes used in the MEGA drive, decrease the value of the quality factor of mechanical resonance Q_m . Based on experiments with piezoelectric stacks made with piezoelectric ceramics having a quality factor of mechanical resonance Q_m value of 1200, the authors conclude that the thickness of the electrode should desirably be as thin as possible within the scope of where electrical conduction can be assured. The authors found best results with higher values of Q_m , between 1400 and 2000, and concluded that $Q_m = 2000$ is the limit value of Q_m for materials available at that time. This is still the case nowadays (2016), as $Q_m = 2000$ is about the upper limit for presently available piezoelectric ceramics. In a later patent [14] Maruyama et.al state that when the electrode thickness is 2 to 3 micrometers (0.002 to 0.003 mm), the current abruptly generated after the start of the polarization process generates sparks that can lead to crack formation in the piezoelectric material. They conclude that the electrode thickness should optimally be 4 to 6 micrometers (0.004 to 0.005 mm) or about 10% of the thickness of the electrodes used in the MEGA drive, because electrodes thinner than that generate sparks.

Fearn et.al. [9] state that six (unified thread standard 4-40) stainless-steel bolts are used between the front aluminum mass and the back brass mass to compress the Langevin piezoelectric stack. The choice of stainless-steel material for these bolts is not optimal, because it is known that the piezoelectric material used for the plates in the MEGA stack for the experiments of Fearn and Woodward, a modified form of PZT-4 (Navy Type I) has a much smaller coefficient of thermal expansion than stainless-steel. For example, Morgan Technical Ceramics (page 8 of [15]) states that the coefficient of thermal expansion in the thickness direction for poled PZT4D is $-0.1 \times 10^{-6} \frac{1}{K}$ in the first heat and $+1.7 \times 10^{-6} \frac{1}{K}$ in subsequent heating, both at 50 °C, and $-6 \times 10^{-6} \frac{1}{K}$ in the first heat and $-1 \times 10^{-6} \frac{1}{K}$ in subsequent heating, both at 100 °C. (The negative sign meaning that PZT4 contracts in the thickness direction upon an increase in temperature). This compares with a coefficient of thermal expansion of $+16.9 \times 10^{-6} \frac{1}{K}$ between 0 °C and 100 °C for stainless steel 304. Therefore, as the MEGA Langevin stack gets heated by internal damping as a result of vibration in the experiments by Fearn and Woodward, the PZT plates will slightly contract, particularly if their temperature exceeds 50 °C, while the stainless steel bolts will expand as a result of the increase in temperature. (Obviously thermal expansion of the brass and aluminum masses located at the ends of the Langevin stack is immaterial to this issue because it is well-known that the stress in the bolt acts between its boundary conditions, which are mainly governed by the first thread the bolt is in contact with. Hence it is the free length of the bolts that matters in this consideration, and thermal expansion of the aluminum and brass mass is immaterial to this). Hence a significant portion of the initial compression may be lost due to internal heat generated from damping during vibration. Thus, the use of stainless-steel bolts is particularly detrimental to their purpose which is to compress the stack. As a significant portion of the compressive stress may be decreased, this will translate into damage to the stack, with a concomitant decrease in modulus of elasticity, hence a decrease in stiffness, and therefore a decrease in the natural frequency of the stack, leading to de-tuning of the MEGA stack as a result of the natural frequency getting away from the excitation frequency. Furthermore this will lead to fatigue damage to the piezoelectric plates as a result of this decrease in compression because of thermal expansion mismatch between the bolts and the PZT plates, and a shortening of the life of the PZT plates. Therefore, it would be a better choice to use bolts with a very small coefficient of thermal expansion, for example invar bolts. For example, Nabeya Bi-tech Kaisha (NBK) [16] supplies hex socket head cap screws with size M3 equivalent to 4-40 bolts, made of super invar with a thermal expansion coefficient of $+0.69 \times 10^{-6} \frac{1}{K}$, a thermal expansion coefficient which is 25 times smaller than the one of stainless steel.

The location of the maximum stress and strain in the PZT stack is a function of the mass distribution in the stack and the boundary conditions. For example, for a symmetric mass distribution, with free-free boundary conditions at the ends, the vibration displacement amplitudes at the two ends are the same, and the vibration displacement node is at the middle of the stack, therefore the maximum stress and strain, and strain energy are located at the middle of the stack. Since internal heat generation is proportional to the strain energy, the resulting heat generation and temperature will also be maximum at the middle of the stack for a symmetric transducer with symmetric, free-free boundary conditions. For piezoelectric materials like PZT it is advisable to limit the amount of stress and strain (because of fracture mechanics and fatigue considerations) and therefore (if no other more important consideration is at play) it is advisable to have a

mass distribution that minimizes the maximum stress and strain in the stack. It must also be taken into account that in order to protect the brittle PZT it is advisable not to have the PZT exposed at the end. Therefore many applications have the PZT stack placed near one end, usually around one quarter of the total length of the Langevin transducer (including the length of the end masses).

A more sophisticated (and complicated) approach is to design a transducer that incorporates more than one mode shape, using several piezoelectric stacks instead of just one, with metal masses in between the stacks. One such design is to use two piezoelectric stacks at different positions within the same transducer, independently excited at two different frequencies. The analysis of such stacks is complicated because (deliberately by design or not) such complicated distribution of the piezoelectric materials may excite unwanted bending modes of vibration as well as the desired longitudinal modes of vibration. Bending modes of vibration are particularly harmful because bending involves tension in one of the surfaces of the bent shape, and as previously discussed, tension should be avoided for brittle ceramics like PZT.

To conclude this section, the present design of the MEGA drive could be improved, as it is essentially similar to Langevin's transducer design of 100 years ago. The present choice of brass for the tail mass could be substituted by copper, in order to increase thermal conductivity by a factor of 3.5 times and to increase thermal diffusivity by a factor of 3.4 times. If the cost of silver at 59 US dollars per 100 grams (compared to copper at 0.49 US dollars per 100 grams, and brass at 0.29 US dollars per 100 grams) is not an issue, silver would be an even better choice for the tail mass, since it would improve thermal conductivity by a factor of 3.7 times and the more important (for unsteady heat conduction) thermal diffusivity by a factor of 5 times, as compared to the present choice of brass. Similar, other choices for the electrode should be investigated instead of the present brass electrodes, for example, copper and silver. The present choice of stainless steel for the bolts that apply the necessary compression to the PZT plates is not optimal, because of thermal expansion mismatch with the PZT plates, leading to loss of compression, and hence to damage and decrease of stiffness of the PZT plates, also leading to de-tuning between the excitation frequency and the natural frequency of the MEGA stack. Instead of stainless-steel, a material with a much smaller coefficient of thermal expansion should be used. For example Nabeya Bi-tech Kaisha (NBK) [16] bolts made of super invar with a thermal expansion coefficient 25 times smaller than the one of stainless steel, will better match the coefficient of thermal expansion of the PZT plates in the thickness direction. The present choice of adhesive (unfilled Bisphenol A epoxy) could be substituted by a filled epoxy to raise thermal conductivity (aluminum nitride or boron nitride filled epoxy), and if desired, the electrical conductivity (a silver-filled epoxy) as well. Also a filled adhesive with a higher glass transition temperature (for example a polyimide adhesive like Creative Materials 124-41 with a thermal conductivity of 11 W/(m K) as compared to the present unfilled epoxy 0.17 W/(m K) should also be investigated, because the present adhesive is limiting the upper temperature of the MEGA Drive due to loss of integrity of the adhesive due to its glass transition temperature being significantly lower than the Curie temperature of the PZT. Also co-sintering of the MEGA PZT-electrodes stack should be investigated, as co-sintering would eliminate the adhesive altogether, and involve much thinner electrodes. Finally, but not least, newer piezoelectric materials should be investigated to replace the 64 year old PZT, materials like high-Curie-temperature ferroelectric single-crystal Mn doped PIN-PMN-PT discussed by Zhang et.al. [17].

3. VARIATION OF INERTIAL MASS FROM HOYLE-NARLIKAR'S COSMOLOGY

In [18], Fearn discusses how Hoyle and Narlikar (HN) [19] [20] [21] in the 1960's developed a theory of gravitation which is Machian and uses both retarded and advanced waves to communicate gravitational influence between mass particles (a gravitational version of the absorber theory derived by Wheeler and Feynman for classical electrodynamics). The HN theory reduces to Einstein's theory of gravity in the smooth mass field approximation, with particles having constant rest mass. The theory was ignored by much of the gravitation community since it was developed with Hoyle's static universe in mind. However, it is trivial to drop the static universe condition (by dropping the "C"-field matter creation terms) and then one obtains a non-static theory of gravitation. Hawking in 1965 pointed out a possible flaw in theory. This involved integrating out into the distant future to account for all the advanced waves which might influence the mass of a particle here and now. Hawking used infinity as his upper time limit and showed the integral was divergent. Fearn recently pointed out that when considering HN without the creation "C" field, theory agrees with the observation that the universe is known to be expanding, and accelerating, and hence the upper limit in the advanced wave time integral should not be infinite but should be bounded by the cosmic event horizon. Fearn showed that the advanced integral is in fact finite when the cosmic event horizon is taken into account. Therefore, Hawking's objection is no longer valid and the HN theory becomes a working

theory once again. Mach's principle can be summarized by stating that the inertia of a body is determined by the rest of the mass content of the universe. Ciufolini and Wheeler [22] simply stated that “inertia here arises from mass there.” The HN inertial interaction is scalar: the inertial mass of a particle is determined by the scalar field contributions from the rest of the particles in the universe. The HN gravitational theory is wider in scope than Einstein’s general relativity and it is conformally invariant: if the measured inertial mass of a particle in a given spacetime metric g_{ik} is m , then in a conformal transformation $\Omega^2 g_{ik}$ of this metric, the inertial mass becomes $\frac{m}{\Omega}$. Most interestingly for this article, HN gravitational theory easily accommodates a rest mass that is variable with time. For example Narlikar and Arp [23] consider an inertial mass that varies with epoch t as $m_o(t) = t^2$ to explain the redshift in cosmology and make the same predictions as the standard expanding model, using instead a static model with particle masses that increase quadratically with epoch, instead of the conventional model of an expanding universe with constant masses. Narlikar and Das [24] argue that the excess redshift of high-redshift quasars may be explained as quasars born in galactic explosions and ejected from galactic nuclei and that the observed quasar alignment and redshift bunching can be understood within the framework of the variable mass HN theory, with the particle masses in them increasing quadratically with epoch. In the following, I consider HN without the creation “C” field, such that the HN theory agrees with the observation that the universe is known to be expanding, and where a HN variable mass hypothesis is used to calculate the Woodward Mach effect thruster hypothesis involving mass fluctuations.

Fearn et.al. [25] [26] outline a derivation of the Woodward Mach effect thruster theory based on the HN field equation that Fearn shows to have the same type of mass fluctuation terms. The force equation, used to predict the thrust in the MEGA drive, can be derived from the mass fluctuation. In General Relativity, length, and hence surface and volume, are observer dependent and hence not invariant like mass. This argues for the time derivatives of the mass field to govern the fluctuation in inertial mass, instead of the mass fluctuation being governed by mass density (which is observer dependent due to the observer-dependence of the volume). This distinction is irrelevant for isochoric media (e.g. perfect fluids or idealized elastomers) or for solid media undergoing isochoric (equivoluminal) deformation, but it is important when considering solids like piezoelectric materials that are not isochoric and that undergo non-isochoric deformation. Fearn basically obtains the following equation for the mass density fluctuation (in SI units), after neglecting a number of derivative terms with respect to space (assuming spatial homogeneity of the mass function in a smooth mass field approximation, such that the time derivatives of the mass function are much more significant than any mass transport through the solid medium):

$$\begin{aligned} \Delta\rho &= \frac{1}{G} \left(\frac{1}{m} \frac{\partial^2 m}{\partial t^2} - \left(\frac{1}{m} \frac{\partial m}{\partial t} \right)^2 \right) \\ &= \frac{1}{G} \frac{\partial^2 \ln [m]}{\partial t^2} \end{aligned} \quad (1)$$

Which I have expressed directly as the second derivative with respect to time of the natural logarithm of the mass. This can be expressed as a function of the kinetic energy.

A few words about the subtleness of the energy mass equivalence. Léon Brillouin (shown behind Bohr, and next to Heisenberg, at the upper right hand corner of Fig. 1, and whose doctor’s thesis committee was composed of Paul Langevin, Marie Curie and Jean Perrin) stated [27], [28], [29]:

“Einstein’s relation between mass and energy is universally known. Every scientist writes

$$E = mc^2 \text{ ([Brillouin] 1)}$$

but almost everybody forgets to use this relation for potential energy. The founders of Relativity seemed to ignore the question, although they specified that relation ([Brillouin] 1) must apply to all kinds of energy, mechanical, chemical, etc. When it comes to mechanical problems, the formulas usually written contain the mass of kinetic energy, but they keep silent about the mass of potential energy. We must investigate this situation carefully and try to understand what sort of difficulties are raised by such a revision. ... The physical body may be moving in a static field of forces and obtain, at a certain instant of time, an external potential energy U . Everybody assumes the total energy to be represented by the formula

$$E_{tot} = mc^2 + U \text{ ([Brillouin] 3)}$$

where U remains unchanged, despite the motion of the body at velocity v ; this fact reveals that one completely ignores any possibility of mass connected with the external potential energy. If this external potential energy had any mass, this mass would somehow be set in motion by the displacement of the physical body, and this moving mass would obtain some kinetic energy. No provision for any such effect can be seen in equation

([Brillouin] 3). We are thus in a strange situation, where the internal potential energy obtains a mass, while the external potential energy does not! The contradistinction is striking and shocking! ”

If external electromagnetic potential energy change needs to be considered, then Brillouin ([27] and [28]) subtracts the potential energy contribution from the total energy:

$$mc^2 = E_{total} - \frac{m_{el}c^2}{\sqrt{1 - \frac{v^2}{c^2}}} - U \left(1 + \frac{1}{2} \left(\frac{1}{\sqrt{1 - \frac{v^2}{c^2}}} - 1 \right) \right) \quad (2)$$

where m_{el} is the total mass associated with the electric field around a mass density point having rest mass m_o and electric charge distributed uniformly, spherically, around it. In those references, Brillouin gives examples of the external potential energy associated with an external electric field, showing that the external electric field itself carries a mass, and shows how, according to the sign of U, the correction can be positive or negative.

Medina ([30] and [31]) states:

“Unlike the inertia of energy, which is well known, many physicists are not aware of the inertia of pressure (stress). In many cases such an effect is negligible, but for the case of the stress produced by electrostatic interactions, it is comparable to the inertial effects of the electromagnetic fields.”

Electromagnetic energy problems may contain components of the mechanical momentum that are of order $\frac{1}{c^2}$, which are sometimes labeled as “hidden” momentum [32]. Brillouin made the above observation in regards to theory of special relativity (which he called restricted relativity). In general relativity and in HN gravitational theory, this energy is implicit in the fields. The important thing is to account for all terms in the equations of conservation of energy and conservation of momentum. While the attribution of meaning to different types of forces is non-unique, what matters is the actual experimentally measured force [33]. For general unsteady behavior, the body force is due to all terms in the equations of motion, and not just one of them. Henceforth I account for the change from the rest mass m_o to m which accounts for the mass of kinetic energy, and I assume that there is no mass change to the mass particle connected with changes in external potential energy.

The standard definition of relativistic kinetic energy is:

$$\begin{aligned} K &= m_o c^2 \left(\frac{1}{\sqrt{1 - \frac{v^2}{c^2}}} - 1 \right) \\ &= mc^2 - m_o c^2 \end{aligned} \quad (3)$$

where m_o is the relativistic rest mass: the mass in the frame in which the velocity is zero, and hence in which the kinetic energy itself is zero. Disregarding time variations of external potential energy, and substituting the expression for the mass m in terms of the kinetic energy Eq. (3) into the expression for the mass fluctuation Eq. (1), one obtains:

$$\begin{aligned} \Delta\rho &= \frac{1}{G} \frac{\partial^2 \ln \left[m_o + \frac{K}{c^2} \right]}{\partial t^2} \\ &= \frac{1}{G} \frac{\partial^2 \ln \left[m_o \left(1 + \frac{K}{m_o c^2} \right) \right]}{\partial t^2} \\ &= \frac{1}{G} \left(\frac{\partial^2 \ln [m_o]}{\partial t^2} + \frac{\partial^2 \ln \left[1 + \frac{K}{m_o c^2} \right]}{\partial t^2} \right) \end{aligned} \quad (4)$$

If the speed v of material points is much smaller than the speed of light c , an assumption that is well satisfied for piezoelectric vibration experiments conducted at less than 100 kHz, it is trivial to show that the kinetic

energy K is

$$K = m_o c^2 \left(\frac{1}{\sqrt{1 - \frac{v^2}{c^2}}} - 1 \right) \quad (5)$$

$$\approx \frac{1}{2} m_o v^2 \quad \text{for } \frac{v}{c} < 1$$

and that the natural logarithm expression becomes

$$\ln \left[1 + \frac{K}{m_o c^2} \right] \approx \frac{K}{m_o c^2} \quad \text{for } \frac{v}{c} < 1 \quad (6)$$

$$\approx \frac{v^2}{2c^2}$$

and therefore the mass fluctuation, Eq. (4), for speed v of material points much smaller than the speed of light c , becomes:

$$\Delta\rho \approx \frac{1}{Gc^2} \left(c^2 \frac{\partial^2 \ln [m_o]}{\partial t^2} + \frac{\partial^2 \left(\frac{K}{m_o} \right)}{\partial t^2} \right) \quad \text{for } \frac{v}{c} < 1 \quad (7)$$

$$\approx \frac{1}{2Gc^2} \left(2c^2 \frac{\partial^2 \ln [m_o]}{\partial t^2} + \frac{\partial^2 v^2}{\partial t^2} \right)$$

Next let us assume the condition that the second derivative with respect to time of the natural logarithm of the rest mass is negligibly small compared to the second derivative with respect to time of the kinetic energy per unit mass:

$$\Delta\rho \approx \frac{1}{Gc^2} \frac{\partial^2 \left(\frac{K}{m_o} \right)}{\partial t^2} \quad \text{for } \frac{v}{c} < 1 \quad \text{and} \quad \frac{\partial^2 \ln [m_o]}{\partial t^2} < \frac{\partial^2 \left(\frac{K}{m_o} \right)}{c^2 \partial t^2} \quad (8)$$

$$\approx \frac{1}{2Gc^2} \frac{\partial^2 v^2}{\partial t^2}$$

Therefore one arrives at the conclusion that the inertial mass fluctuation is due to the second derivative with respect to time of the kinetic energy per unit mass, divided by the gravitational constant G and the square of the speed of light. The only assumptions involved in this conclusion have been: 1. Hoyle-Narlikar's theory of gravity (dropping the creation "C" field, assuming spatial homogeneity of the mass function in a smooth mass field approximation, and assuming negligible mass transport within the solid: neglecting the space gradients of mass terms in the mass fluctuation expression), 2. speed of material points negligibly small compared to the speed of light and 3. second derivative with respect to time of the natural logarithm of the rest mass negligibly small compared to the second derivative with respect to time of the kinetic energy per unit mass.

The second derivative with respect to time of the kinetic energy per unit mass, is a function of the square of the acceleration $\frac{\partial v}{\partial t}$, and the product of the velocity v times the time rate of the acceleration $\frac{\partial^2 v}{\partial t^2}$ (the second derivative with respect to time of the velocity) of the mass points, which is also called the jerk, jolt, surge or lurch:

$$\Delta\rho \approx \frac{1}{2Gc^2} \frac{\partial^2 v^2}{\partial t^2} \quad (9)$$

$$\approx \frac{1}{Gc^2} \left(\left(\frac{\partial v}{\partial t} \right)^2 + v \frac{\partial^2 v}{\partial t^2} \right)$$

The presence of the jerk $\frac{\partial^2 v}{\partial t^2}$ is significant because it has been shown by Sprott [35] [36] in the field of chaotic dynamics that an equation involving the jerk is equivalent to a system of three first order, ordinary, non-linear

differential equations, and such a system is the minimal setting for solutions that can show chaotic behavior. The transient mass fluctuation equation is a nonlinear differential equation involving the jerk, the acceleration and the velocity. Therefore, it is interesting to consider whether the solution of the Machian force due to inertial mass fluctuations (following Fearn's derivation from HN theory) of a piezoelectric/electrostrictive Langevin stack undergoing vibrations may be capable of showing chaotic, complex dynamic behavior. Such chaotic, complex dynamic behavior may result in different dynamic behavior regimes and perhaps it can be exploited to maximize the response if properly engineered.

4. THE MEGA DRIVE MODEL: 2 UNEQUAL MASSES CONNECTED BY A VISCOELASTIC PIEZOELECTRIC/ELECTROSTRICTIVE STACK

Next, I model the MEGA drive as a dynamic system composed of two unequal, lumped, end masses (the front, aluminum, mass and the tail, brass, mass) connected by a linearly viscoelastic piezoelectric/electrostrictive stack. Therefore the two coupled differential equations can be visualized as modeling a 2-mass dynamic system connected by a spring and a dashpot (the spring stiffness and the dashpot's damping given by the viscoelastic piezoelectric/electrostrictive stack and the stiffness of the bolts providing initial compression), undergoing piezoelectric and electrostrictive excitations. The boundary conditions are modeled as free-free, as if the MEGA drive would be vibrating in space. It is critical to take damping into account in addition to considering unequal end masses. To calculate the maximum amplitude of a vibrating system it is imperative to consider non-zero damping because for zero damping, the response will have infinite amplitude at resonance, which is an unphysical result. All piezoelectric dynamic systems obey the second law of thermodynamics, and hence have non-zero damping.

The strain excitation is composed of piezoelectric and electrostriction excitation components, Fig. 15. The piezoelectric strain excitation is proportional to the piezoelectric coefficient d_{33} in the thickness direction of the PZT plates, and proportional to the electric field E_{33} in the thickness direction (voltage differential divided by the thickness of the plate). The electrostrictive strain excitation is proportional to the electrostriction coefficient M_{33} in the thickness direction of the PZT plates, and proportional to the square of the electric field $(E_{33})^2$ in the thickness direction (voltage differential divided by the thickness of the plate). The voltage excitation $V_o \cos(\omega t)$ is assumed to be proportional to a cosine function $\cos(\omega t)$ of time t and angular frequency ω oscillating with zero to peak voltage amplitude V_o . The piezoelectric and electrostrictive force excitations are proportional only to the stiffness of the piezoelectric stack, since the bolts provide no piezoelectric or electrostrictive excitation. By contrast, for the dynamic equations of motion, the stiffness is given by the stiffness of the PZT stack plus the stiffness of the bolts providing initial compression to the stack. The piezoelectric/electrostrictive equations are formulated based on the results of theory for segmented electromechanical stacks developed by Gordon E. Martin [37] at the U.S. Navy Electronics Laboratory, San Diego, California, in the early 1960's. The exact solution to the coupled differential equations of motion for the dynamic system of two unequal masses with damping and stiffness, excited by piezoelectricity and electrostriction, can be decomposed into a piezoelectric solution for the displacement of each end mass, with an in-phase and an out-of-phase component, for a total of 4 terms; and an electrostrictive solution for the displacement of each end mass, with an in-phase and an out-of-phase component, for a total of an additional 4 terms; so the solution has 8 such terms. Piezoelectric resonance occurs when the voltage excitation frequency ω equals the first natural frequency of the MEGA drive ω_o . Calculating the first natural frequency, using the following properties:

length of PZT stack = 0.018288 m
 thickness of PZT plates = 2×10^{-3} m
 thickness of brass electrode = 5×10^{-5} m
 thickness of epoxy adhesive = 5×10^{-6} m
 outer diameter of PZT stack = 0.019 m
 outer diameter of bolts = 0.002845 m
 screw head diameter = 0.00452 m
 screw head length = 0.00277 m
 number of outside bolts = 6
 mass of PZT stack = 0.046 kg
 mass of aluminum (head end) = 0.010 kg
 mass density of steel bolts = 7850 kg/m³
 mass density of PZT SM-111 = 7900 kg/m³
 mass density of aluminum = 2720 kg/m³

mass density of brass = 8525 kg/m^3

Poisson's ratio of PZT stack (radial strain to longitudinal strain ratio) = 0.4375

modulus of elasticity of PZT "SM-111" plates (Y_{33} , stress and strain both in thickness direction "3") = $7.3 \times 10^{10} \text{ Pa}$

modulus of elasticity of brass electrodes = $10 \times 10^{10} \text{ Pa}$

modulus of elasticity of unfilled epoxy Bisphenol A = $0.2 \times 10^{10} \text{ Pa}$

modulus of elasticity of stainless steel bolts = $19 \times 10^{10} \text{ Pa}$

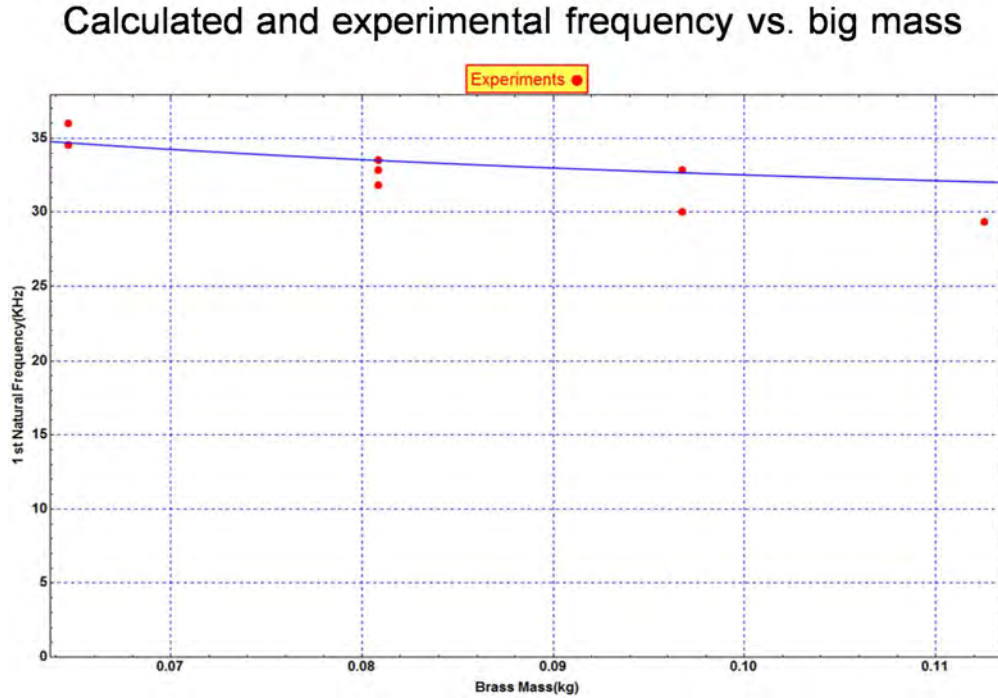


FIG. 14: Calculated (blue line) and measured (red dots) natural frequency vs. mass of brass tail end

one can see, Fig. 14, that the calculated natural frequency falls within the experimentally measured values. The modulus of elasticity in the thickness direction (Y_{33}) of PZT is known to be a complicated nonlinear function of frequency, temperature, voltage, initial compressive stress, fatigue life, and electromechanical history, including polarization history. The calculated values of natural frequency are based on the book value of the modulus of elasticity provided by the supplier (Steiner & Martins), who does not specify the values of these variables during the testing of the PZT that resulted in those book values. Furthermore, the piezoelectric stack is a composite where several layers (PZT plates, brass electrodes and adhesive layers) are sandwiched together by hand, where the adhesive has a modulus of elasticity much lower than the one of the PZT. Also, the actual stack is a continuum with a very large number of material points, rather than a simple 2-mass lumped system connected with a viscoelastic spring and dashpot as in the numerical model, and it is known that the actual natural frequency of such a continuum will be different than the one calculated in this simplified numerical model. Considering all the above factors, the comparison between the calculated and the measured natural frequency is very reasonable, particularly considering the unknown electromechanical state of the piezoelectric stack, and the level of damage (a more damaged stack will have a lower stiffness and hence a lower natural frequency, Fig. 19), at the time of the natural frequency measurements.

Electrostrictive resonance occurs when the electrostriction voltage excitation frequency 2ω equals the first natural frequency of the MEGA drive ω_o , this happens at $2\omega = \omega_o$, or equivalently at $\omega = \frac{1}{2}\omega_o$, so the electrostrictive resonance occurs at the $\frac{1}{2}$ subharmonic of the first natural frequency.

5. THE MACH EFFECT FORCE: ANALYSIS OF INPUT VARIABLES

The Mach effect force on the center of mass is calculated as the product of the total mass times the acceleration of the center of mass [38]. The acceleration of the center of mass contains terms (due to Mach effect inertial mass fluctuations) of the form of the product of the time derivative of the mass fluctuation times the velocity, and of the form of the product of the second time derivative of the mass fluctuation times the displacement, as well as square terms of the previously mentioned expressions. As a result of these multiplications, trigonometric expressions due to the product of harmonic terms at frequency ω (due to piezoelectric excitation) multiplying harmonic terms at frequency 2ω (due to electrostrictive excitation) occur, such as:

$$\begin{aligned} &(\sin(\omega t))^2 \cos(2\omega t) \\ &(\cos(\omega t))^2 \cos(2\omega t) \\ &\cos(\omega t) \sin(\omega t) \sin(2\omega t). \end{aligned}$$

Expressions such as these give constant uniaxial force terms. Such terms comprise a single term with frequency 2ω due to electrostriction times two terms with frequency ω due to the piezoelectric effect. Some terms contain all factors that are completely in-phase (with the excitation frequency) and other terms contain a mixture of out-of-phase and in-phase factors. No term consists entirely of out-of-phase (with the excitation frequency) factors. Mass fractions occur implicitly in these expressions. There are also more complicated terms that result due to the square terms of the derivatives, such terms are composed of the product of five factors that can be in-phase or out-of-phase. In such terms, the electrostrictive effect factors occur from the first power up to the third power, while the piezoelectric factors occur from the first power up to the fourth power. There is a total of $20 + 269 = 289$ such terms that contribute to the Mach effect force. In the interest of saving space these 289 terms are not shown explicitly in this article, but it is remarked that the solution is an exact analytical solution, that is solved using Wolfram *Mathematica*.

The Mach effect force can then be calculated, using the input variables previously discussed in section 4, which were used to calculate the fundamental natural frequency, and also using these additional properties:

$$G \text{ (gravitational constant)} = 6.67408 \times 10^{-11} \text{ N m}^2/\text{kg}^2$$

$$c \text{ (speed of light in vacuum)} = 2.99792458 \times 10^8 \text{ m/s}$$

$$\begin{aligned} d_{33} \text{ (piezoelectric constant: strain due to electric field, both in thickness direction "3")} \\ = 320 \times 10^{-12} \text{ m/V} \end{aligned}$$

$$\begin{aligned} M_{33} \text{ (electrostrictive constant: strain due to (electric field)}^2, \text{ both in thickness direction "3")} \\ = 13.5 \times 10^{-18} \text{ m}^2/\text{V}^2 \end{aligned}$$

$$V_o \text{ (voltage excitation, constant term)} = 200 \text{ V}$$

$$Q_m \text{ (quality factor of resonance due to mechanical dissipation)} = 190$$

$$\text{mass of brass (tail end)} = 0.0809 \text{ kg}$$

$$\text{outer diameter of brass mass} = 0.02819 \text{ m}$$

$$\text{outer diameter of aluminum mass} = 0.02819 \text{ m}$$

$$\text{aluminum bracket mount mass} = 0.007 \text{ kg}$$

$$\text{Mach effect coupling factor on piezoelectric and electrostrictive excitations} = 0.006$$

Both the modulus of elasticity (Y_{33}) and the piezoelectric constant (d_{33}), in the thickness direction of the PZT plates, for plates poled through the thickness, are obtained from the values published in the website of the supplier of the piezoelectric material plates "SM-111," Steiner & Martins [39]. Also, from Steiner & Martins [39] published values, the piezoelectric Poisson's ratio is taken to be the ratio $-d_{31}/d_{33} = -(-140/320) = 0.4375$ of the value of the piezoelectric constant d_{31} (the piezoelectric strain in the radial direction of the circular plates due to electric field applied in the thickness direction) to the piezoelectric constant d_{33} (the piezoelectric strain in the thickness direction of the plates due to electric field applied in the thickness direction). In other words, the piezoelectric strain in the radial direction of the circular plates due to electric field applied in the thickness direction, equals the negative of the piezoelectric Poisson's ratio times the piezoelectric constant d_{33} .

The value for the electrostrictive constant M_{33} for hard PZT is difficult to get, because electrostrictive strains are much smaller than piezoelectric strains, Fig. 15, in hard-doped PZT materials like (Steiner & Martins) "SM-111." Steiner & Martins does not report any electrostriction values. Reviewing the literature, I conclude that the electrostrictive coefficient (giving the strain due to the (electric field)², both in thickness direction "3") for PZT-4 "SM-111" (Navy Type I) used for the MEGA experiments has a value $M_{33} = 13.5 \times 10^{-18} \text{ m}^2/\text{V}^2$. I base this conclusion on the following experimental support (here and in the following I adopt the subscript "3" for the thickness direction for M_{33} and for Q_{33} in agreement with IEEE convention, while the authors in their articles use the "1" convention for the crystallographic axis, the important point

being that I am referring to the diagonal tensor components due to uniaxial electrostriction and not to the off-diagonal shear properties):

1. Haun et.al. [40] present electrostrictive data for a number of PZT compositions, including, most interestingly (Haun et.al. show this value in a chart vs. temperature showing little temperature dependence):

1a. tetragonal PZT 40/60 (40% antiferroelectric lead zirconate $PbZrO_3$, 60% ferroelectric lead titanate $PbTiO_3$), $Q_{33} = 0.1 \text{ m}^4/\text{C}^2$

1b. tetragonal PZT 50/50 (50% $PbZrO_3$, 50% $PbTiO_3$), $Q_{33} = 0.0966 \text{ m}^4/\text{C}^2$

Although Steiner & Martins does not disclose their “SM-111” formulation, one can reasonably ascertain from its properties that it must have a tetragonal structure, with a composition between these two. (This follows from the fact that the Curie Temperature is known to depend heavily on composition and that the Curie Temperature for SM-111 is 320 °C). The fourth order electrostriction tensor component M_{33} and the fourth order electrostriction tensor component Q_{33} (where the IEEE notation convention is used for the fourth order tensor component indices) are related to each other through the value of the electric permittivity of the material. One can derive this relationship as follows: the second order strain tensor component S_{33} and the electric field vector component E_3 , are related through the following electrostrictive constitutive equation (e.g. pages 73 and 79 of Burfoot and Taylor [45]):

$$S_{33} = M_{33}E_3E_3 \quad (10)$$

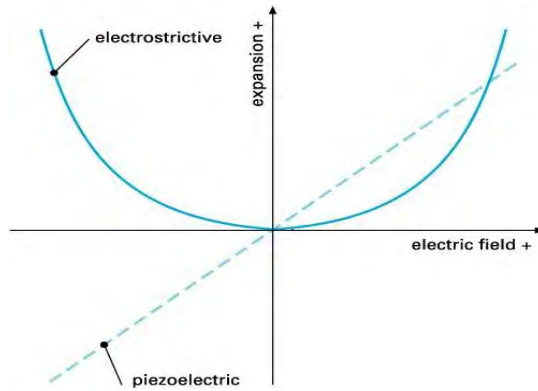


FIG. 15: Comparison of piezoelectric and electrostrictive strains vs. electric field. (Image from PI USA (Physik Instrumente))

Electrostriction is an electromechanical effect that is always present, to some extent, in all dielectric materials, whether isotropic or anisotropic. This is unlike the piezoelectric effect which cannot exist in isotropic dielectrics, Fig. 15. A piezoelectric effect can exist only in special anisotropic dielectrics, that are not centro-symmetric, where the electric vector field \mathbf{E} creates in anisotropic materials a polarization vector field \mathbf{P} that points, in general, not parallel to the electric field \mathbf{E} , and hence for a piezoelectric material, the permittivity and susceptibility are second-order tensors with non-zero off-diagonal components. Crystals are anisotropic materials composed of atoms, ions or molecules that have long range periodic order in three dimensions. Crystals may be grouped into 7 crystal systems which may be characterized in terms of axes of symmetry: cubic, tetragonal, orthorhombic, rhombohedral (or trigonal), hexagonal, monoclinic and triclinic. Each of these systems is subdivided into a number of crystal classes. There are 32 crystal classes corresponding to 32 crystallographic point groups. All piezoelectric coefficients disappear when a crystal has a center of symmetry. This eliminates 11 crystal classes. In addition, the piezoelectric coefficients become zero in crystal class 29 because of holoaxial symmetry (a crystal class with axial symmetry such that all the possible axes of symmetry are present but that has no planes of symmetry). Thus, as Voigt showed [46], of the 32 crystal classes, only 20 of these, all non-centrosymmetric, can exhibit direct piezoelectricity, and 10 of these are polar crystals which show a spontaneous polarization without mechanical stress. Electrostriction causes elongation (extensional strain) in the direction of the electric field, in response proportional to the square of the electric field \mathbf{E} [44]. Thus, an electrostrictive actuator’s movement is independent of the electric field

TABLE IV: Comparison between piezoelectric and electrostrictive effects

Property	Piezoelectricity	Electrostriction
Material direction dependence	Anisotropic, non-centro-symmetric	All dielectrics
Strain's electric field dependence	Linear	Mostly Quadratic
AC strain for zero DC bias	Elongation ($E+$) & Contraction($E-$)	Elongation
Strain's voltage polarity dependence	Dependent	Independent
Inverse effect	Yes	No
Electric poling required	No(natural), Yes(engineered material)	No
Actuators or sensors	Both	Mostly actuators
Property	Hard PZT	PMN-PT
Electric poling required	Yes	No
Electric-field-dependent phase fragility	Smaller	Greater
Strain vs. electric field hysteresis	Larger	Smaller
Tangent d_{33}	Lower	Higher
Tangent d_{33} DC bias dependence	Much smaller	Much greater
Linear stroke	Larger	Smaller
Electric permittivity ϵ_{r33}	Lower	Higher
Coupling coefficient k_{33}	Lower	Higher
Mechanical quality factor of resonance Q_m	Higher	Lower
Curie temperature T_c	Higher	Lower
T_c transition	Sharp, well-defined	Gradual transition over wide range
Single crystal	No	Yes
Cost	Lower	Higher

polarity. The directions orthogonal to the applied electric field contract in proportion to the Poisson's ratio of the material. Electrostriction, unlike piezoelectricity, has no inverse (a strain or stress cannot produce an electric field as a result of inverse electrostriction). Thus, while the piezoelectric effect has been used either for actuators, where an electric field causes strain, or for sensors, where an applied stress generates an electric field, the electrostrictive effect can mostly be used for actuators. Both electrostrictive and piezoelectric actuators are basically capacitive elements [6]. Current only flows during the charging process (while the actuator is providing motion) and so long as leakage currents and losses can be kept small, force is maintained at the end of the stroke without the need of supplying additional energy. Electrostrictive actuators usually have lower (strain vs. electric field) hysteresis than piezoelectric actuators. For most dielectrics, including PZT, the electrostrictive effect is too small to be used for actuator purposes. Relaxor ferroelectrics with extremely high electric permittivity, and having a very gradual transition Curie temperature range, display a more complex strain-electric field response, with an approximately linear range (approximately constant tangent d_{33}) over a narrow range of electric field that can be exploited for actuator purposes using a DC bias. Examples of such relaxor ferroelectrics are lead-magnesium-niobate $\text{Pb}(\text{Mg}_{\frac{1}{3}}\text{Nb}_{\frac{2}{3}})\text{O}_3$ (PMN) and lead magnesium niobate - lead titanate $\text{Pb}(\text{Mg}_{\frac{1}{3}}\text{Nb}_{\frac{2}{3}})\text{O}_3\text{-PbTiO}_3$ (PMN-PT). These electrostrictive relaxor ferroelectrics can produce larger stresses than piezoelectric actuators of similar size, and have larger values of the coupling coefficient k_{33} . Such electrostrictive actuators are ideal candidates for precision optical positioning systems. However, electrostrictive actuators have the drawbacks of a more limited stroke than piezoelectric actuators (because of their limited range of approximately linear strain vs. electric field behavior, under a direct current bias), temperature dependence (because interesting electrostrictive properties occur near phase transition temperatures), lower mechanical quality of resonance Q_m than hard PZT (also because interesting electrostrictive properties occur near phase transition temperatures, that are associated with higher dissipation) and higher cost than PZT materials. PMN-PT are single crystals, and hence do not

have the grain boundaries and inter-grain voids typical of sintered PZT, but, on the other hand, PMN-PT exhibit temperature-dependent and electric-field-dependent phase fragility as well as low fracture toughness, yielding to progressive degradation of polarization, electric permittivity ϵ_{r33} , and tangent d_{33} . Thus, there are several engineering trade-offs to make between electrostrictive and piezoelectric actuators, for example the available force vs. the length of the stroke, Q_m , temperature limitation, phase fragility, etc.

The polarization vector \mathbf{P} is a field (due to the electric dipole moment per unit volume of the dielectric material, and having units of charge per unit area) that only arises from the electric dipoles bound within the material, while the electric field \mathbf{E} (with units of force per unit charge, or volts per unit length) is induced by all charges: external and internal to the material. The electric field \mathbf{E} polarizes a dielectric material by inducing new dipole moments and/or changing the magnitude and orientation of pre-existing dipole moments. This deforms (alters the dimensions of) the dielectric solid by moving electrons and nuclei to new equilibrium positions. An electric field can remove a center of charge symmetry by creating a polar axis. The area inside the hysteresis loop in the polarization \mathbf{P} vs. electric field \mathbf{E} coordinate space has units of stress (force per unit area), or equivalently energy (force times length), per unit volume. Therefore the area inside the polarization vs. electric field hysteresis loop has the physical meaning of energy density loss (due to internal dissipation). The second order strain tensor component S_{33} and the polarization vector component P_3 , are related through this electrostrictive constitutive equation (e.g. pages 73 and 79 of Burfoot and Taylor [45]):

$$S_{33} = Q_{33}P_3P_3 \quad (11)$$

The polarization vector component P_3 and the electric field vector component E_3 are related to each other, in the linear range by (e.g. Eq. (6.4.2) of Haus and Melcher [47], or Eq. (4.36) of Jackson [48], or Eq. (4.30) of Griffiths [49]) the following constitutive equation:

$$\begin{aligned} P_3 &= (\epsilon - \epsilon_o)E_3 \\ &= \epsilon_o(\epsilon_r - 1)E_3 \\ &= \epsilon_o\chi_e E_3 \end{aligned} \quad (12)$$

where, for anisotropic electric susceptibility, the electric susceptibility $\chi_e = \epsilon_r - 1$ (dimensionless, since it expresses the ratio of the bound charge density to the free charge density) and the relative electric permittivity ϵ_r are second order tensors. Piezoelectric materials, for example PZT used in the MEGA drive experiments, have anisotropic electric susceptibility, therefore the electric susceptibility, and the relative electric permittivity in the above equation should be taken to be the value of the anisotropic tensor component coaxial with the thickness direction 3:

$$\begin{aligned} P_3 &= (\epsilon_{33} - \epsilon_o)E_3 \\ &= \epsilon_o(\epsilon_{r33} - 1)E_3 \\ &= \epsilon_o\chi_{e33}E_3 \end{aligned} \quad (13)$$

One can visualize this anisotropic susceptibility by imagining the electron's binding within the crystal as a mechanical system whereby the electron charge distribution is connected to the positively charged nucleus by springs in three orthogonal directions, whereby for an anisotropic crystal, the springs have different stiffness in different directions. (Also, it can be shown by energy considerations (page 30 and chapter 6 of Panofsky and Phillips [50]), that the anisotropic susceptibility tensor must be symmetric and hence it should be possible to express the anisotropic relationship between the polarization and the electric field vectors in terms of principal directions by a set of only three eigenvalues, and hence there are at least three directions in which the polarization and the electric field vectors are parallel in the anisotropic case.) The polarizability starts to saturate at high values of the electric field, depending on the material initial properties, the material electromechanical history and most importantly on the temperature (particularly when the temperature is close to a phase transition temperature or to the Curie temperature). Therefore at high values of the electric field, this saturation must be modeled with a nonlinear susceptibility model, which leads, in that case, to a very nonlinear relationship between the constitutive material properties M_{33} and Q_{33} . Newnham et al. [51] point out that the polarization related electrostrictive material tensor \mathbf{Q} components better describe the electrostrictive strain behavior, than the electric field related electrostrictive material tensor \mathbf{M} components,

in the nonlinear regime of electric field \mathbf{E} vs. polarization field \mathbf{P} , in which the strain ceases to be a quadratic function of the electric field \mathbf{E} .

Assuming that the electric field is low enough below saturation and hence that the linear relationship, Eq. (13), between the polarization vector component P_3 and the electric field vector component E_3 is valid, substituting Eq. (13) into Eq. (11), one obtains:

$$S_{33} = Q_{33}(\epsilon_{33} - \epsilon_o)^2 E_3 E_3 \quad (14)$$

and equating the expressions for the strain component, from Eqs. (10) and (14), one obtains the following relationship between M_{33} and Q_{33} , valid in the linear range of susceptibility, below saturation:

$$\begin{aligned} M_{33} &= Q_{33}(\epsilon_{33} - \epsilon_o)^2 \\ &= Q_{33}(\epsilon_o(\epsilon_r - 1))^2 \\ &= Q_{33}(\epsilon_o \chi_{e33})^2 \end{aligned} \quad (15)$$

where $\epsilon_o = 8.854187817 \times 10^{-12}$ F/m (notice that the units F/m can equivalently be expressed as C/(mV) which is useful for this conversion) is the value of the vacuum permittivity, also known as the permittivity of free space, and as the electric constant. Using the relative electric permittivity value reported for SM-111 in the website of Steiner & Martins [39]: $\epsilon_r = 1400$, and the above-mentioned values in cases 1a and 1b for Q_{33} I obtain the following values for M_{33} using Eq. 15:

1a. for PZT 40/60 (40% $PbZrO_3$, 60% $PbTiO_3$): $M_{33} = 15.34 \times 10^{-18}$ m²/V²

1b. for PZT 50/50 (50% $PbZrO_3$, 50% $PbTiO_3$): $M_{33} = 14.82 \times 10^{-18}$ m²/V²

2. Li and Rao [41] report the following values

2a. $M_{33} = 2.5 \times 10^{-18}$ m²/V² for PZT-7A from 0% to 80% volume fraction PZT ceramic embedded in P(VDF-TrFE) polymer.

2b. $M_{33} = 2.5 \times 10^{-18}$ m²/V² for PZT-5 at 0% volume fraction PZT ceramic embedded in P(VDF-TrFE) polymer to $M_{33} = 8 \times 10^{-18}$ m²/V² at 90% volume fraction PZT ceramic embedded in P(VDF-TrFE) polymer.

2c. $M_{33} = 2.5 \times 10^{-18}$ m²/V² for PZT-5H at 0% volume fraction PZT ceramic embedded in P(VDF-TrFE) polymer to $M_{33} = 13.5 \times 10^{-18}$ m²/V² at 95% volume fraction PZT ceramic embedded in P(VDF-TrFE) polymer.

Taking the value for the composite having 95% volume fraction PZT-5H ceramic as representative of 100% PZT-5H (assuming that 95% is already over the percolation threshold), one obtains $M_{33} = 13.5 \times 10^{-18}$ m²/V²

3. As an extreme upper value comparison, a different type of ferroelectric known for its high electrostrictive material properties, a relaxor ferroelectric, is lead-magnesium-niobate (PMN). Lee et.al. [42] report a value: $Q_{33} = 0.0115$ m⁴/C². Swartz et.al [43], report a high value of $\epsilon_r = 18,000$ for PMN. Using these values for ϵ_r and Q_{33} , I obtain the following value for M_{33} for PMN using Eq. 15:

$$M_{33} = 292 \times 10^{-18} \text{ m}^2/\text{V}^2$$

To obtain a value of $M_{33} = 13.5 \times 10^{-18}$ m²/V², similar to the PZT value, a lower value of the relative electric permittivity would be required: $\epsilon_r = 3,870$, for $Q_{33} = 0.0115$ m⁴/C². Thus, the higher value of $M_{33} = 292 \times 10^{-18}$ m²/V² for PMN is shown to be due mainly to the very high value of $\epsilon_r = 18,000$ for PMN.

Thus, from the above data in points 1 through 3, the value of M_{33} for PZT materials like (Steiner & Martins) "SM-111" can be reasonably ascertained to be between $M_{33} = 13.5 \times 10^{-18}$ m²/V² and $M_{33} = 15.34 \times 10^{-18}$ m²/V².

As previously stated, the constant term in the voltage excitation is taken to be $V_o = 200$ V, and the thickness of the PZT plates = 2×10^{-3} m, therefore the electric field vector component in the thickness direction is $E_3 = \frac{200}{0.002} \frac{\text{V}}{\text{m}} = 1 \frac{\text{kV}}{\text{cm}}$. To assess whether this magnitude of electric field is high enough to result in significant nonlinear effects, one can compare this magnitude of electric field with the magnitude of electric fields responsible for significant hysteresis in the strain vs. electric field plane.

As shown in Fig. 16 (from Fig. 2 of Zhang et.al. [52]), the magnitude of the applied electric field in this example of MEGA drive experiments, 1 kV/cm, is 20 times smaller than the electric field that results in significant nonlinearity (strain vs. electric-field hysteresis due to piezoelectric internal damping losses) for PZT-4.

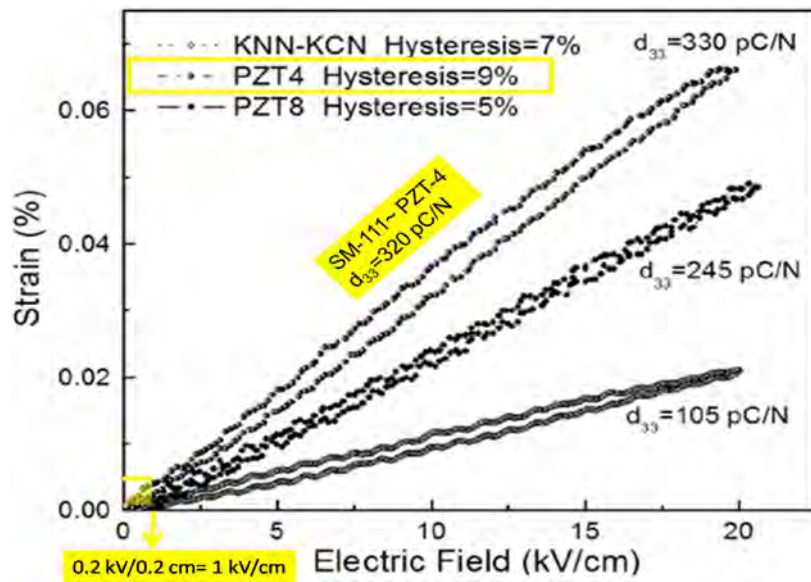


FIG. 16: Hysteresis, strain vs. electric field, for several piezoelectric materials, PZT-4 is the upper curve (from Fig. 2 of Zhang, Lim, Lee and Shrout, [52])

Fig. 17 (from Fig. 1 of Zhang et.al. [52]), shows the polarization hysteresis, plotted with coordinate axes: polarization field vs electric field, for three different piezoelectric materials, including PZT-4. All measured at an electric field of 40 kV/cm and frequency of 1 Hz.

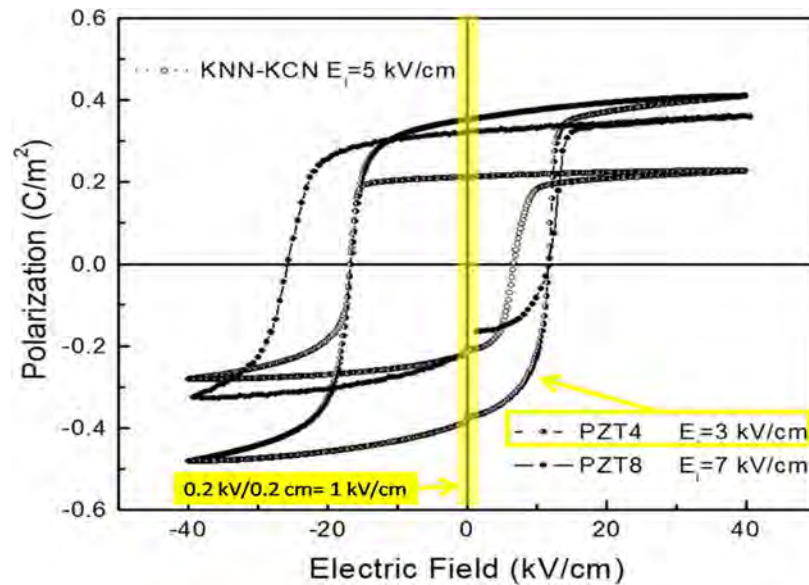


FIG. 17: Hysteresis, polarization vs. electric field, for several piezoelectric materials, PZT-4 has the largest hysteresis (from Fig. 1 of Zhang, Lim, Lee and Shrout, [52])

Hard PZT ceramics such as PZT-4 (Navy Type I) are doped with impurities that introduce an internal bias field, which is made evident by a lateral shifting along the electric field axis of hysteresis loops (described in the polarization vs. electric field domain). This internal field has been attributed to the introduction of acceptor impurity-oxygen vacancy complexes. This internal field increases the coercive field and allows the material to be driven with a higher electric field amplitude. The horizontal (electric field) offset in Fig. 17 is the result of building up of the internal bias field E_i (3 kV/cm for PZT-4). It is evident that PZT-4 has a

larger hysteresis than the other two materials, at this high level (40 kV/cm) of electric field magnitude, but it is also evident that the electric field magnitude used for these MEGA experiments (1 kV/cm) is 40 times smaller than for the example shown in Fig. 17 (and also smaller by a factor of 3 than the internal bias field used in this example). Of course, care should be taken in MEGA drive experiments to perform experiments at identical electric field magnitude, rather than identical voltage excitation magnitude. For example, if the same voltage excitation were used for PZT plates 1 mm thick instead of 2 mm thick, the electric field would be twice as large in the stack with the thinner plates, and hence closer to the region of nonlinearity.

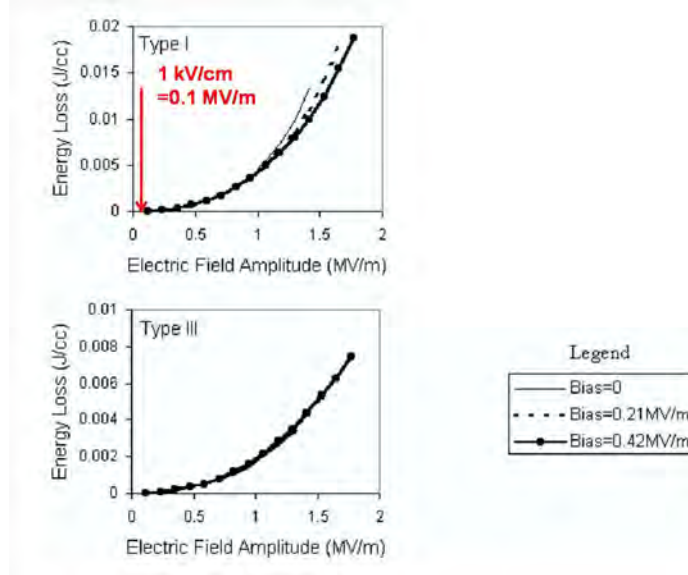


FIG. 18: Energy density loss vs. electric field amplitude for Navy Type I (PZT-4) and Navy Type III (PZT-8), calculated from hysteresis (polarization vs. electric field), for different values of externally applied DC bias (0.21 MV/m = 2.1 kV/cm)(from Fig. 5 of Waechter et.al. [53])

Waechter et.al. [53] report energy density loss data, calculated from integration of (polarization vs. electric field) hysteresis loop data, Fig. 18, for Navy Type I (PZT-4) and Navy Type III (PZT-8) hard-doped PZT materials used in sonar transducers. It is evident from these data that the magnitude of the applied electric field, 1 kV/cm = 0.1 MV/m, in this example of MEGA drive experiments using a modified form (SM-111 from Steiner & Martins) of PZT-4, is very small compared with the amplitude of electric field required for significant energy density loss. Therefore, independently confirming that this magnitude of applied electric field, 1 kV/cm = 0.1 MV/m, should be safely within the approximately linear, small loss range.

The maximum permissible electric field in a sonar transducer involves the choice of a suitable safety margin. Often, the safety margin is determined by the electric field amplitude that would produce excessive internal losses and therefore excessive heating of the material. The previously presented data shows that the magnitude of the applied electric field, 1 kV/cm = 0.1 MV/m, in this example of MEGA drive experiments using a modified form (SM-111 from Steiner & Martins) of PZT-4 is safely within the margin of approximately linear, small hysteretic loss behavior. However, a lower electric field limit is dictated based on long-term reliability (fatigue and fracture toughness) considerations. Fig. 19 shows the impedance vs. frequency spectra vs. stress cycle for Navy Type I (PZT-4) and Navy Type III (PZT-8) experimental data from Waechter et.al. [53], where the piezoelectric samples were excited by a 2 Hz sine wave with peak amplitude of 31.5 kV/cm. This electric field is substantially higher than the coercive field of these materials (the coercive field is the electric field necessary to bring the polarization in the material to zero, typical values are $E_c \approx 14$ kV/cm at room temperature to $E_c \approx 10$ kV/cm at 100 °C for PZT-4). The samples were indented with a Vickers diamond pyramid indenter, using a load of 20 N, applied for a period of 10 sec. This indentation process typically caused cracks of 200 to 300 μm length emanating from the corners of the indenter. For all the material specimens tested, the impedance spectra were shifted to lower frequencies and decreased in magnitude with increasing numbers of cycles. Non-indented samples of Navy Type III (PZT-8) samples that were exposed to the same electric field exhibited only minimal change in the impedance spectra for 5,000 cycles. Non-indented Navy Type I (PZT-4) samples were also more robust than the indented samples, but still showed significant change with as few as 100 cycles. Navy Type I (PZT-4) was the least robust material

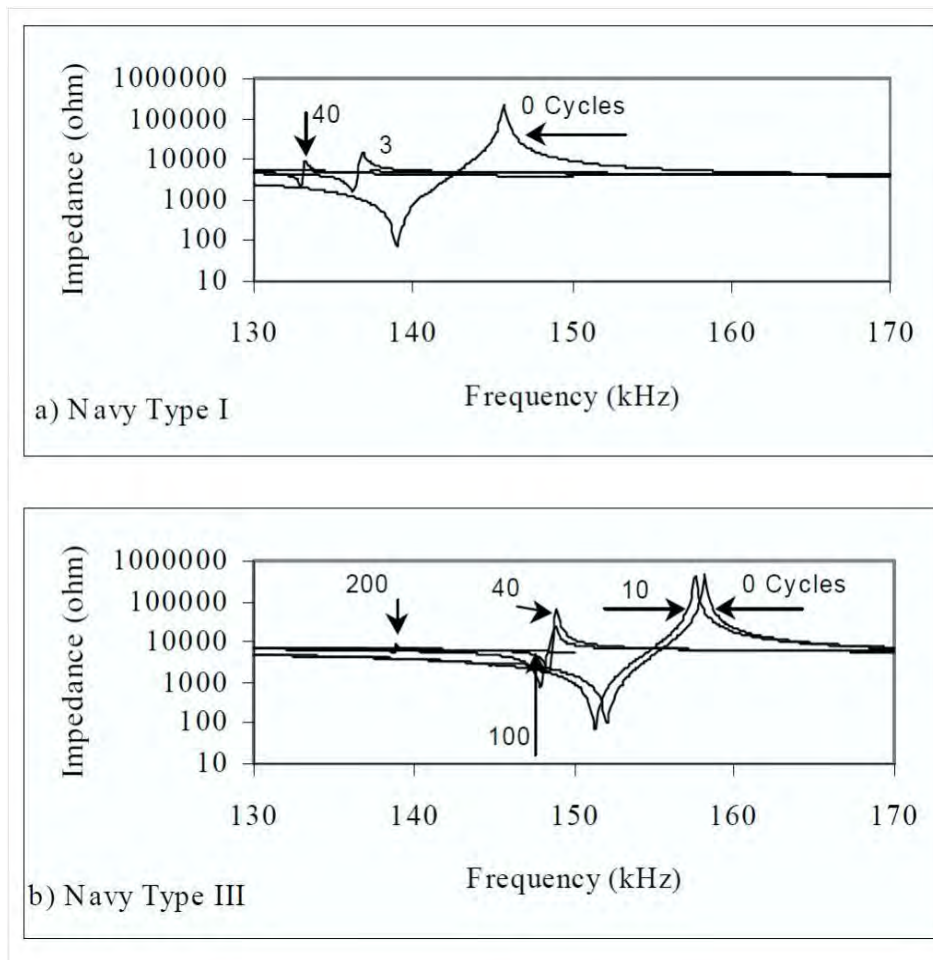


FIG. 19: Impedance vs. frequency spectra vs. stress cycle at 31.5 kV/cm for Navy Type I (PZT-4) and Navy Type III (PZT-8) (from Fig. 6 of Waechter et.al. [53])

tested: it showed the largest resonant frequency shift and the largest impedance peak reduction, with the fewest number of stress cycles.

Impedance vs. frequency spectra measurements of the MEGA drive stack, using non-indented plates made of SM-111 piezoelectric material from Steiner & Martins, measured with a Stanford Research Systems SR-780 dynamic signal analyzer, at California State University, Fullerton, by Heidi Fearn in the summer of 2016, at much lower electric field strength, at frequencies between 22 and 30 kHz, showed similar behavior: the impedance spectra were shifted to lower frequencies and decreased in magnitude with increasing numbers of cycles. It is necessary to perform a rigorous analysis of this cyclic behavior of SM-111 piezoelectric material from Steiner & Martins used in the MEGA drive, in order to characterize the natural frequency dependence on the cyclic stress history, and to assess its fatigue resistance and the appropriate limit of the electric field that should be applied to this material. More robust materials, like Navy Type III, (PZT-8) should also be assessed.

Jones and Lindberg [54] state that for Navy Type III (PZT-8) piezoelectric ceramics, an electric field limit of 10 V/mm = 0.1 kV/cm (determined on a root mean square basis) has been chosen as an industry standard based on considerations of both reliability and acceptable losses. This reliability limit is 10 times smaller than the electric field used for the MEGA experiments and for this numerical example. Since Navy Type III (PZT-8) is a hard-doped PZT with fairly similar properties as the modified Navy Type I (PZT-4) material (with trade name SM-111 from supplier Steiner & Martins) used for the MEGA experiments, and as shown by Waechter et.al. [53] Navy Type III (PZT-8) has significantly greater fracture toughness than Navy Type I (PZT-4), one would expect that the electric field limit for Navy Type I (PZT-4) should be smaller than 0.1 kV/cm and hence this indicates that the 1 kV/cm applied to the MEGA experiments is already more

than 10 times higher than the industry standard based on considerations of reliability.

The mechanical quality factor of resonance Q_m (an inverse measure of mechanical damping, energy dissipation) is known to be a complicated nonlinear function of frequency, temperature, electromechanical history (including fatigue) and electric field. Furthermore, the quality factor of resonance for a stack composed of a number of piezoelectric plates will be affected by the energy dissipation occurring at the adhesive interfaces between the piezoelectric plates and the electrodes. Therefore if one knows empirically the value of the quality factor of resonance (which can be obtained empirically from the width of the resonance bandwidth) one is better off using this empirical value, instead of using book values for just the piezoelectric plates. The supplier of the piezoelectric material with tradename ‘‘SM-111,’’ (a modified form of PZT-4, Navy Type I) used in the MEGA drive experiments, Steiner & Martins, gives a value of $Q_m=1800$ in its website [39]. However, an empirical determination of the value of the mechanical quality factor of resonance Q_m , based on the frequency response, gives a value 10 times smaller: $Q_m=190$, probably due to the dissipation occurring at the adhesive interfaces. It should also be taken into account that the supplier does not provide any information on the experimental test conditions under which the reported values were measured. The value $Q_m=190$ was determined as follows:

1. The peak amplitude response at the resonant frequency f_o was determined.
2. A horizontal line was constructed at the position $\frac{\text{peak amplitude}}{\sqrt{2}}$ ($\sqrt{2}$ is used because the measured response is proportional to the square root of the power). This is equivalent to constructing the horizontal line at the position: peak response minus $10 \log_{10}[(\frac{1}{\sqrt{2}})^2]=3.0103$ dB.
3. The two frequencies f_1 and f_2 at which the constructed horizontal line cuts the amplitude vs. frequency response curve were determined.
4. The mechanical quality factor of resonance was then determined empirically as $Q_m = \frac{f_o}{f_2 - f_1}$.

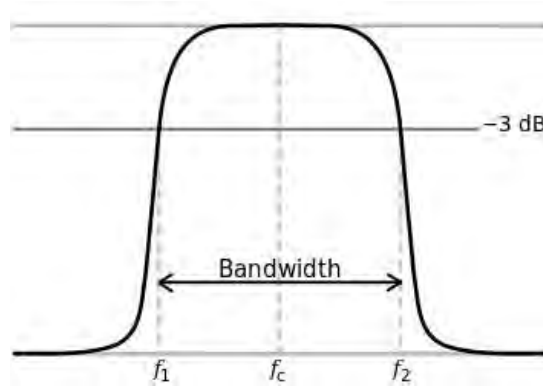


FIG. 20: Empirical calculation of mechanical quality factor of resonance Q_m based on half-power bandwidth (Image from Wikipedia/Wikimedia Commons, author Henrikb4)

(In cases in which the resonant frequency f_o is difficult to determine precisely, it can be approximated, assuming central symmetry, by the central frequency as $f_o \approx f_c = \frac{f_2 + f_1}{2}$, f_c shown in Fig. 20). The difference between the two frequencies f_1 and f_2 at which the constructed horizontal line cuts the amplitude vs. frequency response curve, is known as the half-power bandwidth. Half-power bandwidth is an arbitrary measure that has been adopted by convention to empirically define the mechanical quality factor of resonance from experimental results. This arbitrary measure was adopted by convention by the electrical engineering community to determine the damping ratio from the frequencies for which the power input is half the input at resonance, or, equivalently from the frequencies at which the response is reduced from the peak response by $\frac{\text{peak amplitude}}{\sqrt{2}}$. The half-power bandwidth was determined to be $f_2 - f_1 = 0.2$ kHz. Using a resonant frequency of 38 kHz, then $Q_m = \frac{f_o}{f_2 - f_1} = \frac{38}{0.2} = 190$, while using a resonant frequency of 30 kHz gives $Q_m = \frac{f_o}{f_2 - f_1} = \frac{30}{0.2} = 150$.

Finally, concerning the input variables for this analysis, it is noted that in order to match the experimental results it is necessary to introduce a factor of 0.6% multiplying the piezoelectric coefficient d_{33} and the electrostrictive coefficient M_{33} . This factor is about 100 times smaller than any coupling coefficient one could expect based for electromechanical coupling reasons. As of the time of this writing, the reason for this factor remains to be explained.

6. THE MACH EFFECT FORCE: OUTPUT ANALYSIS

Having described and analyzed the input variables necessary to calculate the Mach effect force, I now proceed to discuss and analyze the results from such calculations. The first results to be discussed are for a MEGA Langevin stack freely floating in space, completely free from any constraints. In contrast, the MEGA Langevin stack measurements by Fearn and Woodward have been conducted with a MEGA Langevin stack that is constrained away from the center of mass, being held at the tail (brass) end. Preliminary analysis for a MEGA Langevin stack with damping force constraints is discussed later in this section.

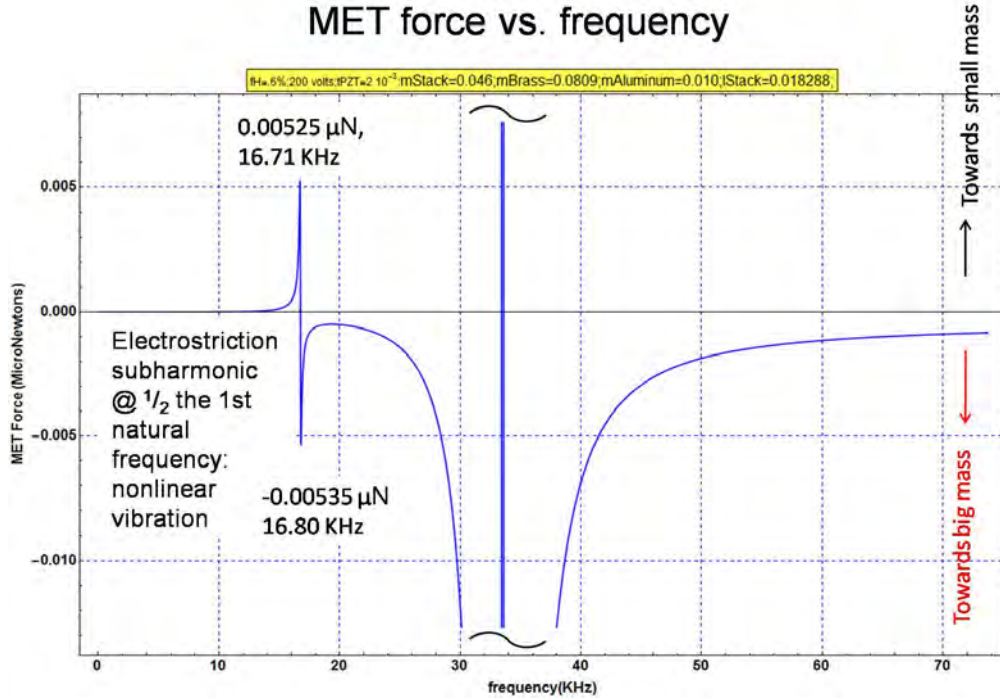


FIG. 21: Mach effect force vs. frequency, detailing the subharmonic resonance due to electrostriction, for brass mass (tail end) = 0.0809 kg

Fig. 21 shows the Mach effect force, in microNewtons (μN), vs. the vibration frequency, in kiloHertz (kHz), zooming-in for a close-up view in detail of the subharmonic resonant frequency due to the electrostrictive effect, occurring at $\frac{1}{2}$ the first natural frequency. This subharmonic response takes place due to the nonlinear excitation proportional to the square of the electric field, when the electrostrictive voltage excitation frequency 2ω equals the first natural frequency of the MEGA drive ω_o . This happens at $2\omega = \omega_o$, or equivalently at $\omega = \frac{1}{2}\omega_o$. As shown in Fig. 21, there is a subharmonic peak at the lower resonant frequency of 16.714 kHz, with a Mach effect force magnitude of only 5.25 nanoNewtons, directed towards the front (aluminum) small mass, immediately followed by a slightly higher subharmonic resonant frequency of 16.802 kHz, oriented in the opposite direction, with a Mach effect force magnitude of only 5.35 nanoNewtons, directed towards the tail (brass) big mass. It is interesting that the response is slightly asymmetric: with a 2% higher amplitude force directed towards the tail (brass) mass, at a 0.53% higher frequency. The amplitude of the response due to the piezoelectric effect is so much larger than this subharmonic response due to the electrostrictive effect that the fundamental natural frequency response needs to be shown cut-off, in this detailed view.

Fig. 22 shows the Mach effect force, in μN , vs. the vibration frequency, in kHz, zooming-in for a close-up view in detail of the fundamental resonant frequency due to the piezoelectric effect. The resonant frequency occurs at 33.514 kHz, with a peak magnitude of 21.576 μN , directed towards the front (aluminum) small mass. This is over 4,000 times greater amplitude than the electrostrictive response amplitude, which shows that the electrostrictive response of hard ferroelectric ceramic materials like PZT-4, Navy Type I, is indeed very small in comparison with the piezoelectric effect response at this amplitude of the electric field (1 kV/cm), and therefore, often times neglected. It is noteworthy that the amplitude vs. frequency approach

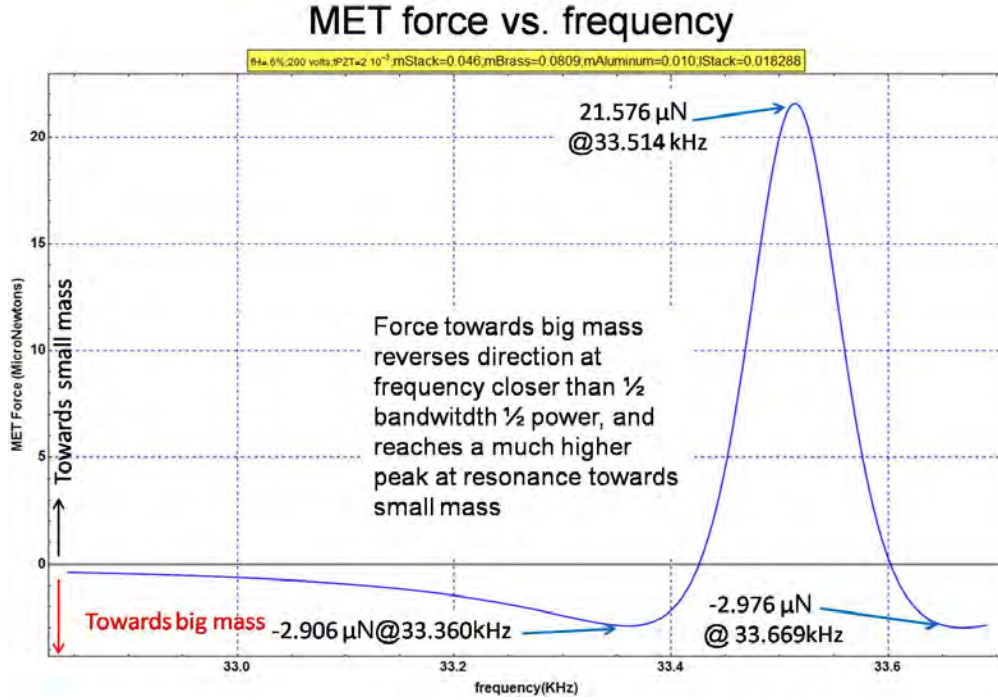


FIG. 22: Mach effect force vs. frequency, detailing the first natural frequency due to piezoelectricity, for brass mass (tail end) = 0.0809 kg

to this resonant frequency response is not monotonic. Rather as the resonant frequency is approached from lower, or higher frequencies, that are more than 0.26% away from the resonant frequency peak, it is observed that the response is actually directed in the opposite direction, towards the tail (brass) big mass, and that as the resonant frequency is approached, the amplitude of the Mach effect towards the tail (brass) big mass increases until it reaches 2.906 μ N directed towards the tail (brass) big mass at 33.360 kHz when approaching from lower frequencies towards higher frequencies. And it reaches 2.976 μ N directed towards the tail (brass) big mass at 33.669 kHz when approaching from higher frequencies towards smaller frequencies. This frequency ratio, between the local peak amplitude response directed towards the tail (brass) big mass (at 33.360 and 33.669 kHz) and the central peak amplitude resonant response (at 33.514 kHz) directed towards the front (aluminum) small mass is due to the mechanical quality factor of resonance, which is assumed, as previously discussed, $Q_m = 190 = \frac{1}{0.53\%}$. The local peak amplitude responses, directed towards the tail (brass) big mass, occur at frequencies that are $(33.514 - 33.360)/33.514 = (33.669 - 33.514)/33.514 = 0.46\% = \frac{1}{1.15Q_m} = \frac{1}{1.15 \times 190} \approx \frac{1}{Q_m}$ from the central resonant frequency. The Mach effect force transitions from being directed towards the tail (brass) mass to being directed towards the front (aluminum) mass by going through zero at a frequency ratio $(\frac{f-f_o}{f_o})$ that is $\pm \frac{1}{2Q_m}$ away from the peak natural frequency response. Thus, the frequency ratio $(\frac{f-f_o}{f_o})$ between the peak natural frequency Mach effect force (directed towards the front (aluminum) mass) and the frequencies at which the Mach effect is zero is $\frac{1}{2Q_m}$, and the distance between the frequencies at which the Mach effect is zero and the local peak responses directed towards the tail (brass) mass is also $\frac{1}{2Q_m}$. The frequency bandwidth between the lower frequency and upper frequency peak responses due to the electrostrictive effect are also separated by a similar factor $(\pm \frac{0.53\%}{2} = \pm 0.26\% = \pm \frac{1}{2Q_m})$. It can be shown that the transient vibration response of the MEGA Langevin stack is also governed by a decaying exponential having the same factor $\frac{1}{2Q_m}$. The (dimensionless) damping ratio ζ (the ratio of the actual damping to the critical value of damping at which the dynamic system does not overshoot its starting position, does not make a single oscillation and returns to equilibrium in the minimum amount of time) is related to the mechanical quality factor of resonance Q_m by $\zeta = \frac{1}{2Q_m}$. Thus the reason for the appearance of the factor $\frac{1}{2Q_m}$ in the dynamic response of the Mach effect force for the vibrating MEGA Langevin stack is easy to understand: the response is governed by the damping ratio ζ . Since the mechanical quality factor of

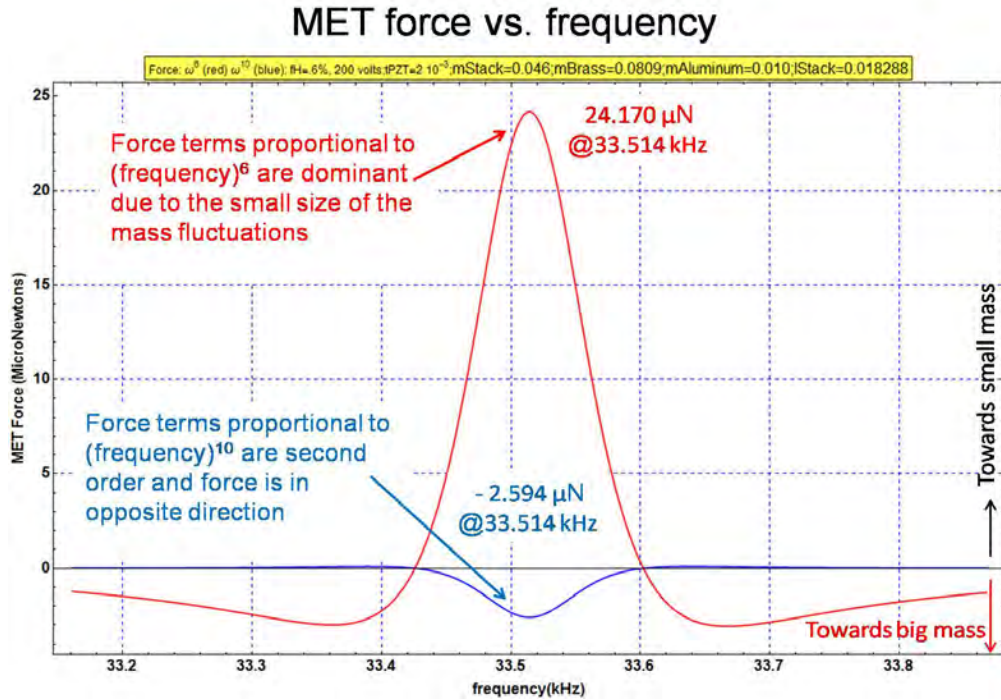


FIG. 23: Mach effect force vs. frequency, showing the first natural frequency due to piezoelectricity, for brass mass (tail end) = 0.0809 kg. In this plot, the Mach effect force is shown to be composed of two terms: a main component proportional to the sixth power of the frequency and a second order term proportional to the tenth power of the frequency.

resonance Q_m is an inverse measure of damping ζ , it governs the amplitude of resonant response. Since the MEGA drive experiments by Fearn and Woodward [26] have been performed with a manual operator chasing the natural frequency, and no frequency control algorithm has been used, it is suspected that the response that they have measured up to now is not the global peak natural frequency response, but rather the significantly lower amplitude local peak directed towards the tail (brass) big mass. Notice that there is a factor of 7.4 ($=21.576/2.906$) times greater response at the natural frequency, but that it is necessary to have equipment that can lock on this frequency with a bandwidth much smaller than $\pm \frac{1}{2Q_m} = \pm \frac{1}{2 \times 190} = \pm 0.26\%$ in order to reach the main resonant peak. This is difficult to do because as the MEGA Langevin stack vibrates, heat gets internally dissipated inside the PZT discs, which raises the temperature, which changes the dimensions of the stack, as well as the piezoelectric and electrostrictive responses, which are all temperature dependent, hence the natural frequency changes during operation and the natural frequency needs to be chased within this small bandwidth. To have the highest Mach effect forces, it is better to have higher quality factor of resonance, but the higher the quality factor of resonance, the smaller the bandwidth at which this peak natural frequency response will be located, hence the higher the quality factor of resonance, the more difficult it is to be at peak resonance and to stay at peak resonance.

Fig. 23 is a plot of the Mach effect force vs. frequency, showing the first natural frequency due to piezoelectricity, for brass mass (tail end) = 0.0809 kg, where the Mach effect force is shown to be composed of two terms: a main component proportional to the sixth power of the frequency and a second order term proportional to the tenth power of the frequency. As was discussed in section 5, the Mach effect force on the center of mass is calculated as the product of the total mass times the acceleration of the center of mass. The acceleration of the center of mass contains terms (due to Mach effect inertial mass fluctuations) of the form of the product of the time derivative of the mass fluctuation times the velocity, and of the form of the product of the second time derivative of the mass fluctuation times the displacement, as well as square terms of the previously mentioned expressions. The term due to the product of the time derivative of the mass fluctuation times the velocity, and due to the product of the second time derivative of the mass fluctuation times the displacement is proportional to the angular frequency to the sixth power, divided by the product of the gravitational constant times the square of the speed of light. The second term, due to the product

of the difference of the displacements, times the square of the difference between the mass fluctuations, is proportional to the angular frequency to the tenth power, divided by the square of the product of the gravitational constant times the square of the speed of light. This is a higher order term, which for small mass fluctuations, should be second order. This is confirmed by these numerical experiments, as Fig. 23 shows that the term proportional to the frequency to the tenth power is an order of magnitude smaller than the term proportional to the frequency to the sixth power. The term proportional to the frequency to the sixth power is dominant. It is also interesting that the direction of the force is in opposite direction for both terms, and both of them cross at the same frequencies at which the Mach effect force is zero.

Fig. 24 is a three-dimensional plot showing the Mach effect force (μN), in the vertical axis, vs. (brass) mass (kg) of tail end, in the horizontal axis, vs. frequency (kHz) in the cross axis. The spikes in the plot are numerical artifacts of the plotting resolution due to the very narrow frequency bandwidth $\pm \frac{1}{2Q_m} = \pm \frac{1}{2 \times 190} = \pm 0.26\%$ associated with the first natural frequency Mach effect force response directed towards the front (aluminum) mass, that make it numerically taxing to plot such a small bandwidth (smaller than $0.0026 \times 33.514 \text{ kHz} = 0.087 \text{ kHz} = 87 \text{ Hz}$) smoothly over an axis scale spanning 40 kHz ($\pm \frac{0.087}{40} = \pm 0.22\%$). In reality the curve should be smooth. Looking at the behavior of the curve along the frequency axis, one can see that the bandwidth around the natural frequency response is very narrow, as expected from the small amount of damping associated with the relatively high value ($Q_m = 190$) of mechanical quality factor of resonance. The positive direction of the vertical axis represents a force towards the front (aluminum) small mass, and the negative direction a force towards the tail (brass) big mass. In this view it is apparent that the amplitude of the Mach effect force diminishes rapidly for a (brass) tail mass smaller than 0.1 kg, and that for a higher (brass) mass than 0.1 kg (of the tail end) the Mach effect force approaches an asymptote in value. In contrast, Fearn and Woodward's experimental results [55] for a held device (not freely floating in space) show the Mach effect force reaching an optimum value below 0.1 kg; more on this later. For a MEGA Langevin stack that is perfectly symmetric about its center of mass, the Mach effect force is zero. This is the reason for the abrupt decrease in Mach effect force for small values of the brass mass. Also observe that the point at which the Mach effect force diminishes rapidly for a (brass) mass (kg) of tail end a little smaller than 0.1 kg is accompanied by a significant increase in the natural frequency.

Fig. 25 is a close-up view of Fig. 24, looking at the Mach effect force (μN), in the vertical axis vs. (brass) mass (kg) of tail end variation from 0 to 0.12 kg instead of 0 to 1 kg. The plot is still a three-dimensional plot of these variables vs. frequency (kHz) in the cross axis. Again, the spikes in the plot are numerical artifacts of the plotting resolution due to the very narrow frequency bandwidth associated with the Mach effect force response at the first natural frequency. This close-up view makes it more apparent that the Mach effect force rapidly changes from a value of zero for a (brass) mass of tail end similar to the (aluminum) mass of the head end (0.010 kg), up to the point at which the brass mass nears 0.060 kg. The Mach effect force variation is smaller for larger values of the brass mass. The plot shows that if the brass mass is less than the aluminum mass, the Mach effect force (associated with an excitation frequency equal to the first natural frequency) is predicted to switch direction.

Figs. 26 and 27 are flipped views of Figs. 24 and 25, respectively, with viewing emphasis on the force directed towards the (brass) mass tail end, instead of the force directed towards the (aluminum) mass front end. The plots are still three-dimensional plots of the Mach effect force (μN), in the vertical axis, vs. (brass) mass (kg) of tail end, in the horizontal axis, vs. frequency (kHz) in the cross axis. Again, the spikes in the plots directed toward the bottom of the plots are numerical artifacts of the plotting resolution due to the very narrow frequency bandwidth. It is evident from the picture that as previously discussed, as the resonant frequency is approached from lower, or higher frequencies, that are more than 0.26% away from the resonant frequency peak, it is observed that the response is actually directed towards the (brass) mass at the tail end, as observed in experiments. And that as the resonant frequency is approached, the amplitude of the Mach effect towards the tail (brass) big mass increases in amplitude until it reaches its local peak ($2.57 \mu\text{N}$ directed towards the tail (brass) big mass at 33.42 kHz when approaching from lower frequencies towards higher frequencies). As previously discussed, the Mach effect force suddenly reverses direction as the frequency gets closer to the resonant frequency peak, and this happens over a very small bandwidth $\pm \frac{1}{2Q_m} = \pm \frac{1}{2 \times 190} = \pm 0.26\%$ centered on the natural frequency. It is also observed that the Mach effect force, as the resonant frequency is approached from lower or higher frequencies that are more than 0.26% away from the resonant frequency peak, is much smoother (it does not present the plotting artifact looking like spikes that occur at the global peak of the fundamental natural frequency).

MET force vs. frequency vs. big mass

`fH=,6%;200 volts;pZT=2 10^-3;mStack=0.046;mAluminum=0.010;IStack=0.018288`

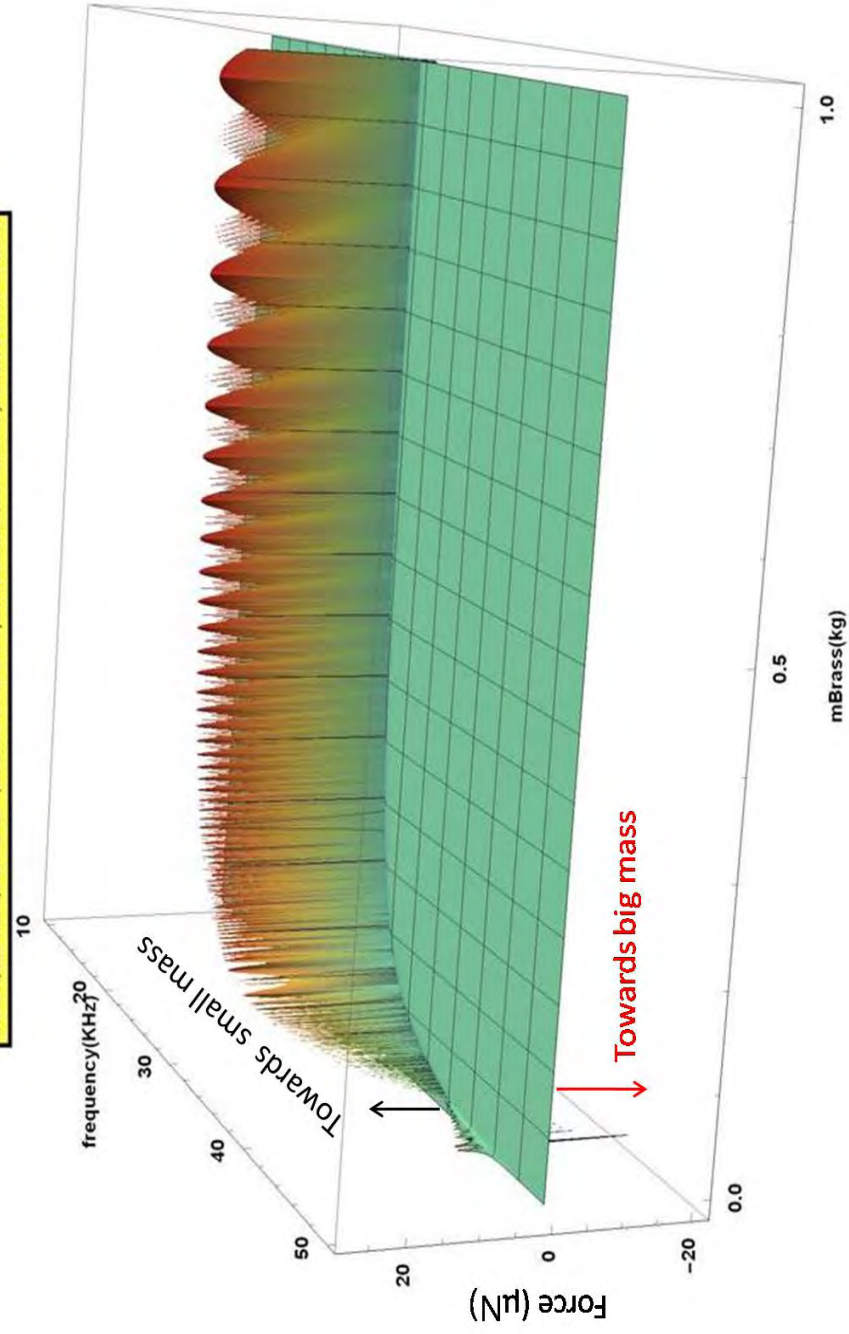


FIG. 24: 3D Plot of Mach effect force (μN) vs. frequency (kHz) vs. (brass) mass (kg) of tail end. MEGA Langevin stack modeled as floating free in space.

It is much smoother because the derivative of the Mach effect force with respect to frequency is much smaller. Therefore one has to be very careful about statements regarding the dependence of the Mach effect force on frequency, like “the force depends on frequency to the sixth power” or “the force depends on frequency to the second power,” as the force’s dependence on frequency is a function of how far away from the resonant frequency the force is calculated at. Again, since the MEGA drive experiments by Fearn and Woodward [26] have been performed with a manual operator chasing the natural frequency, and no frequency control algorithm has been used, it is suspected that the response that they have measured up to now is not the force with global peak natural frequency response shown in Fig. 24, but rather the significantly lower amplitude force directed towards the tail (brass) big mass shown in Fig. 26. There is a factor of 7.4 times greater response at the natural frequency shown in Fig. 24, but in order to reach it, it is necessary to have equipment that can lock on this frequency with a bandwidth much smaller than $\pm \frac{1}{2Q_m} = \pm \frac{1}{2 \times 190} = \pm 0.26\%$.

This is very difficult to do because as the MEGA Langevin stack vibrates, heat gets internally dissipated inside the PZT discs, which raises the temperature, which changes the dimensions of the stack, as well as the piezoelectric and electrostrictive responses, which are all temperature dependent, hence the natural frequency changes during operation and the natural frequency needs to be chased within this small bandwidth.

Fig. 28 is a plot of the first natural frequency vs. (brass) mass (kg) of tail end. As one can see from this plot, as the brass mass increases, the natural frequency decreases, from 44 kHz for zero brass mass to 29 kHz for brass mass=0.3 kg. The natural frequency decreases as the brass mass increases because the natural frequency is inversely proportional to the square root of the reduced mass $m = \frac{m_1 m_2}{m_1 + m_2}$.

Fig. 29 shows the behavior of the Mach effect force vs. (brass) mass (kg) of tail end for a MEGA Langevin stack in space. Each curve is for a constant value of the ratio of excitation frequency to the first natural frequency. Each curve is calculated at a different value of this ratio. The purpose of this plot is to understand the experimental results when the excitation frequency does not match exactly the natural frequency. Recall that the natural frequency is a property of the physical system (regardless of excitation frequency) that is set by the material and geometrical properties of the system. The excitation frequency may not match the natural frequency for a number of reasons, due to inaccuracies of the electronics as well as due to the fact that the natural frequency changes with temperature, and the temperature changes during the test due to transient internal heating. Also the natural frequency changes cycle to cycle due to electromechanical history of the piezoelectric material, and due to the possible growth of internal damage due to micro-cracks and coalescence of internal voids. To understand these curves, we must take into account that as one varies the brass mass, keeping everything else constant, the natural frequency will change as well, due to the fact that the natural frequency is a function of the brass mass. The natural frequency is proportional to the square root of the inverse of the reduced mass $\frac{1}{m} = \frac{1}{m_1} + \frac{1}{m_2}$, so that as one mass (for example the brass mass m_2) is reduced, the natural frequency increases, and vice-versa, as one mass (for example the brass mass m_2) is increased, the natural frequency decreases (up to the point at which the larger mass m_2 becomes so large that its inverse $\frac{1}{m_2}$ is negligible in comparison with the inverse of the smaller mass $\frac{1}{m_1}$). In Fig. 29 the Mach effect force vs. (brass) mass (kg) of tail end (up to 0.12 kg), is shown for $f = f_o(1 - \frac{1}{NQ_m})$ for $N = \frac{1}{2}, 1, \frac{4}{3}, 2, 3, 4$ and ∞ . Since $Q_m = 190$, this means that this plot is for the ratio of excitation frequency to the first natural frequency $\frac{f}{f_o} = (1 - \frac{1}{N190}) = 98.95\%, 99.47\%, 99.61\%, 99.74\%, 99.82\%, 99.87\%$, and 100%. Or, in other words, Fig. 29 shows the calculated behavior for the Mach effect force for different values of the brass mass, where all experiments are conducted such that the excitation frequency is $\frac{1}{NQ_m} = \frac{1}{N190}$ less than the natural frequency (and where the natural frequency decreases as the brass mass increases).

For comparison, consider the experimental data in the “Conclusions” section of page 105 of Fearn et.al.’s [55] article, where they state:

“In addition, it was determined that an optimal brass reaction mass is necessary to give maximal thrust. Several different brass reaction masses 64.7g, 80.9g, 96.8g, 112.6g and 128.3g were tried. We found that for this PZT stack, the preferred brass reaction mass 80.9g. The data is not displayed here since for a different device one would have to run this kind of test again. But it is clearly something that would be worthwhile to optimize the thrust for a given device.”

(The arXiv version of this article [56] also gives the lengths of the brass masses: 0.5, 0.625, 0.75, 0.875 and 1.0 inch, respectively). Unfortunately, the measured force vs. brass mass for brass masses of 64.7g, 80.9g, 96.8g, 112.6g and 128.3g is not shown in [55], and one cannot ascertain from this what was the actual dependence of force vs. brass mass in the experiments.

MET force vs. frequency vs. big mass

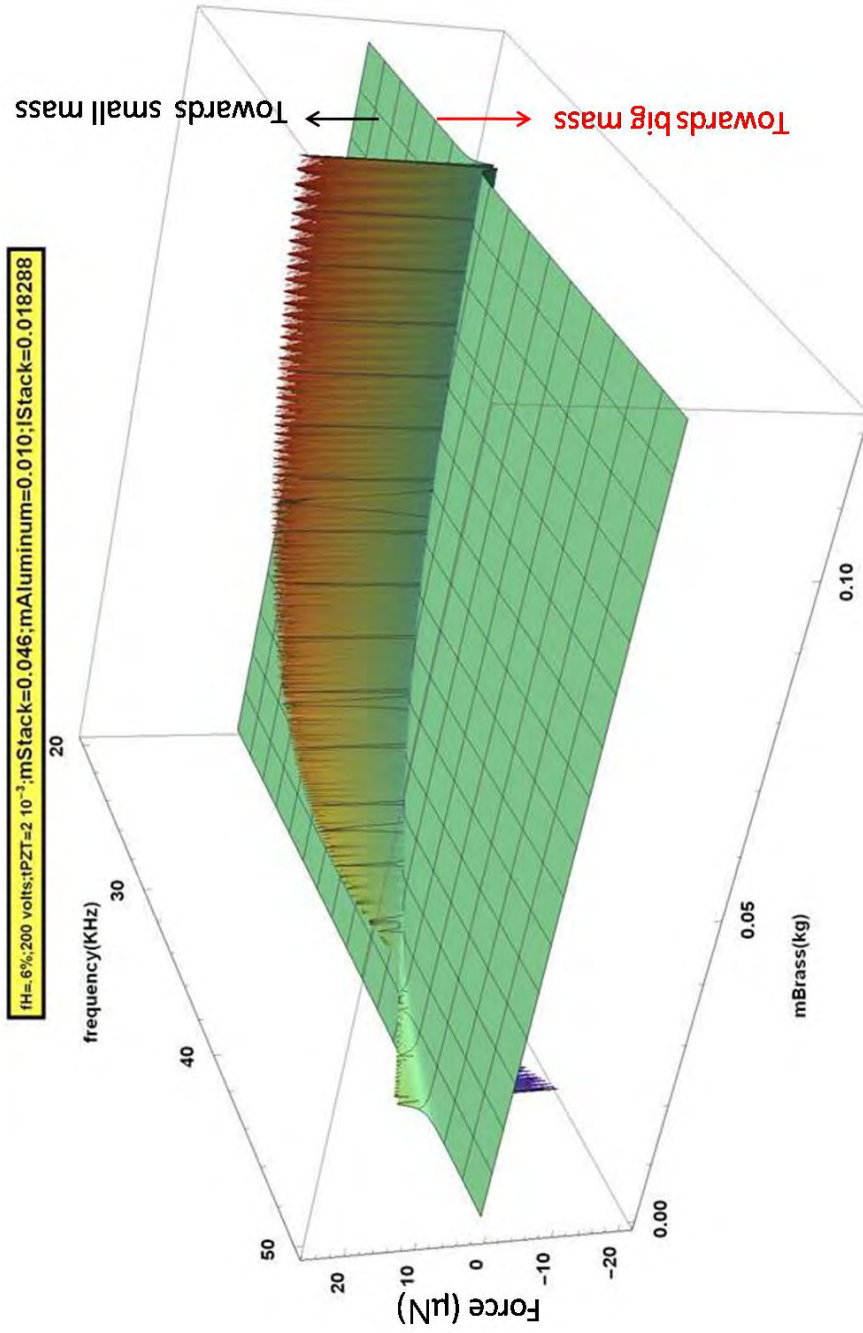


FIG. 25: 3D Plot of Mach effect force (μN) vs. frequency (kHz) vs. (brass) mass (kg) of tail end. Detail close-up of (brass) tail mass lower than 0.1 kg. MEGA Langevin stack modeled as floating free in space.

MET force vs. frequency vs. big mass

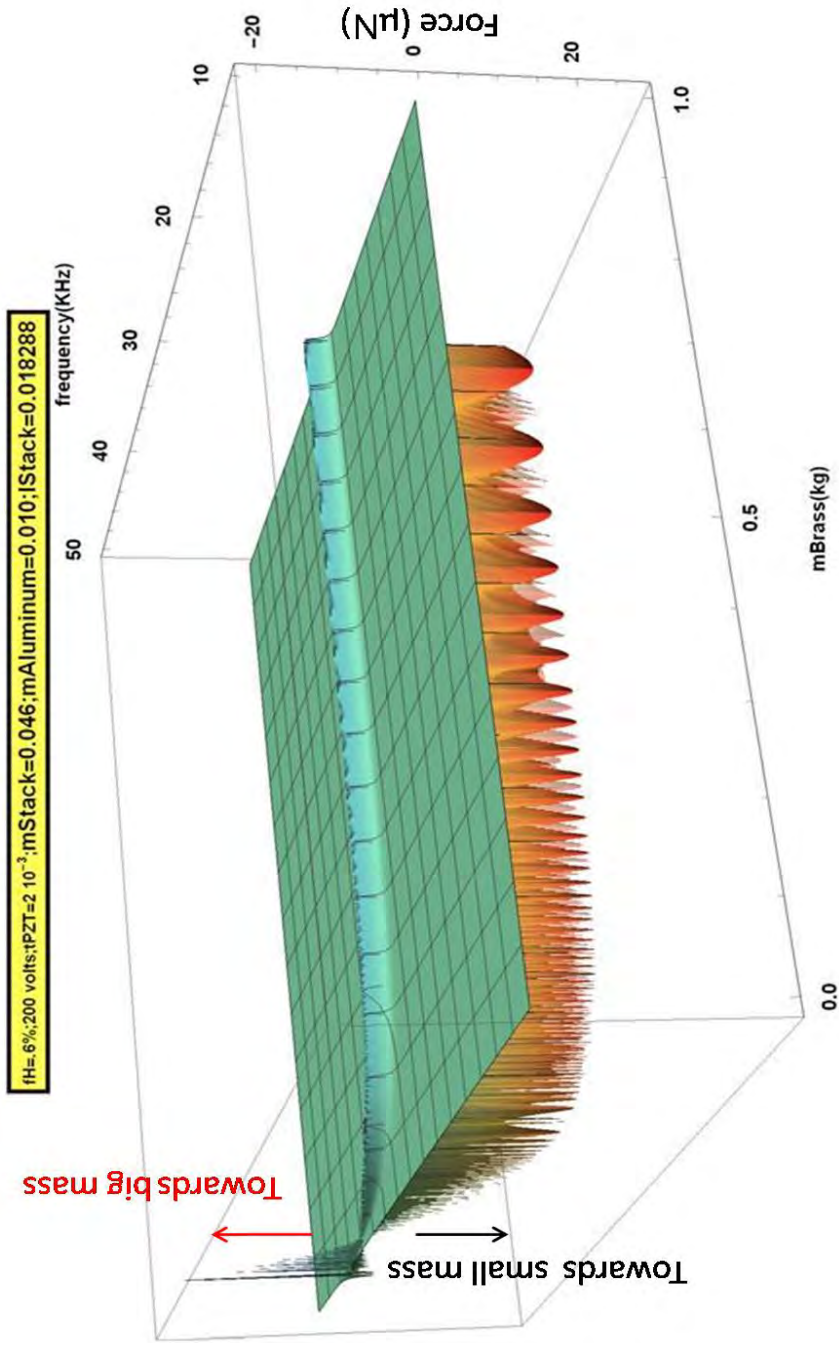


FIG. 26: 3D Plot of Mach effect force (μN) vs. frequency (kHz) vs. (brass) mass (kg) of tail end. View of force directed towards the (brass) mass tail end. MEGA Langevin stack modeled as floating free in space.

However, it looks like there is a discrepancy between the calculated results for a MEGA drive in space, free of any end constraints, for which there is no optimal mass except at an infinity brass mass: as the greater the brass mass, the greater the Mach effect force and the experimental results obtained with the MEGA drive supported at the back of the brass mass in the experiments by Fearn et.al.'s [55], where the optimal mass is reported to be 80.9g. The calculated curves in Fig. 29 show the Mach effect force grows rapidly with brass mass initially up to about 60 grams, in what looks like an exponential decay curve, with the Mach effect force growth exponentially decaying towards an asymptote. The value of the Mach effect force asymptote is different depending on the excitation frequency (depending on how far the excitation frequency is from the natural frequency). The calculations show practically the same results for an excitation frequency $f = f_o(1 - \frac{1}{NQ_m})$ with $N=1$ and $N=\frac{4}{3}$, indicating that the maximum response directed towards the tail (brass) mass occurs when the excitation frequency is between those two values, at approximately $N \approx \frac{7}{6}$, $f \approx f_o(1 - \frac{6}{7Q_m})$, which for $Q_m = 190$ is $f \approx f_o(1 - \frac{6}{7 \times 190})$ or a ratio between the excitation frequency to natural frequency of $\frac{f}{f_o} \approx 99.55\%$, at an excitation frequency approximately 0.45% lower than the natural frequency peak.

One may ask, what happens to the Mach effect force if one wants to attach the MEGA drive to a much larger mass, like a large spacecraft? What is the effect on the Mach effect force, in the limit as the tail mass goes to infinity? Fig. 30 shows the asymptotic behavior of the Mach effect force vs. (brass) mass (kg) of tail end for a MEGA Langevin stack in space. Fig. 30 shows that the Mach effect force grows rapidly as the brass mass increases towards 60 grams and that it rapidly converges towards an asymptotic value for a brass mass of less than 2 kg. It is evident that, to maximize the Mach effect force when using the MEGA drive in space, one should attach it to the most massive part of the spacecraft, preferably at its center of mass, and that the attachment should be as stiff as possible. The spacecraft's mass does not need to be too massive to provide an optimal mass for this size of MEGA stack, since an attachment mass equal or greater to 2 kg works practically as optimally as any greater mass. Of course, this conclusion is for one MEGA Langevin stack of these dimensions, if there is a multiple number of MEGA Langevin stacks, the needed mass of the spacecraft would need to be correspondingly more massive to provide near optimum force.

A preliminary numerical investigation appears to reveal that the optimal mass of 80 grams, discussed on page 105 of Fearn et.al.'s [55] article, is an experimental artifact (there would not be such an optimal brass mass if the MEGA Langevin stack were free in space) due to holding the MEGA Langevin stack behind the brass mass with a rubber pad (page 111 of Woodward's [57] book) between the brass mass and an aluminum bracket that holds the device on the arm of a torque pendulum. Thus, in Fearn and Woodward's experiment, the Mach effect device is not held at its center of mass, but it is held behind the more massive end: behind the tail brass mass, with a rubber pad that provides damping at the tail end of the device. A preliminary numerical investigation was carried out modeling the stack as being supported by a bracket with negligible bending stiffness compared to the uniaxial stiffness of the MEGA Langevin stack, and with the damping force taking place at the ends of the stack, as a first approximation of the situation where the damping provided by the rubber pad between the tail (brass) mass and the aluminum bracket is much greater than the internal damping in the PZT stack (thus providing one possible explanation of the experimentally measured mechanical quality factor of resonance being only $Q_m=190$ instead of the book value $Q_m=1800$ reported by Steiner & Martins for their modified PZT-4 material SM-111).

The following figures show the Mach effect force as a function of frequency and the mass of the tail (brass) mass for a MEGA Langevin stack with damping at the ends, where the damping force is due to a rubber pad between the end mass and a holding bracket. Figs. 31, 32 and 33 cover the same parameters as Figs. 24, 25 and 26, respectively, did for the MEGA Langevin stack floating in space.

Fig. 34 is a plot of the Mach effect force vs. (brass) mass (kg) of tail end for a MEGA Langevin stack with damping at the ends, where the damping force is due to a rubber pad between the end mass and a holding bracket. Each curve is for a constant value of the ratio of excitation frequency to the first natural frequency. Each curve is calculated at a different value of this ratio. The purpose of this plot is to understand the experimental results when the excitation frequency does not match exactly the natural frequency.

For a ratio of excitation frequency to natural frequency equal to $\frac{f}{f_o} = (1 - \frac{1}{0.5 \times 190}) = 98.95\%$, the maximum Mach effect force under such conditions is $0.457 \mu\text{N}$, and it is directed in the direction from the aluminum mass towards the brass mass, and this maximum amplitude Mach effect force occurs for a brass mass equal to 0.206 kg, at a natural frequency of $f_o = 30.19 \text{ kHz}$, and excitation frequency of 29.87 kHz. For $\frac{f}{f_o} = (1 - \frac{1}{190}) = 99.47\%$ the maximum Mach effect force is $1.43 \mu\text{N}$, and it is directed in the direction from the aluminum mass towards the brass mass, and this maximum amplitude Mach effect force occurs for a brass mass equal to 0.106 kg, at a natural frequency of $f_o = 31.87 \text{ kHz}$, and excitation frequency of 31.70 kHz.

MET force vs. frequency vs. big mass

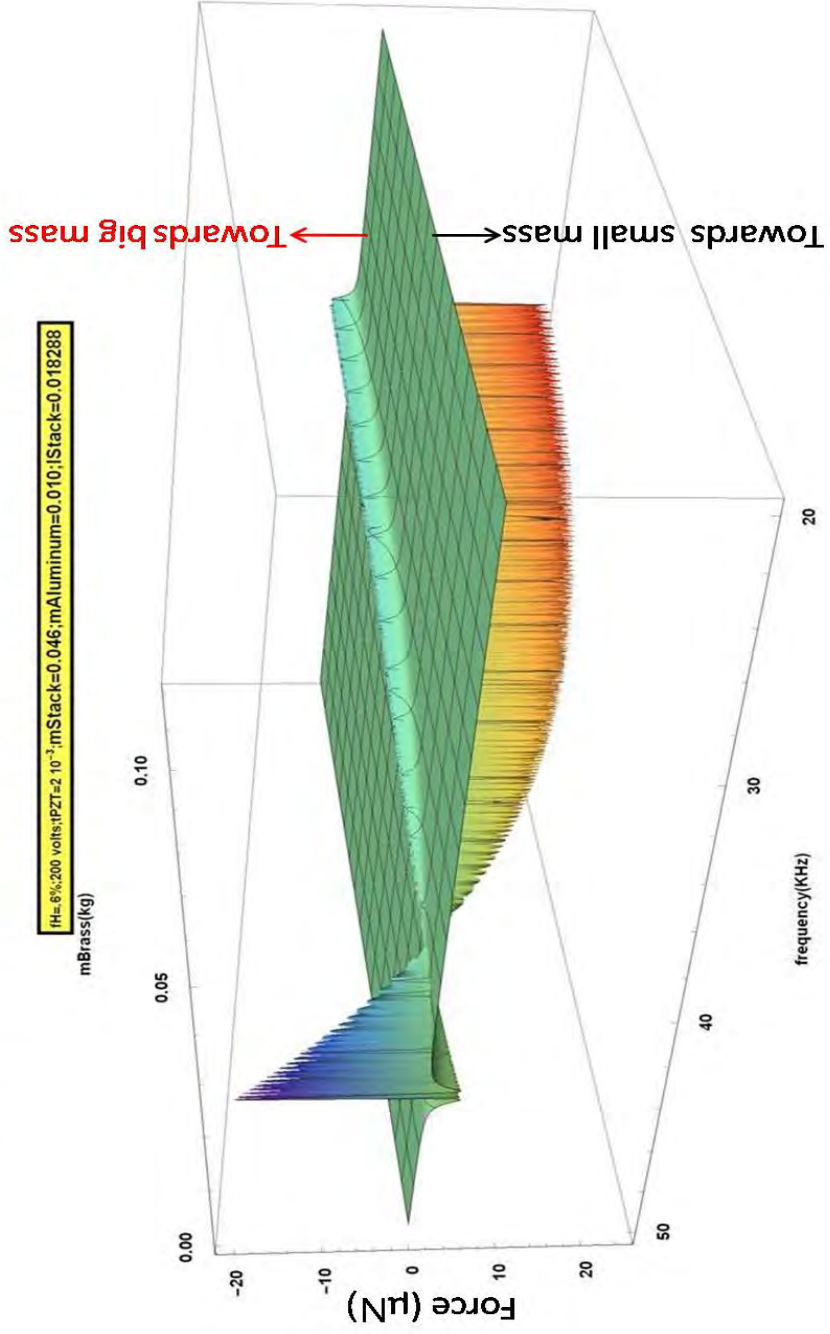


FIG. 27: 3D Plot of Mach effect force (μN) vs. frequency (kHz) vs. (brass) mass (kg) of tail end. View of force directed towards the (brass) mass tail end. MEGA Langevin stack modeled as floating free in space.

Natural frequency vs. big mass

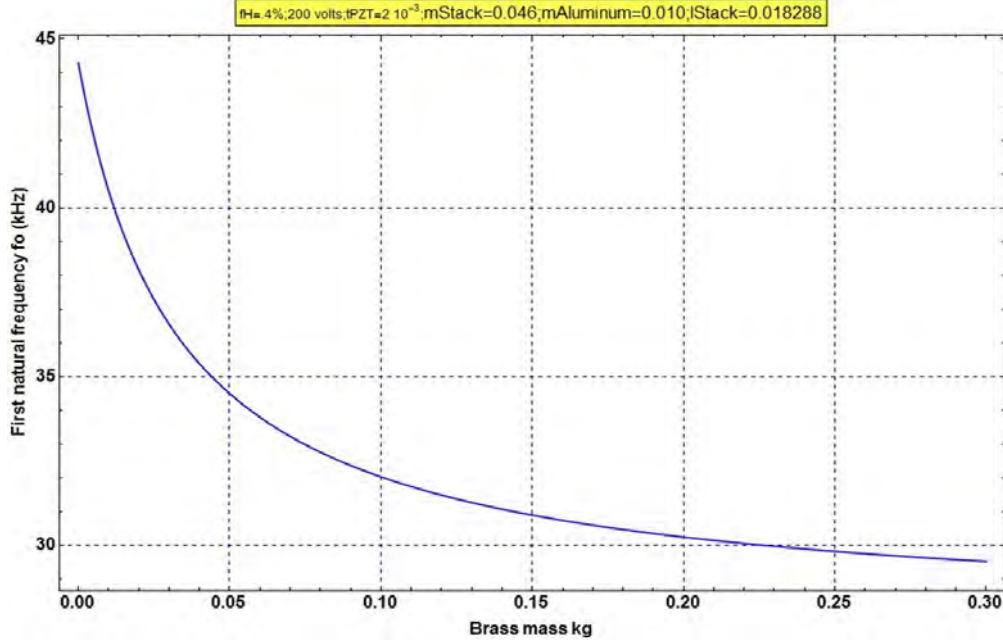


FIG. 28: First natural frequency vs. (brass) mass (kg) of tail end

For $\frac{f}{f_o} = (1 - \frac{0.75}{190}) = 99.61\%$ the maximum Mach effect force is $2.03 \mu\text{N}$, and it is directed in the direction from the aluminum mass towards the brass mass, and this maximum amplitude Mach effect force occurs for a brass mass equal to 0.083 kg , at a natural frequency of $f_o = 32.63 \text{ kHz}$, and excitation frequency of 32.50 kHz .

For $\frac{f}{f_o} = (1 - \frac{1}{2 \times 190}) = 99.74\%$ the maximum Mach effect force is $2.58 \mu\text{N}$, and it is directed in the direction from the aluminum mass towards the brass mass, and this maximum amplitude Mach effect force occurs for a brass mass equal to 0.061 kg , at a natural frequency of $f_o = 33.76 \text{ kHz}$, and excitation frequency of 33.67 kHz . For $\frac{f}{f_o} = (1 - \frac{1}{3 \times 190}) = 99.83\%$ the maximum Mach effect force is $1.59 \mu\text{N}$, and it is directed in the direction from the aluminum mass towards the brass mass, and this maximum amplitude Mach effect force occurs for a brass mass equal to 0.106 kg , at a natural frequency of $f_o = 35.22 \text{ kHz}$, and excitation frequency of 35.15 kHz .

If the excitation frequency exactly matches the natural frequency, the (global) maximum Mach effect force is $17.16 \mu\text{N}$, and it is directed in the direction from the brass mass towards the aluminum mass, and this maximum amplitude Mach effect force occurs for a brass mass equal to 0.083 kg , at an excitation frequency exactly matching the natural frequency of $f_o = 32.64 \text{ kHz}$.

These calculations are summarized in Table V. For comparison, consider the experimental data in the “Conclusions” section of page 105 of Fearn et.al.’s [55] article. It is encouraging that the experiments show the optimal mass to be 81 grams , since this agrees very well with the calculations, (given the sparsity of the experimental data, at increments of 16 grams , or 20% of the optimal mass) within 2% of the optimal mass of 83 grams calculated for the maximum calculated Mach effect force of $17 \mu\text{N}$ when the excitation is exactly identical to the natural frequency and with the optimal mass of 83 grams when the excitation frequency is $\frac{0.75}{Q_m} = 0.395\%$ smaller than the natural frequency, giving a calculated Mach effect force of $2 \mu\text{N}$. As previously discussed, the MEGA drive experiments by Fearn and Woodward [26] have been performed with a manual operator chasing the natural frequency, and no frequency control algorithm has been used. Therefore it is suspected that the response that they have measured up to now is not the global peak natural frequency response predicted to be $17 \mu\text{N}$ directed towards the head aluminum mass, but rather the significantly lower amplitude local peak of $2 \mu\text{N}$ directed towards the tail (brass) big mass. Indeed, the net forces measured by Fearn and Woodward [26] have all been directed towards the tail brass mass. Thus, it is strongly suspected that, on the average they have managed their excitation frequency to be only within $\frac{0.75}{Q_m} = 0.395\%$ of the

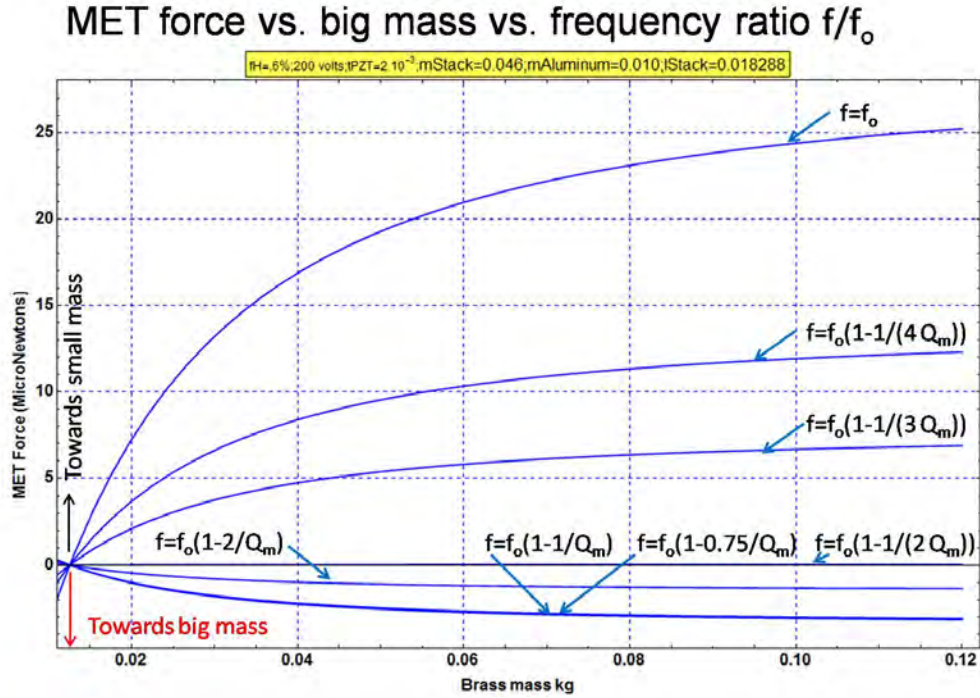


FIG. 29: Mach effect force vs. (brass) mass (kg) of tail end (up to 0.12 kg), for excitation frequency f to natural frequency f_o ratio of $f = f_o(1 - \frac{1}{NQ_m})$ for $N = \frac{1}{2}, 1, \frac{4}{3}, 2, 3, 4$ and ∞ . MEGA Langevin stack modeled as floating free in space.

natural frequency.

TABLE V: Optimal brass mass at which maximum Mach effect force occurs for different values of the excitation frequency to natural frequency ratio $\frac{f}{f_o}$. MEGA Langevin stack modeled as being held at the ends with a bracket much more compliant than the stack and held by a damping force at the ends.

frequency ratio $\frac{f_o - f}{f_o}$	$\frac{1}{NQ_m}$	Opt. brass mass (kg)	Max. Mach force (μN)	Force towards	Optimal f (kHz)	Optimal f_o (kHz)
1.053%	$\frac{1}{0.5Q_m}$	0.206	-0.4571	brass	29.874	30.192
0.526%	$\frac{1}{Q_m}$	0.106	-1.427	brass	31.701	31.869
0.395%	$\frac{0.75}{Q_m}$	0.0831	-2.031	brass	32.503	32.631
0.263%	$\frac{1}{2Q_m}$	0.0606	-2.575	brass	33.669	33.758
0.175%	$\frac{1}{3Q_m}$	0.0417	-1.588	brass	35.153	35.215
0	0	0.0830	17.16	aluminum	32.637	32.637

It is important to understand that this “optimal tail mass” is not a fixed characteristic of a stack and the head mass. First of all, the existence of such an “optimal tail mass” is entirely dependent on the boundary conditions. There is no optimal mass for the tail end of a MEGA Langevin stack floating in space, in which case the greater the tail end mass the greater the force, and it reaches an asymptote fairly quickly with practically no difference for tail end masses greater than 2 kg. The existence of an optimal tail (brass) mass is due to fixing the tail end and providing damping forces with a damper that is held at a fixed point in space. Under a fixed-end condition there is a different optimal tail mass depending on how far the excitation frequency is from the natural frequency. For example, one cannot really distribute at this Estes Advanced Propulsion Workshop to testing groups an “optimal brass mass” for the stack. Because there is no such

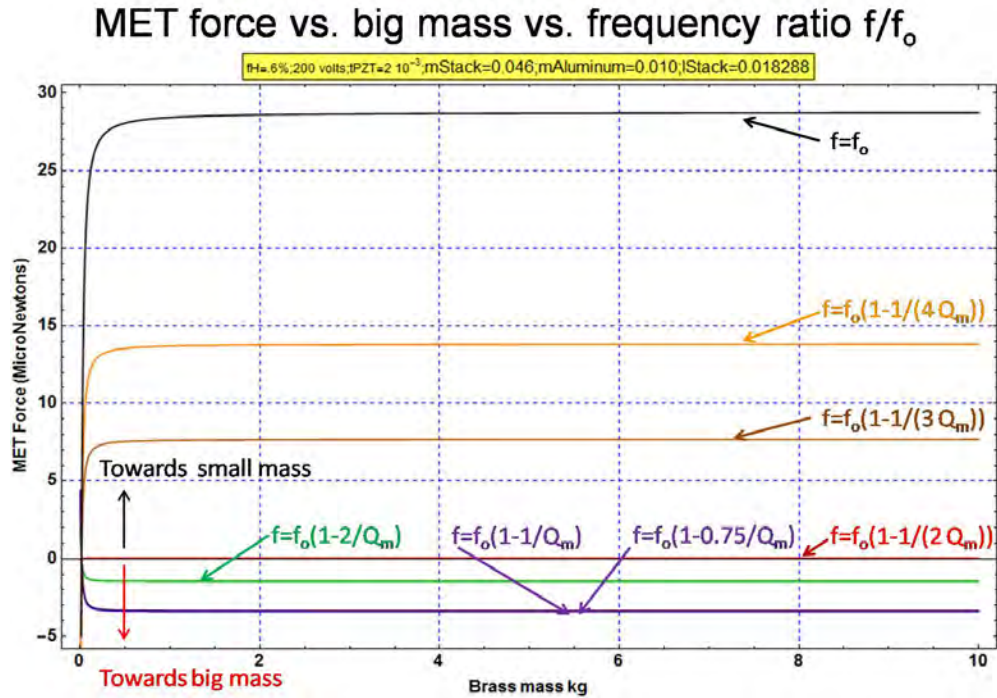


FIG. 30: Mach effect force vs. (brass) mass (kg) of tail end, for different values of the excitation frequency to natural frequency ratio $\frac{f}{f_0}$, showing the asymptotic behavior of the Mach effect force for infinite mass of the brass tail end of the stack (as would happen if the Langevin stack was attached to a very massive and rigid spacecraft in space).

optimal tail mass in general, as the optimal tail mass is a function not just of the head mass, and the material and geometry of the stack, but it is also a function of the stress and electrical history of the stack's material (since the electromechanical properties are history dependent, and the material is subject to internal damage, which affects several properties, including its natural frequency). Not just that, but the optimal tail mass is also a function of how far the excitation frequency is from the natural frequency. Therefore, even in the unlikely case that several groups were testing the same identical stack's material, with identical material history, and geometry, the optimal tail mass would be different if they tested with a different ratio of excitation frequency to natural frequency. For excitation frequencies that are further away than $\frac{1}{2Q_m}$ from the natural frequency, the larger the ratio between the excitation frequency to the natural frequency, the larger the "optimal tail mass" will be. If the excitation frequency is 1% away from the natural frequency, the optimal tail brass mass is twice as large as for a difference of 0.5%.

Fig. 35 is a plot, under a fixed-end condition constraint, of the Mach effect force vs. (brass) mass (kg) of tail end, for different values of the excitation frequency to natural frequency ratio $\frac{f}{f_0}$, showing the asymptotic behavior of the Mach effect force for infinite mass of the brass tail end of the stack. One sees that the Mach effect force decreases, from its optimal value, but that it is still finite for infinite tail mass. For example, for excitation frequency identical to the natural frequency (27.82 kHz for any value of excitation frequency because the brass mass is asymptotically infinite in this example) the Mach effect force is half (8.51 μN) of the value (17.16 μN) for the optimal mass. With an excitation frequency of $\frac{1}{2Q_m}=0.263\%$ less than the resonant frequency, the asymptotic limit for infinite tail brass mass gives a Mach effect force close to zero, while, using the optimal mass, it gives a local maximum for the Mach effect force. And using an excitation frequency of $\frac{1}{0.5Q_m}=1.053\%$ less than the resonant frequency, the asymptotic limit for infinite tail brass mass gives a Mach effect force practically identical (94% or 0.43 μN) to the Mach effect force (0.46 μN) using an optimal tail mass for that difference between the excitation frequency and the natural frequency. This is all summarized in Table 6.

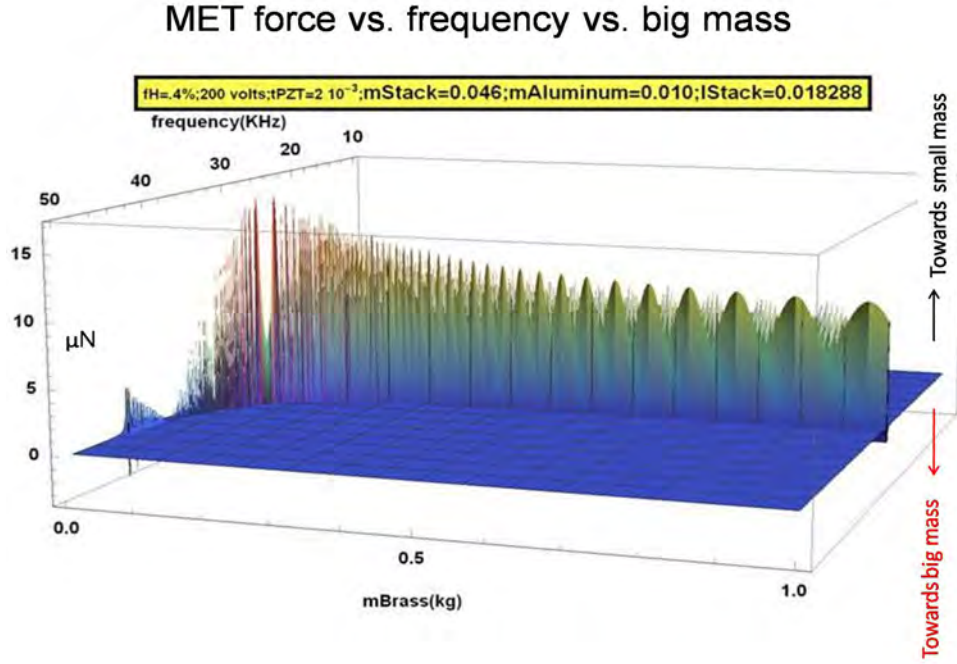


FIG. 31: 3D Plot of Mach effect force (μN) vs. frequency (kHz) vs. (brass) mass (kg) of tail end. MEGA Langevin stack modeled as being held at the ends with a bracket much more compliant than the stack and held by a damping force at the ends.

TABLE VI: Mach effect force for infinite brass mass for different values of the excitation frequency to natural frequency ratio $\frac{f-f_o}{f_o}$. MEGA Langevin stack modeled as being held at the ends with a bracket much more compliant than the stack and held by a damping force at the ends.

frequency ratio $\frac{f-f_o}{f_o}$	$\frac{1}{NQ_m}$	m_∞ Mach force (μN)	Force towards	$m_\infty f$ (kHz)	$m_\infty f_o$ (kHz)
1.053%	$\frac{1}{0.5Q_m}$	-0.43	brass	27.53	27.82
0.526%	$\frac{1}{Q_m}$	-1.01	brass	27.68	27.82
0.263%	$\frac{1}{2Q_m}$	0.009	aluminum	27.75	27.82
0	0	8.51	aluminum	27.82	27.82

7. CONCLUSIONS

It is evident from the images, Figs. 10 and 11, for the MEGA (Mach effect Gravitational Assist) drive stack tested by Fearn and Woodward and its description [25], [26] and [55], that it is a conventional Langevin stack, similar to the typical Langevin transducers that have been used for decades in many applications since Langevin invented it in 1916: with a small aluminum head mass, and a piezoelectric stack composed of modified PZT-4 (US Navy Type I) plates (a material similar to those marketed by US firm Clevite in 1957). The one unconventional choice is the use of a tail mass made of brass, reportedly because it was desired to provide a heat sink for thermal diffusion of heat generated by dissipation in the PZT stack during vibration. The present choice of brass for the tail mass is not optimal: the brass could be substituted by copper, in order to increase thermal conductivity by a factor of 3.5 times and to increase thermal diffusivity by a factor of 3.4 times. If the cost of silver at 59 US dollars per 100 grams (compared to copper at 0.49 US dollars per 100 grams, and brass at 0.29 US dollars per 100 grams) is not an issue, silver would be an even better choice for the tail mass, since it would improve thermal conductivity by a factor of 3.7 times and the more important (for unsteady heat conduction) thermal diffusivity by a factor of 5 times, as compared to the present choice of brass. Other choices for the electrode should be investigated instead of the present

MET force vs. frequency vs. big mass

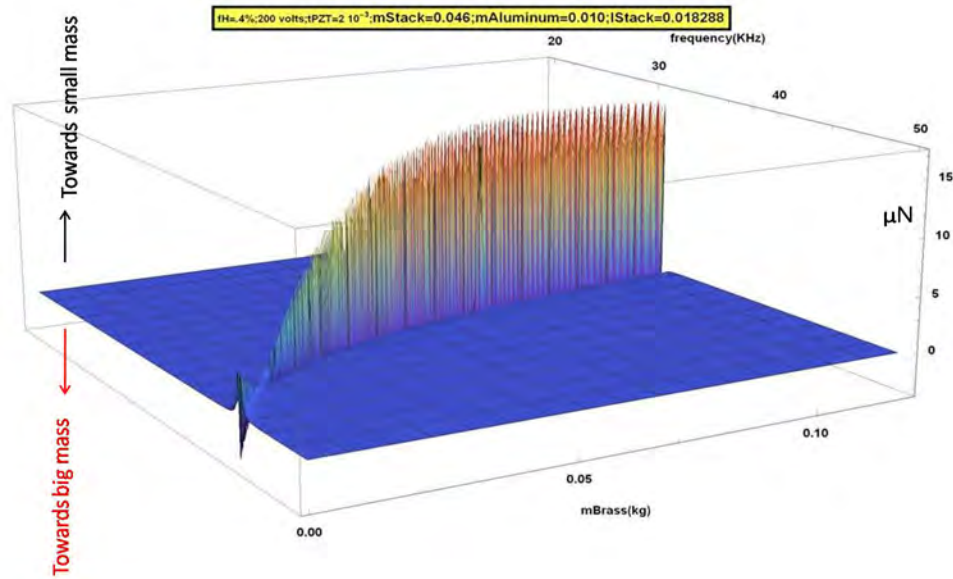


FIG. 32: 3D Plot of Mach effect force (μN) vs. frequency (kHz) vs. (brass) mass (kg) of tail end. Detail close-up of (brass) tail mass lower than 0.1 kg. MEGA Langevin stack modeled as being held at the ends with a bracket much more compliant than the stack and held by a damping force at the ends.

brass electrodes, for example, copper and silver.

The present choice of stainless steel for the bolts that apply the necessary compression to the PZT plates is not optimal, because of thermal expansion mismatch with the PZT plates, leading to loss of compression, and hence to damage and decrease of stiffness of the PZT plates. Worst of all, this thermal expansion mismatch also leads to de-tuning between the excitation frequency and the natural frequency of the MEGA stack, and hence to a substantial decrease in the Mach effect force. This is confirmed by the experimental data of Fearn et.al.[9] displayed in Fig. 13, where the turquoise trace is the output from one or more pairs of 0.3 mm thick passive PZT plates in the MEGA Langevin stack. The direct piezoelectric effect, where the piezoelectric material (PZT) responds to strain by generating an electric voltage, is used in one or more pairs of passive 0.3 mm thick piezoelectric plates in the MEGA drive Langevin stack. They measure the strain, through the thickness of the PZT, resulting from the stress transmitted from the other plates in the stack. They act essentially as strain gauges. Scientific piezoelectric accelerometers are restricted to operating at excitation frequencies lower than 3 dB below the first natural frequency (in other words, approximately below $\frac{1}{2}$ of the first natural frequency). This limit, restricting the excitation frequency to be below $0.5f_o$, $\frac{1}{2}$ of the first natural frequency, marks the frequency where the measuring error becomes 30%. (At approximately $0.3f_o$, $\frac{1}{3}$ of the first natural frequency, the error is 10%, while at approximately $0.2f_o$, $\frac{1}{5}$ of the first natural frequency, the error is 5%). If the exciting frequency becomes closer to the natural frequency, the error becomes much larger (the measured strain becomes unrepresentative of the acceleration, due to the fact that close to the natural frequency the damping term in the equations of motion starts to dominate the amplitude of the response). For the MEGA drive experiments, Fearn and Woodward purposefully operate the stack at an excitation frequency closer than $\frac{0.75}{Q_m}$ to the natural frequency of the Langevin stack (which has a mechanical-quality-factor-of-resonance (Q_m) equal to 190). Therefore, for the MEGA drive experiments conducted by Fearn and Woodward, the output of the passive PZT plates is unrepresentative of the acceleration, and instead should be interpreted strictly as representing solely the strain through the thickness of the PZT plate. Therefore the turquoise trace in Fig. 13 shows the strain vs. time in the MEGA PZT passive plates. As one can see, the strain steadily decreases at a steady slope with time (after a short initial faster nonlinear decay). The compressive strain decreases with time as the temperature in the stack increases, and this is a natural result of loss of compressive stress as the stainless steel bolts expand with temperature with a much higher coefficient of thermal expansion than the one of the PZT plates. Instead of stainless-steel, a material

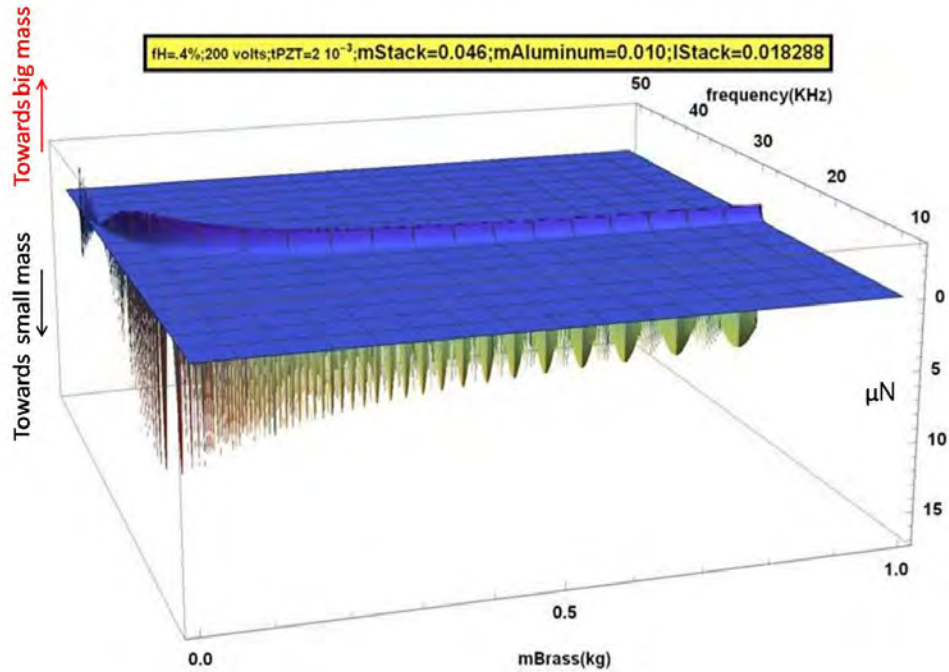


FIG. 33: 3D Plot of Mach effect force (μN) vs. frequency (kHz) vs. (brass) mass (kg) of tail end. View of force directed towards the (brass) mass tail end. MEGA Langevin stack modeled as being held at the ends with a bracket much more compliant than the stack and held by a damping force at the ends.

with a much smaller coefficient of thermal expansion should be used. For example Nabeya Bi-tech Kaisha (NBK) [16] bolts made of super invar with a thermal expansion coefficient 25 times smaller than the one of stainless steel, will better match the coefficient of thermal expansion of the PZT plates in their thickness direction.

The present choice of adhesive (unfilled Bisphenol A epoxy) could be substituted by a filled epoxy to raise thermal conductivity (aluminum nitride or boron nitride filled epoxy) to a similar value as PZT, and if desired, the electrical conductivity (a silver-filled epoxy) as well. Also a filled adhesive with a higher glass transition temperature (for example a polyimide adhesive like Creative Materials 124-41 with a thermal conductivity of $11 \text{ W}/(\text{m K})$ as compared to the present unfilled epoxy $0.17 \text{ W}/(\text{m K})$ should also be investigated, because the present adhesive is limiting the upper temperature of the MEGA Drive due to loss of integrity of the adhesive due to its glass transition temperature being significantly lower than the Curie temperature of the PZT. Also co-sintering of the MEGA PZT-electrodes stack should be investigated, as co-sintering would eliminate the adhesive altogether, and involve much thinner electrodes. Newer piezoelectric materials should be investigated to replace the 64 year old PZT, materials like high-Curie-temperature ferroelectric single-crystal Mn doped PIN-PMN-PT discussed by Zhang et.al. [17].

Fearn et.al. [25] [26] outline a derivation of the Woodward Mach effect thruster theory based on the Hoyle-Narlikar field equation that Fearn shows to have the same type of mass fluctuation terms. The force equation, used to predict the thrust in the MEGA drive, can be derived from the mass fluctuation. In General Relativity, length, and hence surface and volume, are observer dependent and hence not invariant like mass. This argues for the time derivatives of the mass field to govern the fluctuation in inertial mass, instead of the mass fluctuation being governed by mass density (which is observer dependent due to the observer-dependence of the volume) as done for example in other derivations. This distinction is irrelevant for isochoric media (e.g. perfect fluids or idealized elastomers) or for solid media undergoing isochoric (equivoluminal) deformation, but it may be relevant when considering solids like piezoelectric materials that are not isochoric and that undergo non-isochoric deformation. I show that the inertial mass fluctuation is due to the second derivative with respect to time of the kinetic energy per unit mass, divided by the gravitational constant G and the square of the speed of light. The only assumptions involved in this conclusion have been: 1. Hoyle-Narlikar's theory of gravity (dropping the creation "C" field, and neglecting the gradients of mass terms, assuming spatial homogeneity of the mass function in a smooth mass field approximation), 2. speed

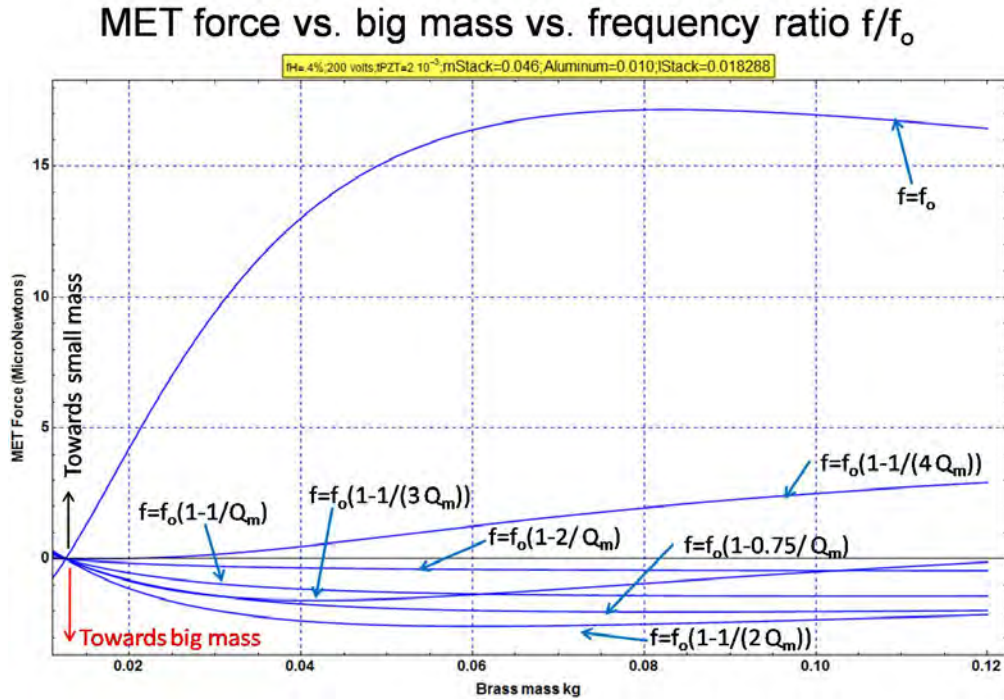


FIG. 34: Mach effect force vs. (brass) mass (kg) of tail end (up to 0.12 kg), for excitation frequency f to natural frequency f_0 ratio of $f = f_0(1 - \frac{1}{NQ_m})$ for $N = \frac{1}{2}, 1, \frac{4}{3}, 2, 3, 4$ and ∞ . MEGA Langevin stack modeled as being held at the ends with a bracket much more compliant than the stack and held by a damping force at the ends.

of material points negligibly small compared to the speed of light and 3. second derivative with respect to time of the natural logarithm of the rest mass negligibly small compared to the second derivative with respect to time of the kinetic energy per unit mass. The second derivative with respect to time of the kinetic energy per unit mass is a function of the square of the acceleration $\frac{\partial v}{\partial t}$, and the product of the velocity v times the time rate of the acceleration $\frac{\partial^2 v}{\partial t^2}$ (the second derivative with respect to time of the velocity) of the mass points, which is also called the “jerk.” The presence of the jerk $\frac{\partial^2 v}{\partial t^2}$ is significant because it has been shown by Sprott [35] [36] in the field of chaotic dynamics that an equation involving the jerk is the minimal setting for solutions that can show chaotic behavior. It is interesting to consider whether the solution of the Machian force due to inertial mass fluctuations (a system of coupled nonlinear differential equations involving the jerk, the acceleration and the velocity) of a piezoelectric/electrostrictive Langevin stack undergoing vibrations may be capable of showing chaotic, complex dynamic behavior. Such chaotic, complex dynamic behavior may result in different dynamic behavior regimes and perhaps it can be exploited to maximize the response if properly engineered.

I modeled two different conditions. In the first and main condition, the MEGA drive is in space, free of any boundary fixity constraints (modeling the MEGA drive as rigidly attached, at the tail end of the Langevin stack, to the spacecraft’s center of mass, with the spacecraft considered a rigid body). In the second condition, I modeled the MEGA drive in the Woodward and Fearn experiments as being held at the ends with a bracket much more compliant than the stack and held by a damping force at the ends. I modeled the MEGA drive as a dynamic system composed of two unequal, lumped, end masses (the front mass and the tail mass) connected by a viscoelastic piezoelectric/electrostrictive stack. Obviously, to calculate the maximum amplitude of a vibrating system it is imperative to consider non-zero damping because for zero damping, the response will have infinite amplitude at resonance, which is an unphysical result. The exact solution to the coupled differential equations of motion for the dynamic system of two unequal masses with damping and stiffness, excited by piezoelectricity and electrostriction, can be decomposed into a piezoelectric solution for the displacement of each end mass, with an in-phase and an out-of-phase component, for a total of 4 terms; and an electrostrictive solution for the displacement of each end mass, with an in-phase and an out-of-phase component, for a total of an additional 4 terms; so the solution has 8 such terms. Piezoelectric resonance occurs when the voltage excitation frequency ω equals the first natural frequency of the MEGA

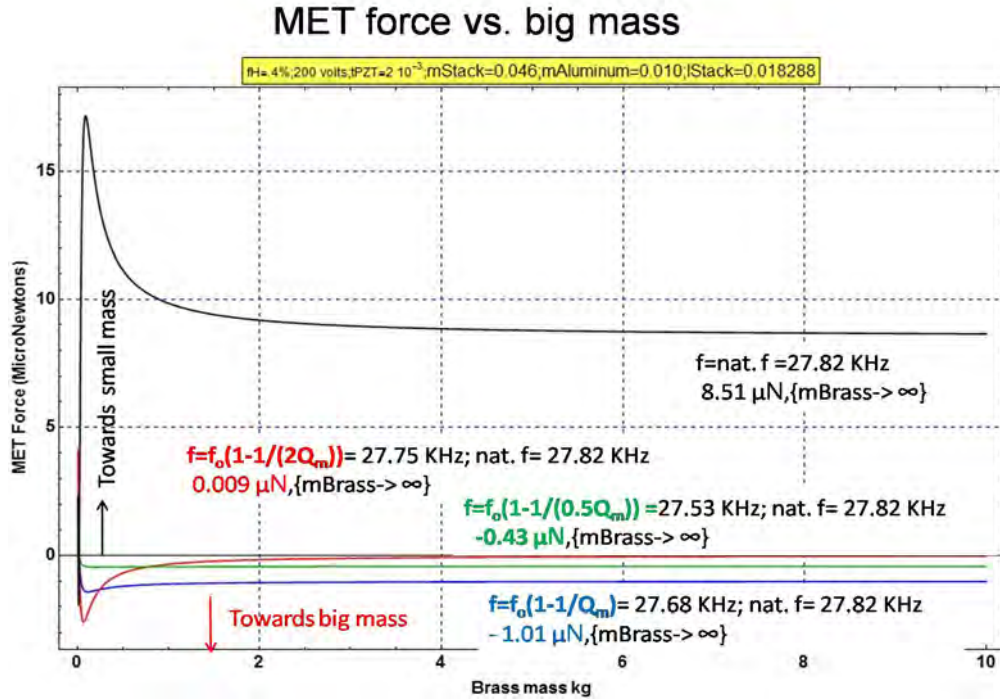


FIG. 35: Mach effect force vs. (brass) mass (kg) of tail end, for different values of the excitation frequency to natural frequency ratio $\frac{f}{f_o}$, showing the asymptotic behavior of the Mach effect force for infinite mass of the brass tail end of the stack. MEGA Langevin stack modeled as being held at the ends with a bracket much more compliant than the stack and held by a damping force at the ends.

drive ω_o . One can see, Fig. 14, that the calculated natural frequency falls within the experimentally measured values. The calculated values of natural frequency are based on the book value of the modulus of elasticity provided by the supplier, who does not specify the values of these variables during the testing of the PZT that resulted in those book values. Furthermore, the piezoelectric stack is a composite where several layers (PZT plates, brass electrodes and adhesive layers) are sandwiched together by hand, where the adhesive has a modulus of elasticity much lower than the one of the PZT. Also, the actual stack is a continuum with a very large number of material points, rather than a simple 2-mass lumped system connected with a viscoelastic spring and dashpot as in the numerical model, and it is known that the actual natural frequency of such a continuum will be different than the one calculated in this simplified numerical model. Considering all the above factors, the comparison between the calculated and the measured natural frequency is very reasonable, particularly considering the unknown electromechanical state of the piezoelectric stack, and the level of damage (a more damaged stack will have a lower stiffness and hence a lower natural frequency, Fig. 19), at the time of the natural frequency measurements.

The Mach effect force on the center of mass is calculated as the product of the total mass times the acceleration of the center of mass [38]. The acceleration of the center of mass contains terms (due to Mach effect inertial mass fluctuations) of the form of the product of the time derivative of the mass fluctuation times the velocity, and of the form of the product of the second time derivative of the mass fluctuation times the displacement, as well as square terms of the previously mentioned expressions. As a result of these multiplications, trigonometric expressions due to the product of harmonic terms at frequency ω (due to piezoelectric excitation) multiplying harmonic terms at frequency 2ω (due to electrostrictive excitation) occur, that give constant uniaxial force terms. There is a total of 289 such terms that contribute to the Mach effect force. The solution is an exact analytical solution, that is solved using Wolfram *Mathematica*.

A fundamental difference between the exact solution discussed in this article and previous efforts by Fearn and Woodward [25], [26], [55] at calculating the Mach effect force is that I have taken into account that the problem is one of vibration and hence that damping (or the inverse measure, the mechanical quality of resonance) and stiffness of the stack have a most important role in the value of the Mach effect force. The previous solutions by Fearn and Woodward [25], [26], [55] did not involve important material properties

like the mechanical quality of resonance or the modulus of elasticity. Note that Fearn and Woodward [25], [26], [55] use *dimensional* ad-hoc factors in their Mach effect force calculation. One can readily extract this information from their unconventional definitions of their piezoelectric constant K_p and their electrostrictive constant K_e , where Fearn and Woodward define their constitutive equations in terms of the strain to voltage ratio, instead of the strain to electric field ratio. They define the piezoelectric strain as $\epsilon_{p33} = K_p V_3$ instead of the proper constitutive relationship $\epsilon_{p33} = d_{33} E_3 = d_{33} \frac{V_3}{l_{plate}}$, where l_{plate} is the thickness of the piezoelectric plates, and the electric field in the thickness direction E_3 is assumed constant through the thickness of the plate. Therefore $K_p = \frac{d_{33}}{l_{plate}}$. Similarly, Fearn and Woodward use an unconventional definition of the electrostrictive constant K_e , in terms of the strain to voltage ratio, instead of the strain to electric field ratio. They define the electrostrictive strain as $\epsilon_{e33} = K_e (V_3)^2$ instead of the proper constitutive relationship $\epsilon_{e33} = M_{33} (E_3)^2 = M_{33} (\frac{V_3}{l_{plate}})^2$. Therefore $K_e = \frac{M_{33}}{l_{plate}^2}$. In Fearn and Woodward's experimental example, the thickness of the plates l_{plate} is taken as 0.002 m, therefore their piezoelectric constant is $K_p = \frac{d_{33}}{0.002} = \frac{d_{33}}{0.2\%}$ and their electrostrictive constant is $K_e = \frac{M_{33}}{0.002^2} = \frac{M_{33}}{0.04\%}$. The thickness of the PZT plate (0.002 m for their PZT plate thickness example) appears as an extraneous factor in these material constants, due to the unconventional choice of constitutive parameters. Then, for the piezoelectric constant K_p , they take the book value of $d_{33} = 320 \times 10^{-12}$ m/V from Steiner & Martins SM-111, to be the value of K_p (and in doing so, they disregard the different units of d_{33} (m/V) and K_p (1/V)). Therefore they set the magnitude of $K_p = 320 \times 10^{-12}$ (1/V), but since their definition for K_p was $K_p = \frac{d_{33}}{0.002} = \frac{d_{33}}{0.2\%}$, in doing so they effectively set $d_{33} = 0.2\% \times 320 \times 10^{-12}$ m/V instead of the correct book value for d_{33} , which amounts to using an ad-hoc constant of 0.2% multiplying the book value of the Steiner & Martins SM-111 piezoelectric constant d_{33} . The reason for the appearance of these extraneous length dimensional factors is that Fearn and Woodward define their constitutive equations in terms of the strain to voltage ratio, instead of the strain to electric field ratio. The proper field variable in piezoelectric and electrostrictive constitutive relations should be the electric field instead of the voltage. Fearn and Woodward [26] state $N f_p \approx l_o$ and therefore that their *dimensional* coupling factor is $f_p \approx \frac{l_o}{N} \approx l_{plate}$ where N is the number of PZT plates and l_o is the length of the stack, and therefore that their coupling factor is the thickness of each plate ($l_{plate} = 0.002$ m in their example), but I find this justification for the coupling factor unconvincing, based on a) correct dimensions of the constitutive variables (the constitutive variables should be formulated in terms of the electric field instead of the voltage), b) the well-established constitutive equations of theory of electroelasticity and c) the thorough analysis of a Langevin stack by Martin [37] at the U.S. Navy Electronics Laboratory, San Diego, California, in the early 1960's.

Concerning the input variables for this analysis, it is noted that in order to match the magnitude of the experimentally measured Mach effect force, using book values for the material constants it is also necessary in my analysis to introduce an ad-hoc *non-dimensional* factor of 0.6% multiplying the piezoelectric coefficient d_{33} and the electrostrictive coefficient M_{33} , when modeling the MEGA Langevin stack free in space. Preliminary modeling of the MEGA Langevin stack restrained at the ends by a damping force needs an ad-hoc *non-dimensional* factor of 0.4% multiplying the piezoelectric coefficient d_{33} and the electrostrictive coefficient M_{33} to match the magnitude of the experimentally measured Mach effect force, when using book values for the material constants. This *non-dimensional* factor is about 100 times smaller than the coupling coefficient one would expect based on electromechanical coupling. Since the total Mach effect force is comprised of the multiplication of three force excitation factors, (one factor with frequency 2ω due to the electrostrictive excitation force times two factors with frequency ω due to the piezoelectric excitation force) the total *non-dimensional* coupling factor for the Mach effect force (multiplying the reduced mass times the excitation frequency to the sixth power, divided by the product of the gravitation constant G times the square of the speed of light) is of the order of $(10^{-2})^3 = 10^{-6}$.

The reason for the need of this coupling factor (10^{-2} on the excitation force) based on book values of material properties (needed to match the experimental results on this study and, as shown above, also used in previous papers by Fearn and Woodward) remains to be fully explored. Following is a consideration of different possible explanations:

- Arguable validity of the Mach effect propulsion hypothesis for our Universe. If the argument were made that it is physically invalid, one would need to otherwise explain: a) the physical nature of the net unidirectional force that has been measured by Woodward and Fearn, as well in other replication experiments independently conducted by N. Buldrini at Forschungs- und Technologietransfer in Austria, G. Hathaway in Canada and by M. Tajmar at TU Dresden in Germany (described in other articles in this workshop proceedings), b) the fact that experimental measurements with a symmetric Langevin stack (with equal tail and head masses) result in no measured net unidirectional force, c)

reported experimental measurements of the force scaling like the fourth power of the exciting voltage, and therefore (for uniform thickness of the piezoelectric plates in the Langevin stack) like the fourth power of the exciting electric field (the Mach effect force is predicted to be proportional to the fourth power of the electric field because it is due to the product of the second power of the piezoelectric strain excitation times the first power of the electrostrictive strain excitation), and d) the success of the present calculations to correctly predict the experimental measurements for the direction of the Mach effect net force as well as accurately predicting the experimentally measured optimal mass of the tail brass end, that maximizes this Mach effect force.

- The effect of neglecting the gradients of mass terms appearing in the full derivation of the mass fluctuation based on Hoyle-Narlikar theory. Such mass transport might take place for example due to electric gradients, and due to coupling with temperature gradients. This may be particularly relevant at the interface of the electrodes with the piezoelectric (PZT) plates, due to migration of metallic species (e.g. copper) from the electrode into the dielectric.
- The effect of neglecting a number of mass fluctuation (time differential) terms in the derivation, assuming they were too small. Most important among these neglected terms are the derivatives of mass with respect to time terms that would multiply the velocity in the equations of motion, as for low damping materials (high mechanical quality factor of resonance) these mass fluctuation terms may not be negligible.
- Fluctuations in internal energy that have been disregarded in the analysis. The analysis considers only the mass fluctuations due to kinetic energy. I also take the position that external potential energy terms (see the previous discussion regarding the analysis of Brillouin, Medina and others regarding hidden momentum terms) that such external energy and momentum carried by the fields is automatically taken into account in the Hoyle Narlikar theory of gravitation through the energy-stress tensor, physically through advanced-retarded waves, and that they do not need to be incorporated as extra mass terms.
- The Mach effect mass fluctuations, rather than affecting the whole mass density of an object, as assumed in this analysis, may mainly affect the bonds that hold the mass particles together, as when a solid is deformed, the strain affects mainly the bonds between the particles.
- Material properties: modulus of elasticity Y_{33} and masses: it is unlikely that the discrepancy is due to either the modulus of elasticity or the mass values because the calculated natural frequency is very close to the measured natural frequency and because the optimal brass mass is accurately calculated.
- Material nonlinearity: strain vs. electric field hysteresis. As shown in Fig. 16 (from Fig. 2 of Zhang et.al. [52]), the magnitude of the applied electric field in this example of MEGA drive experiments, 1 kV/cm, is 20 times smaller than the electric field that results in significant nonlinearity (strain vs. electric-field hysteresis due to piezoelectric internal damping losses) for PZT-4. Hence, the data shows that strain vs. electric field nonlinearity is unlikely to be the reason for the ad-hoc factor needed to be used in these calculations.
- Material nonlinearity: polarization vs. electric field hysteresis nonlinearity. Fig. 17 shows that PZT-4 has a larger hysteresis than the other two materials, at the high level (40 kV/cm) of electric field magnitude used in the experiments plotted in that figure. The electric field magnitude used for the MEGA experiments (1 kV/cm) is 40 times smaller than for the example shown in Fig. 17 (and also smaller by a factor of 3 than the internal bias field used in this example). Of course, care should be taken in MEGA drive experiments to perform experiments at identical electric field magnitudes, rather than identical voltage excitation magnitudes. For example, if the same voltage excitation were used for PZT plates 1 mm thick instead of 2 mm thick, the electric field would be twice as large in the stack with the thinner plates, and hence closer to the region of nonlinearity. Waechter et.al. [53] report energy density loss data, calculated from integration of (polarization vs. electric field) hysteresis loop data, Fig. 18, for Navy Type I (PZT-4) and Navy Type III (PZT-8) hard-doped PZT materials used in sonar transducers. It is evident from these data that the magnitude of the applied electric field, 1 kV/cm = 0.1 MV/m, in this example of MEGA drive experiments using a modified form (SM-111 from Steiner & Martins) of PZT-4, is very small compared with the amplitude of electric field required for significant energy density loss. Therefore, independently confirming that this magnitude of applied electric field, 1 kV/cm = 0.1 MV/m, should be safely within the approximately linear, small loss range. Therefore, the data shows that polarization vs. electric field nonlinearity is unlikely to be the reason for the ad-hoc factor needed to be used in these calculations.

- Thermal effects. As shown in Figs. 12 and 13 (from Figs. 3 and 4 of [9]) the transient temperature peak measured in the front aluminum mass was reported as 18 °C above initial temperature, and the transient temperature peak measured in the back brass mass was reported as 8 °C (which is consistent with the aluminum mass having 2.56 times higher thermal diffusivity than the brass mass, and therefore being able to more rapidly diffuse the temperature generated in the PZT stack). Also, the maximum transient temperature measured in the aluminum was 45 °C. This temperature is much lower than the Curie temperature of 320 °C for the modified PZT-4 material used in the stack (SM-111 from Steiner & Martins), even allowing for the fact that the transient temperature inside the PZT must have reached a higher temperature than the temperature measured at the end metal masses. Furthermore, the mechanical quality factor of resonance Q_m for PZT-4 is fairly constant from room temperature to at least 150 °C (page 11 of [15]), a temperature much higher than the measured temperatures in the MEGA stack experiments of Fearn et.al. [9]. Similarly, Hooker, on page 19 Fig. 10 of [58], shows that the effective electro-mechanical coupling coefficients of PZT-4 only begin to have a gentle drop-off after 150 °C. Also (polarization vs. electric field) hysteresis data for PZT-4 show appreciable changes only for temperatures exceeding 125 °C. Therefore, the temperatures measured by Fearn et.al. [9] do not indicate that the MEGA stack reached temperatures high enough to appreciably influence the material properties. Fig. 13 shows that the temperatures in the aluminum and brass masses were still increasing at the end of the 14 second run of the MEGA stack, because the internally generated heat exceeded the heat being transiently conducted in both the aluminum and the brass masses. Therefore, the maximum temperature that a MEGA stack will reach under the present design is a function of the time duration of the run. The shorter the run, the lower the temperature. The longer the run, the higher the temperature. Besides using a back mass with significantly higher thermal diffusivity (copper, or preferably silver instead of the present inferior choice of brass), active cooling may be required. Therefore, under the present design of the MEGA drive, care has to be exercised regarding temperature effects, because with the present design (relying only on passive cooling and using a material like brass that has lower thermal diffusivity than copper or silver) the stack may reach temperatures that will affect material properties if run long enough. I would recommend that more detailed temperature measurements are made to further characterize the transient temperatures throughout the stack during a test, and that a detailed numerical model of the MEGA stack, as well as of thermal expansion changes (including viscoelastic compression set of the PZT stack) are carried out.
- Material properties: since the ad-hoc factor multiplies the piezoelectric constant d_{33} and the electrostrictive constant M_{33} , the book values taken for these material constants are prime suspects for the need to adopt an ad-hoc multiplying factor. Perhaps the tested materials have values substantially lower than book values, either due to damage (due to micro cracks, and voids between grains) and/or electroelastic history. The piezoelectric constant d_{33} and the electrostrictive constant M_{33} of the actual stack should be measured, for example, using strain gauges. For example, the book value (from the supplier, Steiner & Martins) of the mechanical quality factor of resonance Q_m is 1800, but the measured value for the actual stack used for the MEGA experiments is only 190, which shows a severe degradation of the actual mechanical quality factor of resonance Q_m compared to the book value. If these calculations had been carried out using the book value of mechanical quality factor of resonance Q_m instead of the actual value, there would have been a huge discrepancy between calculated and actual magnitudes of response, as the amplitude of resonant response near the natural frequency is very dependent on the magnitude of the mechanical quality factor of resonance Q_m .
- The electric field limit used in MEGA experiments is 10 times higher than industry standard based on reliability. Jones and Lindberg [54] state that for Navy Type III (PZT-8) piezoelectric ceramics, an electric field limit of 10 V/mm = 0.1 kV/cm (determined on a root mean square basis) has been chosen as an industry standard based on considerations of both reliability and acceptable losses. This reliability limit is 10 times smaller than the electric field used for the MEGA experiments and for this numerical example. Since Navy Type III (PZT-8) is a hard-doped PZT with fairly similar properties as the modified Navy Type I (PZT-4) material (with trade name SM-111 from supplier Steiner & Martins) used for the MEGA experiments, and as shown by Waechter et.al. [53] Navy Type III (PZT-8) has significantly greater fracture toughness than Navy Type I (PZT-4), one would expect that the electric field limit for Navy Type I (PZT-4) should be smaller than 0.1 kV/cm and hence this indicates that the 1 kV/cm applied to the MEGA experiments is already more than 10 times higher than the industry standard based on considerations of reliability. This is another prime suspect reason for the need to apply an ad-hoc multiplying factor on the book values of the piezoelectric and electrostrictive

constants. The importance of the fracture mechanics and fatigue reliability limit has been known for a long time. For example, W. Mason (head of Mechanics Research at Bell Labs), pointed out in 1958 (p. 157 of [59]) that:

“For dynamic conditions, the amount of strain can be increased by the buildup of vibrations as a function of time. Here the limitation is either the strength of the material, the heat produced by the electrical input to the transducer, or the Q of the transducer with its associated load.... For relatively high Q systems, it is usually the breaking or fatiguing strength of the transducer material or associated vibrating parts that provides the limitation.... The third limitation, that of heating, is generally worse for a magnetostrictive transducer than for a piezoelectric or electrostrictive transducer, and usually requires auxiliary cooling to overcome it.”

It is clear that several of the effects discussed above cannot be responsible for the piezoelectric and electrostrictive coupling factor of 10^{-2} needed to match the experimental results. For example, material nonlinearity due to strain vs. electric field hysteresis, or due to polarization vs. electric field hysteresis cannot be responsible because the strains and electric field values in Woodward and Fearn’s experiments are significantly lower than the values needed for material nonlinearity. On page 261 of his book [57], Woodward states: “More difficult than the forgoing theoretical activities is investigation of the way in which Mach effects are generated. That is, the detailed examination of how changes in the internal energies of materials take place, and how that relates to the production of Mach effects should be examined. Although it is clear that internal energy is stored in the interatomic bonds of the dielectric materials in the capacitors involved in the experiments described in Chaps. 4 and 5, it is not clear how that process produces the Mach effects predicted, or where exactly the mass fluctuations take place.” Also, on page 100 of [55] Fearn and Woodward state “Capacitors store energy in the electric field between the plates or, as in this case, in the electric polarization of the dielectric medium by ion core displacements. The condition that the capacitor rest mass vary in time is met as the ions in the lattice are accelerated by the changing external electric field. If the amplitude of the proper energy density variation and its first and second time derivatives are large enough, a small (10^{-11} Kg) mass fluctuation should ensue. That mass fluctuation, δm_o , is given by Eqn.(8) above. Note that the assumption that all of the power delivered to the capacitors ends up as a proper energy density fluctuation is an optimistic assumption. Some of this energy is likely stored in the gravitational field, and some will dissipate as heat. Nonetheless, it is arguably a reasonable place to start.”

Yes, indeed, if the Woodward mass fluctuation propulsion hypothesis is real, the most plausible explanation for the small value of the coupling factor seems to be that the mass fluctuations do not take place uniformly over the entire piezoelectric-electrostrictive material mass, but most significantly take place only over a small proportion of its total inertial mass. However, why the coupling factor on the piezoelectric and electrostrictive forces should be 10^{-2} or the coupling factor on the total Mach effect force should be 10^{-6} is unclear, as for example the electron-to-proton (dimensionless) mass ratio is 5.446×10^{-4} . Another reason to back this view, that the Mach effect mass fluctuations take place only over a small proportion of its total inertial mass, is shown in Fig. 23. This figure shows that the Mach effect force is composed of two terms: a main component proportional to the sixth power of the frequency and a second order term proportional to the tenth power of the frequency. The term proportional to the tenth power of the frequency is negligible compared to the main component proportional to the sixth power of the frequency, as long as the inertial mass fluctuations are negligibly small. Using a coupling factor on the piezoelectric and electrostrictive forces of 0.6% results in the term proportional to the tenth power of the frequency being negligible, as shown in Fig. 23. However, increasing the magnitude of this coupling factor results in greater mass fluctuations and this term proportional to the tenth power of the frequency becomes dominant, which is unphysical and unintuitive. In other words, if there were no need for a coupling factor on the piezoelectric and electrostrictive forces of 0.6%, the mass fluctuations would be orders of magnitude larger, the Mach effect force would be orders of magnitude larger, and it would be governed mainly by the tenth power of the frequency, with unphysical results. Such forces would have already been measured in countless experiments, man-made and natural phenomena. If the mass fluctuations were orders of magnitude larger this would also be in contradiction with this mathematical analysis, since the mathematical derivation was conducted under the assumption of small mass fluctuations.

Focusing now on the calculated Mach effect force results, a very small amplitude subharmonic response Mach effect force is calculated to take place due to the electrostrictive effect: a nonlinear excitation proportional to the square of the electric field, when the electrostrictive voltage excitation frequency 2ω equals the first natural frequency of the MEGA drive ω_o , this happens at one half the first piezoelectric natural frequency: $\omega = \frac{1}{2}\omega_o$. As shown in Fig. 21, there is a subharmonic peak at the lower resonant frequency of 16.714 kHz (16.74 kHz for damping force with restrained end), with a Mach effect force magnitude of only

5.25 nanoNewtons (2.38 nanoNewtons for damping force with restrained end), directed towards the front (aluminum) small mass, immediately followed by a slightly higher subharmonic resonant frequency of 16.802 kHz (16.78 kHz for damping force with restrained end), oriented in the opposite direction (towards the tail (brass) big mass), with a Mach effect force magnitude of only 5.35 nanoNewtons (2.78 nanoNewtons for damping force with restrained end). The magnitude of the Mach effect force at the first piezoelectric natural frequency is 4,000 times (7,000 times for damping force with restrained end) larger than this subharmonic electrostrictive response, because the value of the piezoelectric constant d_{33} (strain linearly proportional to the electric field) is 24 million times greater than the value of the electrostrictive material constant M_{33} (strain due to the square of the electric field), and the electric field (1 kV/cm) is not high enough to fully compensate for this difference, Fig. 15.

As the first fundamental frequency due to piezoelectricity is approached from lower, or higher frequencies, that are more than $\frac{1}{2Q_m} = \frac{1}{2 \times 190} = 0.26\%$ ($\frac{1}{3Q_m} = \frac{1}{3 \times 190} = 0.17\%$ for damping force with restrained end) away from the resonant frequency peak, it is observed that the response is actually directed towards the tail (brass) big mass, and that as the resonant frequency is approached from below, the amplitude of the Mach effect towards the tail (brass) big mass increases in amplitude until it reaches $2.906 \mu\text{N}$ ($2.57 \mu\text{N}$ for damping force with restrained end) directed towards the tail (brass) big mass at 33.360 kHz (33.42 kHz for damping force with restrained end) when approaching from lower frequencies towards higher frequencies. The mechanical quality factor of resonance is an inverse measure of damping, and hence governs the amplitude of resonant response. Since the MEGA drive experiments by Fearn and Woodward [26] have been performed with a manual operator chasing the natural frequency, and no frequency control algorithm has been used, it is suspected that the response that they have measured up to now is not the global peak natural frequency response, but rather the significantly lower amplitude local peak directed towards the tail (brass) big mass. Notice that there is a factor of 7.4 (6.5 times for damping force with restrained end) greater absolute magnitude response at the natural frequency, but that it is necessary to have equipment that can lock on this frequency with a bandwidth much smaller than $\pm \frac{1}{2Q_m} = \pm \frac{1}{2 \times 190} = \pm 0.26\%$ ($\pm \frac{1}{3Q_m} = \pm \frac{1}{3 \times 190} = \pm 0.17\%$ for damping force with restrained end). This is very difficult to do because as the MEGA Langevin stack vibrates, heat gets internally dissipated inside the PZT discs, which raises the temperature, which changes the dimensions of the stack, as well as the piezoelectric and electrostrictive responses, which are all temperature dependent, hence the natural frequency changes during operation and the natural frequency needs to be chased within this small bandwidth. To have the highest Mach effect forces, it is better to have higher quality factor of resonance, but the higher the quality factor of resonance, the smaller the bandwidth at which this peak natural frequency response will be located, hence the higher the quality factor of resonance, the more difficult it is to be at peak resonance and to stay at peak resonance.

Fearn et.al. [55] tested the MEGA drive with several different brass tail masses: 65 g, 81 g, 97 g, 113 g and 128 g, while keeping everything else, the PZT stack and the aluminum head mass, constant. They found that for this PZT stack, the optimal brass tail mass was 81 grams. This experimental finding by Fearn et.al. agrees very well with my preliminary calculations of the effect of the tail brass mass based on my exact electroelasticity solution of the Mach effect force modeling the MEGA drive as being held at the ends with a damping force. An optimal mass of 83 grams is calculated for the maximum calculated Mach effect force of $17 \mu\text{N}$ when the excitation is exactly identical to the natural frequency. Also an optimal mass of 83 grams is calculated for an excitation frequency $\frac{0.75}{Q_m} = 0.395\%$ smaller than the natural frequency, giving a calculated Mach effect force of $2 \mu\text{N}$. As previously discussed, the MEGA drive experiments by Fearn and Woodward [26] have been performed with a manual operator chasing the natural frequency, and no frequency control algorithm has been used. Therefore it is suspected that the response that they have measured up to now is not the global peak natural frequency response predicted to be $17 \mu\text{N}$ directed towards the head aluminum mass, but rather the significantly lower amplitude local peak of $2 \mu\text{N}$ directed towards the tail (brass) big mass. Indeed, the forces measured by Fearn and Woodward [26] have all been directed towards the tail brass mass. Thus, it is strongly suspected that, on the average they have managed their excitation frequency to be only within $\frac{0.75}{Q_m} = 0.395\%$ of the natural frequency.

The optimal tail mass is a function not just of the head mass, and the material and geometry of the stack, but it is also a function of the stress and electrical history of the stack's material. It is important to understand that this "optimal tail mass" is not a fixed characteristic of a stack and the head mass, but it is an experimental artifact due to the end fixity conditions in the experiments run by Fearn and Woodward. A MEGA drive in space does not have an optimal tail mass. For a MEGA drive in space, the greater the tail mass the better, with diminishing returns as the tail mass gets larger, see Fig. 30. For the experiments run by Fearn and Woodward, with end fixity at the tail end, there is a different optimal tail mass that depends on how far the excitation frequency is from the natural frequency. For excitation frequencies that are further

away than $\frac{1}{3Q_m}$ from the natural frequency, the larger the difference between the excitation frequency from the natural frequency, the larger the “optimal tail mass” will be. If the excitation frequency is 1% away from the natural frequency, the optimal tail brass mass is twice as large as for a difference of 0.5%.

What happens to the Mach effect force if one attaches the MEGA drive to a much larger mass, like a large spacecraft? Fig. 30 is a plot of the Mach effect force vs. (brass) mass (kg) of tail end, for different values of the excitation frequency to natural frequency ratio $\frac{f}{f_0}$, showing the asymptotic behavior of the Mach effect force for infinite mass of the brass tail end of the stack (as would happen if the Langevin stack was attached to a very massive and rigid spacecraft). For the modeled response of the Mach effect force when one attaches the MEGA drive to a much larger mass, for the experiments run by Fearn and Woodward, with end fixity, see Fig. 35 summarized in Table 6.

References

- [1] B. Jaffe, W. Cook and H. Jaffe, “*Piezoelectric Ceramics*,” Academic Press (1971).
- [2] “Military Standard, Piezoelectric Ceramic Material and Measurement Guidelines for Sonar Transducers,” MIL-STD-1376B(SH), Document Date 24 February 1995, US Naval Sea Systems Command, Department of the Navy, Arlington, VA. (This US Military standard describes six types of piezoelectric ceramic materials utilized to manufacture sonar transducers for the US Naval service. The 1376B standard was cancelled in 1999, among many defense standards that were cancelled as a result of the 1994 memo by US Secretary of Defense William Perry that prohibited the use of most defense standards without a waiver. This action was motivated by criticism that standards imposed unnecessary restrictions, increased cost to contractors, impeded the incorporation of the latest technology, and that if an enemy discovers a drawback in a standardized system, the system’s uniformity leaves it vulnerable to total incapacitation rather than a limited compromise. The US Navy Types of piezoelectric ceramic materials, created as guidelines specifically for sonar transducer design, survive today as industry standards, used by manufacturers to classify their PZT materials and referenced by scientists and engineers working in a broad range of industries.) http://quicksearch.dla.mil/qsDocDetails.aspx?ident_number=116168
- [3] Y. Shindo and F. Narita, “Piezomechanics in PZT Stack Actuators for Cryogenic Fuel Injectors,” Chapter 24 of “*Smart Actuation and Sensing Systems - Recent Advances and Future Challenges*,” edited by G. Berselli, R. Verthey and G. Vassura, ISBN 978-953-51-0798-9 (October 17, 2012). <http://www.intechopen.com/books/smart-actuation-and-sensing-systems-recent-advances-and-future-challenges/piezomechanics-in-pzt-stack-actuators-for-cryogenic-fuel-injectors>
- [4] N. Zhang, H. Yokota, A. Glazer, Z. Ren, D. Keen, D. Keeble, P. Thomas and Z. Ye, “The Missing Boundary in the Phase Diagram of $PbZr_{1-x}Ti_xO_3$,” *Nature Communications*, 5 (2014). <http://www.nature.com/articles/ncomms6231>
- [5] T. Zhang, T. Wang and M. Zhao, “Failure Behavior and Failure Criterion of Conductive Cracks (Deep Notches) in Thermally Depoled PZT-4 Ceramics,” *Acta Materialia*, Volume 51, Issue 16, (2003), pp. 4881-4895.
- [6] G. Monkman, S. Hesse, R. Steinmann and H. Schunk, “*Robot Grippers*,” Wiley-VCH (December 15, 2006).
- [7] E. Lierke, W. Littmann, T. Morita and T. Hemsel, “Various Aspects of the Placement of a Piezoelectric Material in Composite Actuators, Motors, and Transducers,” *Journal of the Korean Physical Society*, Volume 57, No. 4, (October 2010), pp. 933-937. http://www.ems.k.u-tokyo.ac.jp/morita/Papers/51_tobias.pdf
- [8] A. Mathieson, A. Cardoni, N. Cerisola and M. Lucas, “The Influence of Piezoceramic Stack Location on Nonlinear Behavior of Langevin Transducers,” *IEEE Transactions on Ultrasonics, Ferroelectrics, and Frequency Control*, Jun. 2013, Volume 60, Issue 6, (2013), pp. 1126-1133.
- [9] H. Fearn, A. Zachar, K. Wanser and J. F. Woodward, “Theory of a Mach Effect Thruster I,” *Journal of Modern Physics*, Volume 6, (2015), pp. 1510-1525. <https://physics.fullerton.edu/~heidi/JMP-MachII.pdf>. http://file.scirp.org/pdf/JMP_2015091711084670.pdf
- [10] J. Den Hartog, “*Mechanical Vibrations*,” 4th edition, McGraw-Hill (1956).
- [11] R. Scanlan and R. Rosenbaum, “*Aircraft Vibration and Flutter*,” Dover (1968).
- [12] R. Clough and J. Penzien, “*Dynamics of Structures*,” McGraw-Hill (1975).
- [13] Y. Maruyama, N. Kojima, T. Ezaki and T. Yamakawa, US Patent 6114798 A, “Stacked Element and Vibration Drive Device,” publication date: Sep. 5, 2000, filing date: Mar. 25, 1997, priority date: Mar. 25, 1996.
- [14] Y. Maruyama, N. Kojima, T. Ezaki and T. Yamakawa, US Patent 6951048 B2, “Method for Producing a Stacked Piezoelectric Element,” publication date: Oct. 4, 2005, filing date: Nov. 5, 2003, priority date: Feb. 17, 1998.
- [15] D. Berlincourt, H. Krueger and C. Near, “Properties of Morgan Electro Ceramic Ceramics,” Technical Publication TP-226 Properties of Piezoelectricity Ceramics. <http://www.morgantechnicalceramics.com/media/1885/tp226.pdf>
- [16] NBK Hex Socket Head Cap Screws - Super Invar. <https://www.nbk1560.com/en-US/products/specialscrew/nezicom/specialmaterialscrew/SNSIV/>
- [17] S. Zhang, F. Li, N. Sherlock, J. Luo, H. Lee, R. Xia, R. Meyer, W. Hackenberger and T. Shrout, “Recent Developments on High Curie Temperature PIN-PMN-PT Ferroelectric Crystals,” *Journal of Crystal Growth*, Volume 318, Issue 1, (March 2011), pp. 846-850. https://www.researchgate.net/publication/51073215_Recent_developments_on_high_Curie_temperature_PIN-PMN-PT_ferroelectric_crystals

- [18] H. Fearn, "Mach's Principle, Action at a Distance and Cosmology," *Journal of Modern Physics*, Volume 6, Issue 3, (February 2015). <https://physics.fullerton.edu/~heidi/JMP-Mach0.pdf>
- [19] F. Hoyle and J. V. Narlikar, "A New Theory of Gravitation," *Proc. Roy. Soc. Lon.*, Volume A282, Issue 191 (1964).
- [20] F. Hoyle and J. V. Narlikar, "On the Gravitational Influence of Direct Particle Fields," *Proc. Roy. Soc. Lon.*, Volume A282, Issue 184 (1964). See also "A Conformal Theory of Gravitation," *Proc. Roy. Soc. Lon.* Volume A294, Issue 138 (1966).
- [21] F. Hoyle and J. V. Narlikar, "*Action at a Distance in Physics and Cosmology*," W. H. Freeman and Company, San Francisco (1974).
- [22] I. Ciufolini and J. Wheeler, "*Gravitation and Inertia*," Princeton University Press (1995).
- [23] J. Narlikar and H. Arp, "Time Dilation in the Supernova Light Curve and the Variable Mass Hypothesis," *The Astrophysical Journal*, Volume 482, (June 20, 1997), pp. L119-L120. <ftp://ftp.lal.in2p3.fr/pub/flower/bibliographie/cosmology/narkilar-arp-1997.pdf>
- [24] J. Narlikar and P. Das, "Anomalous Redshifts of Quasi-Stellar Objects," *The Astrophysical Journal*, Part 1, Volume 240, (September 1, 1980), pp. 401-414. http://repository.iucaa.in:8080/jspui/bitstream/11007/1523/1/105A_1980.PDF
- [25] H. Fearn, J. F. Woodward and N. van Rossum, "New Theoretical Results for the Mach Effect Thruster," 51st AIAA/SAE/ASEE Joint Propulsion Conference, AIAA Propulsion and Energy Forum (July 27-29, 2015), Orlando, FL, (AIAA 2015-4082). <http://arc.aiaa.org/doi/abs/10.2514/6.2015-4082>.
- [26] H. Fearn, N. van Rossum, K. Wanser and J. F. Woodward, "Theory of a Mach Effect Thruster II," *Journal of Modern Physics*, Volume 6, (2015), pp. 1868-1880. <https://physics.fullerton.edu/~heidi/JMP-MachII.pdf>
- [27] L. Brillouin, "The Actual Mass of Potential Energy, a Correction to Classical Relativity," *Proceedings of the National Academy of Sciences, USA*, Volume 53, Issue 3, (March 15, 1965), pp. 475-482. <https://www.ncbi.nlm.nih.gov/pmc/articles/PMC336961/pdf/pnas00155-0003.pdf>
- [28] L. Brillouin, "The Actual Mass of Potential Energy, II," *Proceedings of the National Academy of Sciences, USA*, Volume 53, Issue 6, (June, 1965), pp. 1280-1284. <https://www.ncbi.nlm.nih.gov/pmc/articles/PMC219831/pdf/pnas00158-0114.pdf>
- [29] L. Brillouin, "*Relativity Reexamined*," Academic Press (1970).
- [30] R. Medina, "The Inertia of Stress," *American Journal of Physics*, Volume 74, (2006), pp. 1036-1040. <https://arxiv.org/pdf/physics/0609144.pdf>
- [31] R. Medina, "Radiation Reaction of a Classical Quasi-Rigid Extended Particle," *Journal of Physics A: Mathematical and General*, Volume 39, (2006), pp. 3801-3816. <http://citeseerx.ist.psu.edu/viewdoc/download?doi=10.1.1.205.7077&rep=rep1&type=pdf>
- [32] K. McDonald, "Stress and Momentum in a Capacitor that Moves with Constant Velocity." <http://citeseerx.ist.psu.edu/viewdoc/download?doi=10.1.1.412.5459&rep=rep1&type=pdf>
- [33] P. Penfield and H. Haus, "*Electrodynamics of Moving Media*," The MIT Press (August 15, 1967).
- [34] C. Leibovitz, "Rest Mass in Special Relativity," *American Journal of Physics*, Volume 37, Issue 8, (August 1969), pp. 834-835. <http://cleibovitz.upwize.com/physics/>
- [35] J. Sprott, "Some Simple Chaotic Jerk Functions," *American Journal of Physics*, Volume 65, Issue 6, (June 1997), pp. 537-543.
- [36] J. Sprott, "*Chaos and Time-Series Analysis*," Oxford University Press (2003).
- [37] G. Martin, "On the Theory of Segmented Electromechanical Systems," *The Journal of the Acoustical Society of America*, Volume 36, Issue 7, (July 1964), pp. 1366-1370.
- [38] K. Wanser, "Center of Mass Acceleration of an Isolated System of Two Particles with Time Variable Masses Interacting with Each Other via Newton's Third Law Internal Forces: Mach Effect Thrust 1," *Journal of Space Exploration*, Volume 2, Issue 2, (2013), pp. 121-130.
- [39] Steiner & Martins, Inc., "Piezo Material Properties." https://www.steminc.com/piezo/PZ_property.asp.
- [40] M. Haun, Z. Zhuang, E. Furman, S. Jang and L. Cross, "Electrostrictive Properties of the Lead Zirconate Titanate Solid-Solution System," *Journal of the American Ceramic Society*, Volume 72, Issue 7, (July 1989), pp.1140-1144.
- [41] J. Li and N. Rao, "Dramatically Enhanced Effective Electrostriction in Ferroelectric Polymeric Composites," *Applied Physics Letters*, Volume 81, Issue 10, (September 2002), pp. 1860-1862.
- [42] S. Lee, R. Monteiro, R. Feigelson, H. Lee, M. Lee and S. Park, "Growth and Electrostrictive Properties of $Pb(Mg_{1/3}Nb_{2/3})O_3$ Crystals," *Applied Physics Letters*, Volume 74, Issue 7, (February 1999), pp. 1030-1032.
- [43] S. Swartz, T. Shrout, W. Schulze and L. Cross, "Dielectric Properties of Lead-Magnesium Niobate Ceramics," *Journal of the American Ceramic Society*, Volume 67, Issue 5, (May 1984), pp. 311-314.
- [44] A. von Hippel, "*Dielectrics and Waves*," John Wiley & Sons (1954).
- [45] J. Burfoot and G. Taylor, "*Polar Dielectrics and their Applications*," University of California Press, Berkeley and Los Angeles, (June 1979).
- [46] W. Voigt, "*Lehrbuch der Kristallphysik*," Teubner, Leipzig, 1910; Springer Fachmedien Wiesbaden (1966).
- [47] H. Haus and J. Melcher, "*Electromagnetic Fields and Energy*," Prentice Hall, (September, 1989).
- [48] J. Jackson, "*Classical Electrodynamics*," Third Edition, John Wiley & Sons (August, 1998).
- [49] D. Griffiths, "*Introduction to Electrodynamics*," Fourth Edition, Pearson (October, 2012).

- [50] W. Panofsky and M. Phillips, “*Classical Electricity and Magnetism*,” Second Edition, Addison-Wesley Publishing Company, (1962).
- [51] R. Newnham, V. Sundar, R. Yimnirun, J. Su and Q. Zhang, “Electrostriction: Nonlinear Electromechanical Coupling in Solid Dielectrics,” *The Journal of Physical Chemistry B*, Volume 101, Issue 48, (1997), pp. 10141-10150.
- [52] S. Zhang, J. Lim, H. Lee, T. Shrout, “Characterization of Hard Piezoelectric Lead-Free Ceramics,” *IEEE Transactions on Ultrasonics Ferroelectrics and Frequency Control*, Volume 56, Issue 8, pp. 1523-1527, (September, 2009).
- [53] D. Waechter, S. Prasad, R. Blacow and B. Yan, “Internally Biased PZT Materials for High-Power Sonar Transducers,” Proceedings of the 11th CF/DRDC International Meeting on Naval Applications of Materials Technology, Dartmouth, Nova Scotia, Canada, (June 7th-9th, 2005). <http://sensortechcanada.com/wp-content/uploads/2014/08/2005-06-Internally-Biased-PZT-Materials-for-High-Power-Sonar-Transducers.pdf>
- [54] D. Jones and J. Lindberg, “Recent Transduction Developments in Canada and the United States,” Proceedings of the Institute of Acoustics (Institute of Acoustics, St. Albans, Herts, UK), Volume 17, Part 3, (1995), pp. 15-33.
- [55] H. Fearn and J. Woodward, “Experimental Null Test of a Mach Effect Thruster,” *Journal of Space Exploration*, Volume 2, Issue 2, (2013), pp. 98-105. <https://physics.fullerton.edu/~heidi/JSE13.pdf>
- [56] H. Fearn and J. Woodward, “Experimental Null Test of a Mach Effect Thruster,” arXiv:1301.6178, (Jan 25, 2013), pp. 1-10. <https://arxiv.org/abs/1301.6178>
- [57] J. Woodward, “*Making Starships and Stargates: The Science of Interstellar Transport and Absurdly Benign Wormholes*,” Springer 2013 edition (December 15, 2012).
- [58] M. Hooker, “Properties of PZT-Based Piezoelectric Ceramics Between -150 and 250 °C,” NASA/CR-1998-208708, prepared for Langley Research Center under Contract NAS1-96014, Lockheed Martin Engineering & Sciences Co., Hampton, Virginia, (September, 1998). <https://ntrs.nasa.gov/archive/nasa/casi.ntrs.nasa.gov/19980236888.pdf>
- [59] W. Mason, “*Physical Acoustics and the Properties of Solids*,” D. van Nostrand Company, (1958).